Alberta Environment Research Proposal RS77-42

FINAL REPORT

PARTICULATE AIR POLLUTION AND VISIBILITY OVER CALGARY

by

A.W. HARRISON and C.V. MATHAI
PHYSICS DEPARTMENT
UNIVERSITY OF CALGARY
February 1980

under

ALBERTA ENVIRONMENT
CONTRACT NO. AE 79-0076

to the:

Research Secretariat
Alberta Environment
9820-106 Street
Edmonton, Alberta
T5K 2J6

RMD-80/2

91-02983/

THIS REPORT IS MADE AVAILABLE AS A PUBLIC SERVICE. THE DEPARTMENT OF ENVIRONMENT NEITHER APPROVES NOR DISAGREES WITH THE CONCLUSIONS EXPRESSED HEREIN, WHICH ARE THE RESPONSIBILITY OF THE AUTHOR(S).

SUMMARY

The particle size distribution n(R) of ambient aerosol in the Calgary boundary layer has been investigated in the size range $R \sim 0.1$ μm to $R \sim 1.0$ μm, the range which is important in determining visibility or visual range. This study was made in conjunction with nephelometer, cascade impactor, high volume air sampler, COH, NO_x, O_3, CO and HC sampling and acoustic sounder monitoring. Comparison of the aerosol in the SE (industrial) sector with that in the NW (residential) sector of the city was accomplished through the use of a mobile unit. The relationship between the shape of the size distribution n(R) and visual range and the relationship between n(R) and the aerosol scattering coefficient was examined under a variety of atmospheric conditions and at different times of the year. Correlation studies of COH, NO_x, O_3, CO and HC data collected by Alberta Environment at CRMU and nephelometer data collected in this study at the University of Calgary showed an almost one to one correspondence between the two sets of data. This correlation covered a two month period. A comparison of the Andersen impactor collection technique with the particle size spectrometer measurement of the same ambient aerosol showed that both instruments give good agreement with one another concerning the particle spectrum deduced. This spectrum is best described by the Junge power law or by the lognormal mass size distribution. A significant result of monitoring through chinook and temperature inversion events was that the particle size spectrum changed significantly and that this change was accompanied by corresponding changes in aerosol scattering coefficient and meteorological parameters.

TABLE OF CONTENTS

Page

SUMMARY i

TERMS OF REFERENCE iv

LIST OF FIGURES v

LIST OF TABLES vii

LIST OF SYMBOLS viii

1. INTRODUCTION 1

2. LITERATURE SURVEY 2

2.1 Introduction 2

2.2 Background 3

2.3 Particle Size Distributions (General) 4

2.4 Particle Size Distributions (Optical) 5

2.5 Particle Size Distributions (Environmental) 6

2.6 Background aerosol. 8

2.7 Self Preserving Distributions 9

2.8 Density of Suspended Particulates 9

2.9 Chemical Composition 10

2.10 Visual Range and Nephelometers 11

2.11 Visibility, Relative Humidity and Mass Loading 12

2.12 Visibility and Particle Size 14

2.13 Wavelength Dependence of Visibility 14

Table of Contents (cont'd)

		Page
3.	EXPERIMENTAL PROGRAMME	15
	3.1 Instrumentation	15
	3.2 Observing Sites	22
	3.3 Observing Programme	24
4.	RESULTS AND EVALUATION	26
	4.1 Mobile Study of Particle Size Distribution	26
	4.2 Visual Range and Particle Size Distribution	34
	4.3 Impactor Data and Particle Size Distribution	46
	4.4 Influence of Chinook on Particle Size Distribution	70
	4.5 Nephelometer, Impactor and CRMU Data Correlation	77
5.	CONCLUSIONS	86
6.	RECOMMENDATIONS	88
7.	ACKNOWLEDGEMENTS	89
8.	REFERENCES	91

TERMS OF REFERENCE

1. To review aerosol and particulate air pollution research literature relevant to Alberta.

2. To investigate particle size distribution in ambient air over Calgary in different seasons using an integrating nephelometer and through the use of a mobile unit.

3. To relate the particle size distribution to visual range.

4. To validate the optically determined particle size distribution with a mechanical particle size distribution technique such as the Andersen impactor. (Data to be supplied by Alberta Environment).

5. To study the influence of Chinook (as determined by acoustic sounder) on particulate size distribution.

6. To investigate correlations of NO_x, coefficient of haze (COH), total suspended particulates as measured by hi-volume sampler, and integrating nephelometer measurement, for specific situations.

LIST OF FIGURES

		Page
Figure 3.1	Relative response of multiwavelength nephelometer to 398, 467, 557, and 696 nm light	18
Figure 3.2	Relative response of multiwavelength nephelometer to white light	19
Figure 3.3	Outline map of City of Calgary showing location of observation sites	23
Figure 4.1	Log n(R) versus log R for ambient aerosol in SE and NW Calgary, Nov. 22, 1979	28
Figure 4.2	Summary of power law exponent ν, wind vector and scattering coefficient a(480) for the transit study of SE and NW sectors of City of Calgary, October-December, 1979	32
Figure 4.3	Summary all SE and NW sector results for ν and a(480) obtained in the transit study, October-December, 1979	33
Figure 4.4-4.7	Particle size spectrum n(R) versus particle size R for clean air, light haze, light pollution and light fog respectively	37-40
Figure 4.8-4.11	Volume differential scattering coefficient $a(\lambda)$ versus wavelength (λ) for clean air, light haze, light pollution and light fog respectively . . .	42-45
Figure 4.12	Log-probability plot of Andersen impactor data for November 22-24, 1978	49
Figure 4.13-4.20	Log-normal best fit and point histogram plot of $\Delta M/M\Delta \log D$ versus D for Andersen impactor samples Nov. 22-24, 24-27, Nov. 27-Dec. 1, Dec. 1-4, 4-8, 11-14, 14-17 and 17-20 respectively.	53-60
Figure 4.21-4.28	Particle size spectrum n(R) calculated from Andersen impactor data and measured by ASAS-300 versus R for samples Nov. 22-24, 24-27, Nov. 27-Dec. 1, Dec. 1-4, 4-8, 11-14, 14-17 and 17-20, 1978. respectively	62-69
Figure 4.29	Acoustic sounder records of boundary layer turbulence for the three chinooks Feb. 17/18, March 3 and March 9/10, 1978	73

List of Figures (cont'd)

		Page
Figure 4.30	Detailed meteorological data (temperature and wind vector), volume scattering coefficient a(480), and particle size power law exponent ν for the chinook of Feb. 17/18, 1978	74
Figure 4.31-4.33	Volume scattering coefficient (a), smoke index (s), NO_x concentration (n), ozone concentration (o), hydrocarbon concentration (h), and carbon monoxide concentration (c) for the University of Calgary, Feb. 1 to March 31, 1978	79-82

LIST OF TABLES

		Page
Table 3.1	Summary of experimental programme	25
Table 4.1	Summary of mobile unit aerosol data	30
Table 4.2	Comparison of measured (ν) and calculated ($\bar{\nu}$) power law exponent with standard visibility V(550) . . .	46
Table 4.3	Summary of Andersen impactor data for University of Calgary Campus, winter 1978/79	50-51
Table 4.4	Correlation coefficients for CMRU and UC data February 1, 1978 to March 31, 1978	83
Table 4.5	Aerosol mass concentration and differential scattering coefficient for summer and winter 1978	85

LIST OF SYMBOLS

a	Broad band (white light) scattering coefficient
$a(\lambda)$	Volume differential scattering coefficient
D	Aerodynamic equivalent diameter
D_m'	Mass median diameter (MMD)
m	Complex index of refraction
M	Mass concentration of total suspended particulates
ΔM	Mass fraction concentration of total suspended particulates
n	Aerosol particle number per unit volume
$n(R)$	Particle size distribution
$Q(R,\lambda,m)$	Mie scattering efficiency factor
R	Radius of spherical aerosol particle
RH	Relative humidity
T	Temperature
α	Angstrom coefficient
ν	Power law exponent (measured)
$\bar{\nu}$	Power law exponent (calculated)
ν_1	Slope of log n(R) vs log R (Andersen data)
ν_2	Slope of log n(R) vs log R (ASAS data)
λ	Wavelength
σ_g	Geometric (mass) standard deviation (GSD)
ρ	Average bulk density of ambient aerosol

1. INTRODUCTION

Of all the possible adverse effects of atmospheric pollution perhaps none is more apparent to the average city of Calgary resident as impaired visibility. Nearly everyone has experienced the shroud of brown or white haze which now and again covers the city and which then obscures the view of the Rocky Mountains to the west. Under these conditions a view of the city itself from a high vantage point outside the city to the north or west will show a pronounced and apparently uniform layer of "pollution" with a ceiling varying anywhere between about 100 m and 300 m in altitude. The optical depth of this layer is taken as an indicator of the severity of the prevailing atmospheric pollution by the casual observer but as is well known the foreign particulates or aerosols in the local atmosphere at any given time may or may not give rise to this visual effect. In other words the COH, NO_x, O_3, and HC levels may be relatively high without the visibility being necessarily low. On the other hand during temperature inversion conditions the reverse is often the case.

Since Calgary is situated in the zone of chinook occurrence and is built around a major river valley, local conditions will be considerably atypical so that predicted relationships between atmospheric particulate loading and visibility may not apply. The aim of the study has been to obtain preliminary data in several situations and areas on particle size distributions relevant to visibility. Further, to compare visual range and particle size data with simultaneous measurements of COH, NO_x, O_3 and HC during periods of chinook, temperature inversions or other specific atmospheric conditions. The study has incorporated several lines of

investigation all of which are preliminary in the sense that most of the instrumentation and experimental techniques employed have not been used before in Calgary.

The terms of reference outlined for this project are only loosely related to one another so that in the interests of clarity the format of the report has been shaped accordingly. The results for each term of reference are dealt with separately within the Results and Evaluation section. However, the equipment used for the project as a whole is described under the Experimental Programme section because in many instances the same instrument was employed for more than one investigation (term of reference).

2. LITERATURE SURVEY

2.1 Introduction

The following survey is intended to focus on particle size distributions in the boundary layer with emphasis on continental aerosols such as might be expected to occur in the central and southern regions of Alberta. Properties of such aerosols relating to visibility and atmospheric transmission have been emphasized in accord with the general tone of the terms of reference for the contract under which this work was carried out. What follows represents a small portion of the overall field of "aerosol science". Topics such as electrical properties, stratospheric aerosols, mechanics of aerosols, diffusion and coagulation, generation of aerosols, radioactivity of aerosols, density, size and shape, etc. have been excluded as such. On the other hand optical properties, scattering, chemical composition, particle spectra, visibility, etc. have

been included where appropriate. It should be realized that to attempt to divorce one topic from all others is in itself a difficult task. In attempting this however, subsidiary topics relating to particle size distributions have been reviewed as indicated below under corresponding headings. All research journals referred to are available in either library at the University of Alberta, Edmonton or at the University of Calgary. Textbooks referred to are available in current holdings at the University of Calgary.

2.2 Background

An aerosol can be defined as a suspension of solid or liquid matter in a gaseous medium (air). The particles in such a suspension range from clusters of a few molecules to particles with radii of $\sim$ 20 μm. Raindrops and cloud particles are usually excluded in such a definition. The upper limit of size is controlled by sedimentation processes in natural air. The lower limit is determined by coagulation processes. Very small particles ($\leq 10^{-3}$ μm) rapidly adhere to larger particles while very large particles ($\geq$ 20 μm) rapidly fall out of suspension due to gravity. A complete discussion of sedimentation and coagulation can be found in Fuchs, (1964). Of practical interest are particles in the general range $\sim 10^{-3}$ μm to 20 μm). This range is usually subdivided into,

Aitken particles : $R \leq 0.1$ μm

Larger particles : $R \sim 0.1$ μm to 1.0 μm

Giant particles : $R \geq 1.0$ μm

Of interest in this review are the larger particles since they are responsible for the optical effects concerning visibility in the natural atmosphere. Due to the large range in size and concentration of aerosols it is customary to use logarithmic scales as in the log radius - number

distribution

$$n(R) = dN/d(\log R) \text{ cm}^3 \qquad [2.1]$$

where N is the total concentration of aerosol particles of radius smaller than R. The number ΔN between the limits of the interval $\Delta(\log R)$ is then

$$\Delta N = n(R)\ \Delta(\log R). \qquad [2.2]$$

The methods used for measuring aerosols vary with the size range. For Aitken particles (nuclei) the Aitken counter is often used, based on the Wilson expansion chamber. Larger particles are now measured most conveniently with an optical particle spectrometer and giant particles can be measured by direct optical microscopy. A survey of different methods can be found in Dennis (1976). Due to the rapid accumulation of data over the past decade it has become possible to identify particular types of distribution and aerosol content according to geographical location. Two particularly well defined atmospheric aerosols are the Maritime and Continental aerosols (Junge, 1963). The former contains a preponderance of NaCl particles and are to be found on or near the oceans of the world. Continental aerosols are comparatively "dry" aerosols and are to be found over large land masses. This aerosol is characteristic of those found in the Calgary area.

2.3 Particle Size Distribution (General)

Aerosols in the natural air vary in size and concentration over several orders of magnitude so that distributions are expressed in logarithmic scales, (Davies, 1974a; Brock, 1971; McCartney, 1976). Many studies in different environments have shown that characteristic distributions can be attached to particular backgrounds, e.g. mountain background, Pacific ocean background, continental background, "urban pollution" background, etc., (Slin 1975). In a great many cases it has

been found that over the size range $R \gtrsim 0.1$ μm to 1.0 μm, of significance in visibility studies, the Junge power law is a good representation of the particle size distribution, i.e.

$$n(R) = c\, R^{-\nu} \ (cm^{-3}\ \mu m^{-1}) \qquad [2.3]$$

with $\nu \gtrsim 3.5$ to 5.0 and where c is a constant. Other distributions often used to describe a natural aerosol are the exponential size distribution, (Twomey 1977),

$$n(R) = c\, R^{\alpha} \exp(-bR^{\gamma}) \qquad [2.4]$$

and the Gaussion or log-normal distribution

$$n(\log R) = c\, R \exp\left[-\log(R/\bar{R})^2/b\right] \qquad [2.5]$$

The Junge power law is the one mostly used in studies of continental and urban pollution aerosols involving a wide variety of origins and compositions. This distribution gets its name from the extensive earlier studies of Junge in Germany, (Junge, 1958). Later studies have confirmed this generality, (Clark and Whitby, 1967; Pueschel and Noll, 1967; Blifford and Ringer, 1969; and Whitby et.al., 1972). Size, area, and weight distributions are often interdependant and a particular characterization of the aerosol depends on the study being made, (Stern, 1976). More details of distributions in general can be found in texts by Davies, (1966), Cadle, (1975), and Rasool, (1973).

2.4 Particle Size Distributions (From Optical Measurements)

While particle size can be measured by a variety of different techniques, depending on the size range covered, of interest here is the dependance of optical properties on aerosol size, (Cadle, 1975). The

interaction of suspended particulates with visible electromagnetic radiation is of interest to all studies involving the transmission of natural (solar) or artificial light through the atmosphere. Many attempts have been made to use spectral attenuation measurements through haze and fogs to deduce the corresponding size distributions, (Curcio, 1961; Eldridge, 1966). This approach has met with partial success only due to the ambiguous predictions which result from application of Mie scattering theory. Only when the size distribution can be characterized by some particular distribution law (e.g. power law) does this method become feasible, (Heintzenberg, 1975). Measurements of atmospheric turbidity have been used to estimate the gross aerosol loading of the atmosphere over the observing site and world-wide turbidity monitoring has been conducted for several years. More recently attention has been given to the estimation of size distributions from daytime sky measurements, (Tashenov, et.al., 1973, Yamamoto and Tanaka, 1969).

2.5 Particle Size Distributions (Environmental)

During the past decade there have been several studies dedicated to particular urban areas in which particle size distributions have been measured and characterized. A seasonal study of particulates using air samplers determined surface area and densities in Pittsburgh air, (Stern, 1976). Similar studies have been made in Melbourne, Australia as a function of altitude, (Mainwaring and Harsha, 1976), and in relation to chemical composition in Nagoya, Japan using Andersen impactors, (Kadawaki, 1976). Comparison of two sites in the Denver area, one with little anthropogenic activity, the other with typical city core activity

was made by Willeke, et.al., (1974) and a similar comparative study has been carried out in Los Angeles and Anaheim using the Andersen impactor technique, (Wadley, et.al., 1978). The early classic study of Los Angeles smog, (Whitby, et.al, 1972) has been followed by a similar large city study for New York, (Leaderer, et.al., 1978) in both of which the relationship between particulate mass and scattering (visibility) has been emphasized. One particularly interesting work which relates to urban freeway aerosols is that of Whitby, et.al., (1975) for the Los Angeles area. The work of Kelkar and Joshi, (1977) at Bombay, India showed that environment to be similar to Los Angeles. One study with an integrating nephelometer in the Puget Sound area, Washington related vertical distribution of particulates to meteorological conditions, (Ahlquist and Charlson, 1968), while the study of Peterson et.al., (1969) from a television tower in Minneapolis and St. Paul followed particulate size distribution through a temperature inversion. Monitoring of distributions in remote areas has been carried out by Jennings and Elleson (1977) in the Lake District, England and by Sverdrup, et.al, (1975) in the Mojave desert. An example of a comprehensive study involving nephelometer, lidar, radiometer and air sampler measurements can be found in the work of DeLuisi, et.al. (1976) and serves as an example of the advantages gained by combining different instruments and techniques. Such a study would be appropriate to the Calgary area where temperature inversions and Chinooks are likely to create unusual altitude distributions. In this connection vertical diffusion effects are important and have been considered by McCormick and Holzworth, (1976). Finally mention should be

made of the aerosol size distribution studies made recently by Twomey, (1976), using nuclepore filters as an example of a relatively inexpensive method compared with the contemporary optical particle spectrometers now available.

2.0 Background Aerosol

The effect of atmospheric aerosols on the world climate has become a prominent feature of aerosol studies due to the increased pollution on a global scale. It is necessary to establish a background level against which future trends may be measured. Earliest methods of estimating a background aerosol level were based on searchlight and Volz sunphotometer techniques. As early as 1970 the integrating nephelometer was employed to measure the aerosol scattering coefficient at remote locations such as Point Barrow, Alaska and Mount Olympus, Washington, (Porch, et.al., 1970). Subsequent studies and discussions have indicated that certain remote locations, such as Greenland should be chosen for long term monitoring, (Megaw 1973). A detailed experimental investigation of the background aerosol at several remote locations using an integrating nephelometer was carried out by Charlson, et.al., (1974). This showed that the aerosol scattering coefficients could be as low as 1.1 to 2.3 times the pure Rayleigh gas scattering coefficient with an anomalous wavelength dependence, $\alpha < 0$ on some occasions. A unique aspect of the background aerosol has been explained by Porch, et.al., (1975) in connection with the visibility of distant mountains and might be considered as a basis for visibility studies in the Calgary-Rocky Mountain environment. General properties of the background aerosol

have been summarized by Shaw, (1976) on the basis of measurements made at the South Pole, in Alaska and Hawaii. A model of radiative transfer and global heating and cooling as a function of background aerosol levels is referred to.

2.7 Self Preserving Distributions

It was realized early on that aerosols in which both sedimentation and coagulation occur simultaneously should tend toward a common size distribution, (Friedlander, 1960). In the case of the natural tropospheric aerosol it has been argued that turbulent coagulation, washout by rain, etc. must also be considered as well as local mechanisms for removal dependent on climate and terrain, (Rasool, 1973). The steady state hypothesis put forward by Friedlander has been argued by Junge, (1969) who accounts for the observed similarity in size distributions as the result of statistical mixing of particles from many sources. In a detailed experimental test of this theory Clark and Whitby, (1967) analyzed 58 size distributions in the range R = 0.001 μm to 3.0 μm under a variety of conditions and found consistent accord with theory. In the range R = 0.05 μm to 3.0 μm the power law was found to hold good with $\nu = 4$. In connection with the self preservation theory is the question of residence times for aerosols in the atmosphere. In general studies indicate that for material injected into the troposphere, a fraction $1/e$ still remains after a time of one to six days, (Rasool, 1973). An up-to-date account of self preserving steady-state solutions may be found in Twomey, (1977).

2.8 Density of Suspended Particulates

The intrinsic density of particulate material itself is poorly known but is estimated to vary from 0.5 to 6.5 g cm^{-3},

(Rasool, 1973). Measurements of the particle density have been made in Pittsburgh yielding 1.8 - 2.3 g cm^{-3} while in Denver values of 1.6 - 1.8 and 1.1 - 1.5 g cm^{-3} were obtained, (Durham, 1975). Closely coupled with the intrinsic density is the shape and size of individual particles. For a definition of shape factors used in this context both Stern, (1976) and Cadle, (1975), should be consulted. The relationship between size distribution and particle shape for Pittsburgh air has been examined by Stein, et.al., (1969). Parallel to studies of intrinsic particle density are those relating to the overall mass loading of the atmosphere or density of the aerosol itself. A summary of suspended particulate matter (µg per m^3) at urban locations in the United States is given by Rasool, (1973). Values range from a minimum of 11 µg m^{-3} to a maximum of 978 µg m^{-3}. In Los Angeles a mean value of 213 µg m^{-3} was reported with 7.5% of this due to sulphates and 4.4% due to nitrates. The investigation carried out by Suck, et.al., (1977) provides an explanation for the occurrence of multimodel density functions resulting from combined deposition, coagulation, convection and other processes. From a practical viewpoint cascade sampler techniques should be used with caution by taking account of particle blow-off and bounce-off and subsequent reentrainment. This matter is discussed in a most recent paper by Wangen, (1978).

2.9 Chemical Composition

It was realized many years ago that the chemical composition of suspended particulates is highly dependent upon locality and that composition is size dependent. This has significance in toxilogical

effects of pollution, particulate pollution potential for corrosion, visibility and crop damage. Specific studies related to sulphates, lead, nitrates, aromatic hydrocarbons, chlorides, vanadium, etc., are numerous and have been summarized by Stern, (1976). Most investigations have relied upon cascade impactor collection followed by chemical analysis. Particular analyses of large organic compounds in American urban atmospheres and of selected anions (Na, K Cu etc.) and cations (phosphate, sulphate etc.) in heavily populated areas are too numerous to mention. The effect on visual range of natural and man made aerosols is treated generally by Davies, (1974a) and in some detail by McCartney, (1976). Another excellent review of composition as related to total concentration is given by Rasool, (1973). A unique study in which the effect of relative humidity on visibility was explained in terms of $(NH_4)_2SO_4$ aerosol content, (Garland, 1969), can be compared with the work of White and Roberts, (1977), for the Los Angeles area. In the later case the visibility was considered in relation to both nitrates and sulphates. Using electron and optical microscopy evaluation in conjunction with chemical analysis Meszaros, (1977) examined the effects of solar radiation, wind speed and temperature on the ammonium sulphate content of aerosols in Budapest, Hungary. A similar and more extensive study has been made in St. Louis, U.S.A. by Orsini, et. al., (1977).

2.10 Visual Range and Nephelometers

The scattering of radiation by aerosols has been a subject of academic interest for a long time embracing the elegant Mie theory of scattering as well as numerous experimental studies embodied in

classical researches on colloidal suspensions. Estimation of aerosol concentration through scattering photometry was recognized by Gucker and Peterson, (1955) and by Crosby (1960). The later's was among the early attempts to produce a workable integrating nephelometer. The nephelometer of Crosby and Koerber, (1963), was followed by a similar instrument perfected by Charlson, et.al., (1967). In a series of papers involving the later group the utility of the integrating nephelometer is described, (Ahlquist and Charlson, 1967; Charlson, et.al., 1969; Ensor and Waggoner, 1970). The integrating nephelometer measures the scattering coefficient due to aerosols and this can be related directly to the visual range. Two other groups have helped in the nephelometer development. An open air version was built by Garland and Rae (1970), and used for visibility studies, (Rae and Garland, 1970). In Australia, Koerber and Dale, (1972) and Cutten, et.al, (1975) have developed a visibility meter based on the integrating nephelometer concept. In Canada, Harrison, (1977c), has constructed a spectronephelometer which measures the wavelength dependence of aerosol scattering coefficient, and can thus be used to investigate the variation of visual range with wavelength. A recognized work on the theory of visual range determinations through the use of nephelometers is given by Middleton, (1968), and experimental studies validating the relationship between aerosol scattering coefficient and visual range have been described by Horvath and Noll, (1969).

2.11 Visibility, Relative Humidity and Mass Loading

Soon after the introduction of the integrating nephelometer as an instrument for routine air pollution monitoring it was established that a strong correlation exists betwen mass concentration and visibility, (Noll, et.al, 1968). The proportionality constant was measured in

California to be 1.0 - 1.9 g m^{-2}. A review of this result and related features is given by Charlson, (1969) and by Tombach, (1971). Use of the integrating nephelometer to infer mass loading of the atmosphere is thus inferred from this result and has been tested in a transit study of an urban area in Adelaide, Australia, (Lyons and Cutten, 1975). In this study the effect of temperature was also included. Other values of the proportionality constant have been reported e.g. 0.45 g m^{-2} by Griggs, (1972). The effect of relative humidity on visibility and the implications concerning particle size were noted by Buma, (1960), in a study near Leeuwarden in the Netherlands. A quantitative investigation by Lundgren and Cooper, (1969), showed that light scattering by aerosols begins to increase for relative humidities above about 70%, a result which has been confirmed by other workers in the field, (Tombach, 1971; Andreev, et.al., 1974; and Zdnunkowski, 1976). Theoretical considerations in relation to water content of a fog and visibility are given by Eldridge, (1971). More detailed and more recent experimental studies include those of Paterson, (1973) for visibility and humidity in Sydney, Australia, and of Livshits, et.al., (1974) for the Odessa region, U.S.S.R. The effect of varying both relative humidity and chemical composition of aerosol particles on visibility has been studied most recently by Sinclair, et.al., (1974) and by Thudium, (1978). Other experimental investigations involving the effects of mass loading and/or relative humidity on visibility include those of Charlson, et.al., (1968); Eccleston, et.al., (1974); Patterson and Wagman, (1977); and Patterson and Gillette, (1977).

2.12 Visibility and Particle Size

The scattering of radiation by particles in the atmosphere is responsible for the degradation in visibility in a polluted atmosphere. The dependence of scattering on particle size, refractive index, and wavelength is well known and has been discussed by Peuschel and Noll, (1967) in connection with particle size distributions. As a general working rule it is usually assumed that only particles in the size range $\sim$ 0.1 μm to 1.0 μm are effective in moderating the visual range, (McCartney, 1976). This is confirmed in theoretical predictions of visual range for power law distributions using Mie theory, (Davies, 1975). Simultaneous visibility and size-number distribution measurements have been compared with theory in the recent study of Patterson, et.al., (1976) for soil erosion particles in Texas. In this case it is found that large particles $\sim$ 20 μm are also important in determining the visual range. However, the investigation of visibility deterioration for St. Louis measured aerosol size spectra showed that particles in the 0.1 μm to 1.0 μm range only are important. This applies to the urban atmosphere.

2.13 Wavelength Dependence of Visibility

In natural (solar) light the physiological concept of visibility is readily discernable and has been put onto a quantitative basis by Middleton, (1968). The definition of visual range properly takes account of the horizon sky brightness compared with the apparent brightness of a black object in so-called contrast theory. A measuring instrument such as an integrating nephelometer uses an artificial light source and an electronic detector so that strict agreement between visual range estimated by eye and that estimated by the nephelometer

cannot be obtained. The wavelength dependence of visual range is thus important in providing a link between eye and instrumental estimates of visual range. Multiwavelength measurements of light scattering in an atmospheric haze are thus of considerable interest in visibility studies. Such measurements were first made by Ahlquist and Charlson (1969) using a multiwavelength nephelometer. A more comprehensive study was made by Charlson et.al., in 1972. More recently the work of Harrison, (1977c) with a spectronephelometer has shown the extent to which spectral measurements of the aerosol scattering coefficient can be put. A thorough treatment of expected nephelometer response under a variety of atmospheric pollution conditions has been given by Harrison, (1979).

3. EXPERIMENTAL PROGRAMME

3.1 Instrumentation

Several instruments were used throughout the two year period of the investigation. These will now be described in turn.

(a) Particle size spectrometer. This instrument is a Particle Measuring Systems Inc., (Boulder, Colorado), model ASAS-300 (Active Scattering Aerosol Spectrometer) and was calibrated using latex spheres of known diameter and refractive index according to the manufacturers instructions. The calibration aerosol was generated in the laboratory with the aid of a Sierra Instruments, Inc. Fluid Atomization Generator (Model 7330). This utilizes a collision type atomizer to produce the primary aerosol spray from aqueous suspensions of latex particles or from solutions of a low vapour pressure liquid dissolved in a volatile

solvent. The ASAS system, which is based on Mie scattering theory counts aerosol particles passing through a defined volume at the rate of 0.13 cm^3 s^{-1} in the radius interval R = 0.078 to 1.46 μm and sizes them into four ranges, each with fifteen channels of equal width. For clean ambient air the sampling time is about 30 minutes. Only those size spectra were acceptable for which $a(\lambda)$ values were stable during the entire sampling period, thereby ensuring that the particle size distribution did not change during that sampling interval. A microprocessor was attached to the ASAS-300 to calculate $\Delta N/\Delta R$, where ΔN is the particle count in any of the 60 channels and ΔR the radius range of the channel. The $\Delta N/\Delta R$ data was printed out on a teletype and also stored on paper tape which was later transferred to a CDC computer for further analysis.

(b) Spectronephelometer. A nephelometer is an instrument used for measurement of the white light (broad band) scattering coefficient "a" of atmospheric aerosol. By coupling the optical output of a nephelometer to a conventional visible region spectrometer it is possible to measure the differential scattering coefficient $a(\lambda)$. The combination of nephelometer and spectrometer is called a spectronephelometer. Such an instrument has been designed and built at the University of Calgary (Harrison, 1977c) and has been used for part of the work described in this report. The calibration procedure takes account of the truncation error and utilizes pure freon-12 gas ($C Cl_2 F_2$) of 99.9% purity secured from Union Carbide of Canada Ltd., and which has a known scattering coefficient throughout the wavelength region of interest. Facilities exist for flushing the instrument with clean air or aerosol as well as for extracting a small sample of aerosol for particle size analysis. The overall dimensions of the nephelometer section including baffles,

light trap, and scattering chamber are 230 cm x 27 cm x 27 cm. The automatic scanning spectrometer of the Czerny-Turner design equipped with a cooled (-20°C) photomultiplier tube (EMl 9558) records the spectrum of scattered light from 400 to 700 nm.

(c) Multiwavelength nephelometer. This nephelometer was built by Rosalin Pi as part of an M.Sc. thesis project and has been described in detail elsewhere (Rosalin Pi, 1979). It consists of a conventional nephelometer with a rotating filter wheel in front of the photomultiplier detector so that scattered light in one particular wavelength interval only is recorded at any one time. Automatic rotation of the filter wheel synchronously coupled to the time sweep of an automatic signal analyser (Tracor-Northern NS-570) enables long term averaging of the multiwavelength nephelometer output. This is particularly useful when results are to be compared with particulates collected in a high volume sampler over a period of several hours or days. The wavelengths of the filters used in this study were at λ = 398, 467, 557, and 696 nm. In addition a fifth channel employed a broad-band or white light response characteristic determined by the combination of nephelometer light source spectral radiance and photomultiplier spectral responsivity. The spectral response characteristics of the nephelometer in these five spectral channels are given in Figs. 3.1 and 3.2.

(d) Integrating Nephelometer. A commercially available conventional white light integrating nephelometer, the Meteorology Research Incorporated model 1550, was employed in part of the routine monitoring reported here. The MRl 1550 measures the broad-band scattering coefficient "a" of

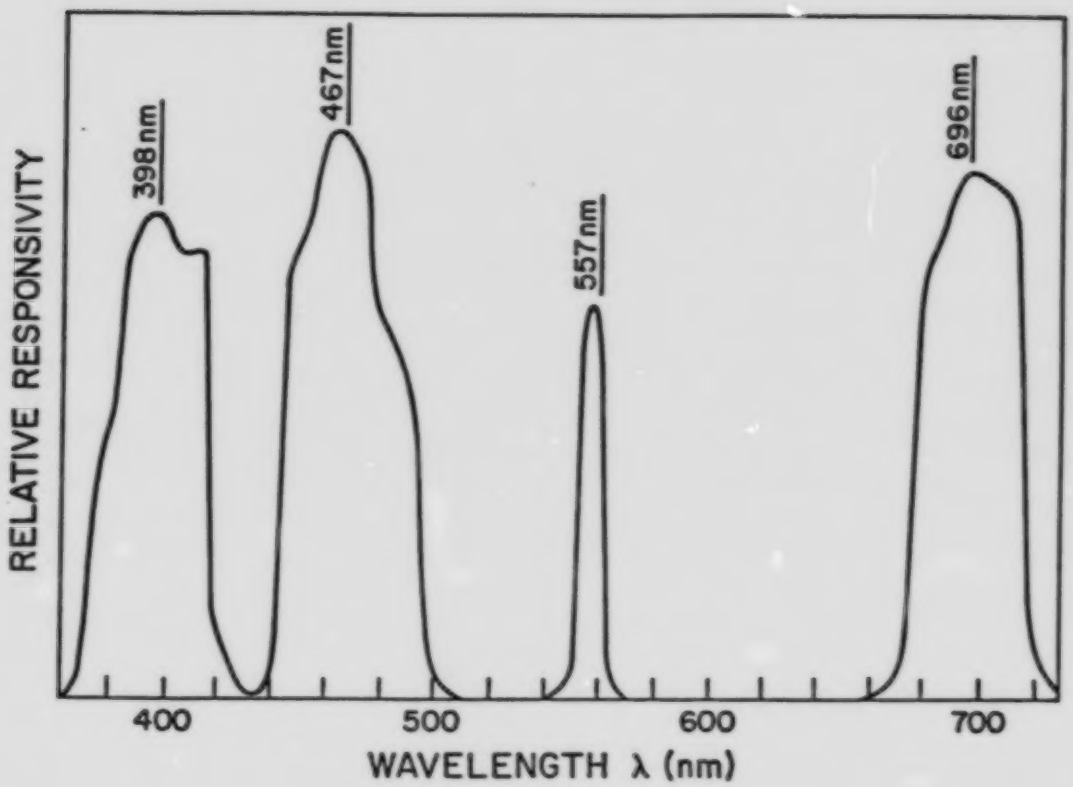

Figure 3.1. Relative response of multiwavelength nephelometer to 398, 467, 557, and 696 nm light.

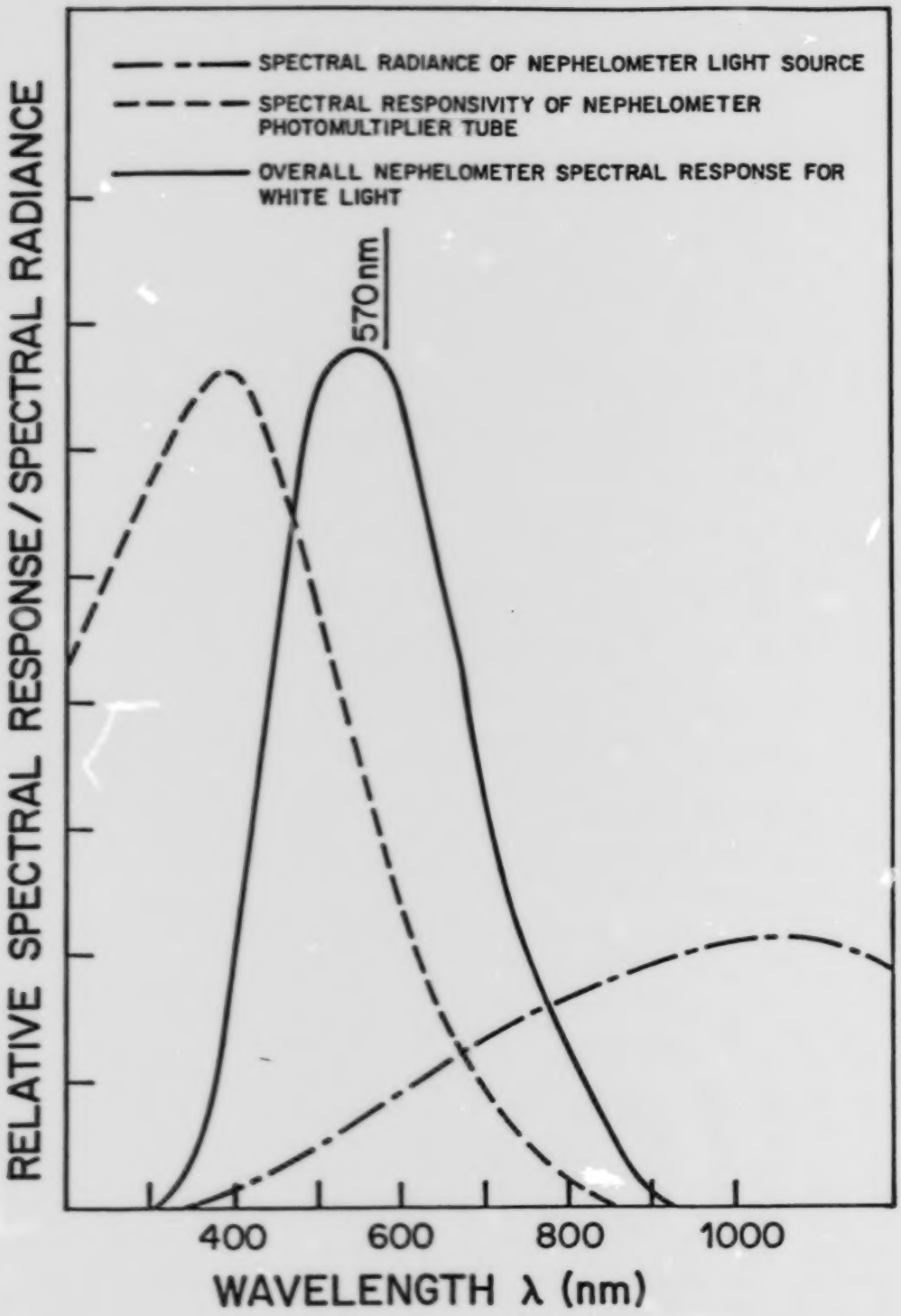

Figure 3.2. Relative response of multiwavelength nephelometer to white light.

ambient aerosol and has an effective wavelength for scattering, $\lambda \sim 480$ nm. Calibration was carried out periodically according to manufacturers instructions. The calibration method is based on the known Rayleigh scattering coefficient for a gas. In this case the gas used was freon-12 for which the volume scattering coefficient is 3.4×10^{-4} m^{-1} at 480 nm, (Harrison, 1977a). Confirmation of the calibration was obtained by comparison of the MRI instrument with the spectronephelometer constructed and operated at the University of Calgary, (Harrison, 1977b). This latter instrument was independently calibrated with laboratory generated monodisperse aerosols for which the volume scattering coefficient can be calculated exactly from Mie scattering theory. Latex hydrosols manufactured by Dow Chemical of Canada, Ltd., were used in this primary calibration procedure. As a result of these calibrations the results given in the report for the integrating nephelometer have an associated standard error of less than 2×10^{-5} m^{-1}.

(e) Andersen Impactor. Two high volume air samplers were used at different times during the monitoring of ambient aerosol described below. One sampler was equipped with a five-stage impactor (Andersen 2000 Inc., Model 65-000) operated at 20 cfm. The aerodynamic equivalent cut-off diameters of the different stages are 7.0, 3.3, 2.0 and 1.1 μm. Gelman type A glass fibre filters were used for collecting the aerosol particulate fractions. Both filters and samples were aged for at least 24 hours in a constant temperature and relative humidity enclosure before weighing on a Mettler microbalance (model H54). Sampling times usually varied between 2 and 7 days. A standard high volume air sampler

was also operated in parallel with the Andersen sampler from time to time as a check on the total mass collected by the latter. In some samples the Andersen impactor gave lower readings by as much as 5% indicating loss of particles to the walls of the impactor.

(f) Acoustic sounder. An Aerovironment model 300 monostatic acoustic sounder has been in operation at the University of Calgary for several years and was made available to this contract for a limited period. A detailed description of the installation and operation of the sounder is given by Hicks et.al. (1977). The acoustic sounder transmits a brief (50 ns) burst of pure tone (1600 Hz) and then receives back scattered signals from various heights as the sound pulse travels upwards. Filtered signal strengths, compensated for range losses, are indicated by shade of blackness on a vertical line as a pen moves over a chart paper. This form of recording quickly reveals the degree of turbulence and the height of turbulent zones. Mathews and Hicks (1979) have shown that an acoustic sounder can provide more information on the development and occurrence of chinooks than is available with conventional measurements. Typical profiles during chinooks indicate a series of descending layers followed by an increase in altitude of the near ground turbulent layer.

(g) Wind direction and wind speed. In general meteorological data was obtained from a variety of sources throughout the two year period of the contract work. These sources included Environment Canada, Alberta Environment (Calgary International Airport and Bonnybrook Meteorological Tower) and the Department of

Geography, University of Calgary. However; in certain specific experiments it was necessary to have on site measurements of wind (speed and direction) and temperature. These were obtained with a Meteorology Research Inc., Mechanical Weather Station, Model 1071, loaned by Alberta Environment.

(h) Temperature and Relative Humidity. For all Andersen impactor, ASAS-300, and nephelometer monitoring at the University of Calgary and in field studies, the ambient temperature and relative humidity were monitored with a Phys-Chemical Research Corp., (New York) Humitemp Model PCRC-11HPT unit. Permanent chart records of both parameters were obtained in the form of voltage readings which could be transposed to T and R.H. through the manufacturer's calibration chart.

3.2 Observing Sites

An outline map of Calgary is shown in Fig. 3.3. Much of the work reported here was carried out on the roof of the Science B building on the University of Calgary campus especially when the less portable instruments had to be employed. Field studies took one of two different forms. Equipment was either set up temporarily at a particular site for a period of several weeks or equipment was mounted in a small van and moved from site to site during the monitoring period. The van was supplied by Alberta Environment and was used as a means of transport to service equipment in the field as well as a "mobile laboratory". The various sites indicated in Fig. 3.3 are,

(a) CRMU (Calgary residential monitoring unit). Operated by Alberta

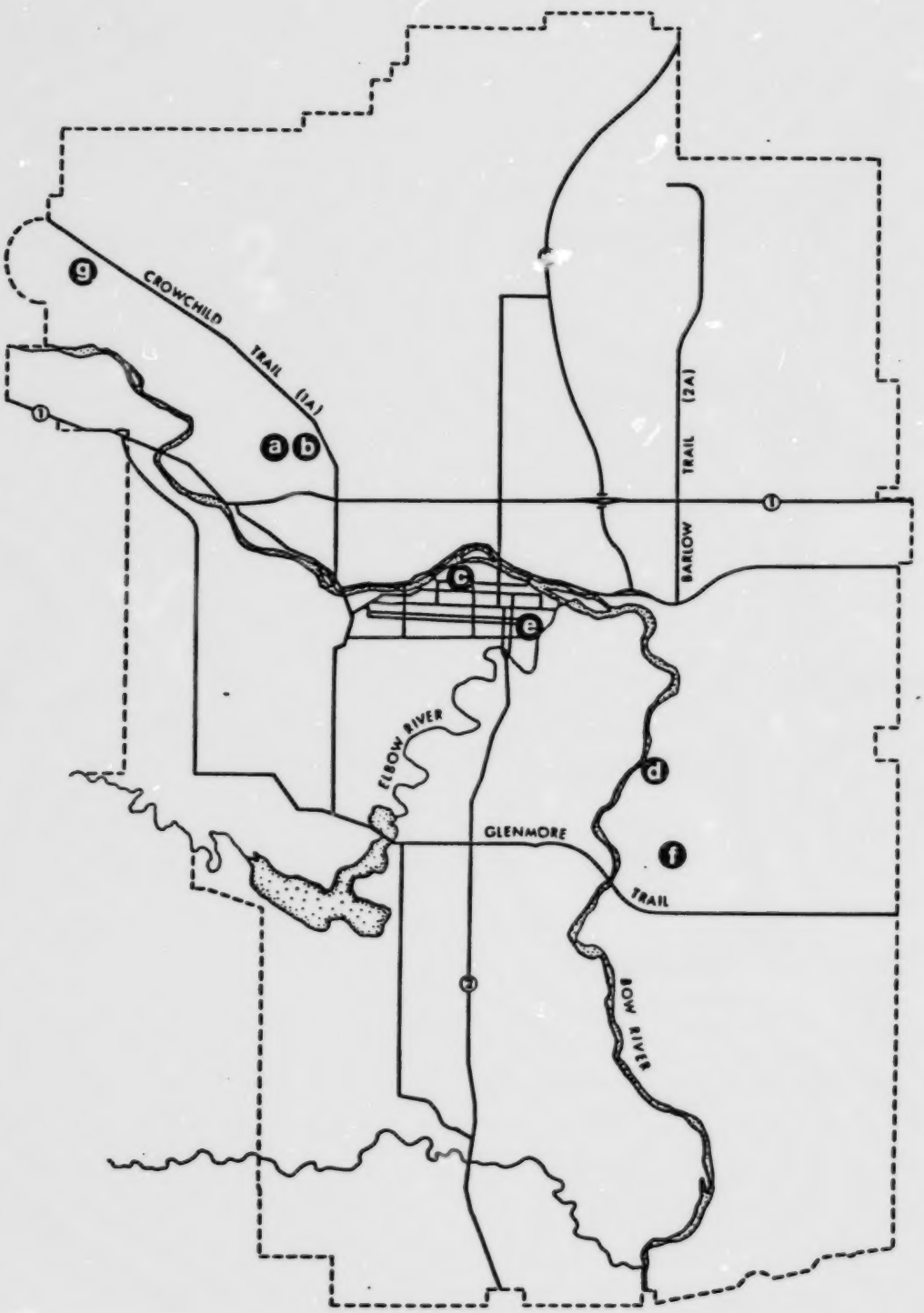

Figure 3.3. Outline map of City of Calgary showing location of observation sites.

Environment, situated on the western edge of the University campus.

(b) Physics Department, University of Calgary. Situated on the roof of the Science B building ∿ 20 m above ground level.

(c) CDMU (Calgary downtown monitoring unit). Operated by Alberta Environment, situated in the John Bowlen building, 7 Ave., S.W., and ∿ 12 m above ground level.

(d) CIMU (Calgary industrial monitoring unit). Operated by Alberta Environment, situated near the Bonnybrook Meteorological Tower in the S.E. Calgary industrial area. The site is at ground level.

(e) Stampede grounds, 17 Ave., S.E., Calgary. This site has been used extensively by Dr. T. Mathews, University of Calgary for the acoustic sounder monitoring of chinook and temperature inversion phenomena. The site is at ground level.

(f) City of Calgary Fire Department, Fire Hall #9, located in S.E. Calgary ∿ 2 km from CIMU and within the Calgary industrial area.

(g) City of Calgary Fire Department, Fire Hall #21, located in the Silver Springs residential district in N.W. Calgary ∿ 5 km from CRMU.

3.3 Observing Programme

An inspection of the Terms of Reference for the work reported here (see page vi) will show how varied and open ended are the topics suggested for investigation. In most cases the planned experiments were contingent upon the prevailing atmospheric conditions so that a large fraction of time and effort were spent in a "waiting" mode for some optimum event to occur. As a result most of the studies were done within a very flexible time schedule. In retrospect it is now possible to give a summary of the equipment used, the observing site

Table 3.1

Summary of experimental programme.

Terms of Reference	Instrumentation	Location	Observing Period
2. Mobile study of particle size distribution.	Particle size spectrometer. Integrating nephelometer. MRI Wind speed/direction. Humitemp PCRC-11HPT.	Fire Hall #9 (S.E. Calgary) Fire Hall #21 (N.W. Calgary)	OCT.-DEC. 1979
3. Visual range and particle size distribution.	Particle size spectrometer. Spectronephelometer. Humitemp PCRC-11HPT.	Physics Department, University of Calgary.	MARCH-JULY 1978
4. Impactor data and particle size distribution.	Particle size spectrometer. Andersen impactor. High volume air sampler. Humitemp PCRC-11HPT.	Physics Department, University of Calgary.	NOV.-DEC. 1978
5. Influence of chinook on particle size distribution.	Acoustic sounder. Integrating nephelometer. Particle size spectrometer.	Stampede grounds. CDMU.	JAN.-FEB. 1979
6. Nephelometer, impactor O_3, COH data.	Integrating nephelometer. CRMU data. Multiwavelength nephelometer. Andersen impactor. High volume air sampler.	Physics Department, University of Calgary.	FEB.-MARCH 1978 JUNE-JULY 1978

employed and the observing period for each of the experimental lines of study suggested in the Terms of Reference #2-6 inclusive. This summary is given in Table 3.1.

4. RESULTS AND EVALUATION

4.1 Mobile study of particle size distribution

Calgary is not a heavy industrial city as such but it does have some light industry in the south-east sector including a fertilizer plant, several ferrous and non-ferrous foundries, concrete, paving and gravel companies and a stockyard. In 1973 Alberta Environment carried out an inventory of air pollution sources in Calgary and concluded that more than 70% of the larger air pollutors were located in S.E. Calgary (Alberta Environment, 1973). In 1978 the City of Calgary commissioned Western Research and Development Corporation to evaluate the air quality in the city. According to the City of Calgary report (1979) the air quality in S.E. Calgary is comparable to that found elsewhere in the city. In connection with these reports it was decided here to investigate both particle size distribution and aerosol scattering coefficient in those spectral regions relevant to visual range. This was done using the particle size spectrometer and the integrating nephelometer (section 3.1). In order to obtain relative measurements of aerosol in the S.E. and N.W. (a purely residential sector of the city), the instruments were mounted inside a small van along with temperature and humidity measuring instrumentation. This mobile unit was then used to monitor the volume scattering coefficient a(480) and the particle size distribution n(R) at the two fire hall

locations in the S.E. and N.W. sectors (sites f and g in Fig. 3.3). This was done by moving the equipment from one location to the other every 2-3 hours. The time taken to move location was approximately 1-2 hours.

During the period October-December 1979 several sequences of S.E.-N.W. observations were obtained. The results are summarized in Table 4.1. Smoke (COH) data from CIMU and CRMU located $\sim$ 2 and 5 km from the S.E. and N.W. fire hall locations respectively is included in Table 4.1 for comparison.

The atmospheric aerosol in the Calgary atmosphere can be represented adequately by the Junge power law distribution or by the lognormal distribution (Harrison and Mathai, 1979). The power law distribution is given by

$$n(R) = c\, R^{-\nu} = \frac{\Delta N}{\Delta R} \qquad [4.1]$$

where c is a constant and ν might have a value between 3.0 and 5 for a typical atmospheric haze, (Bullrich, 1964). In [4.1] N is the total number of particles per unit volume. While ν varies from one aerosol to another; its value serves to characterize a particular aerosol and has been found to vary according to atmospheric conditions in Calgary region, (Mathai, Harrison and Mathews, 1980). In the experiment conducted here the particle size spectrum n(R) was measured in discrete size intervals from R = 0.1 μm to R = 1.0 μm. By plotting log n(R) against log R the Junge power law exponent ν could be derived from each observation made. An example of such a plot is shown in Fig. 4.1 which indicates the size intervals ΔR in which particle concentrations ΔN are obtained. These values of ΔR are characteristic of the particle size spectrometer used

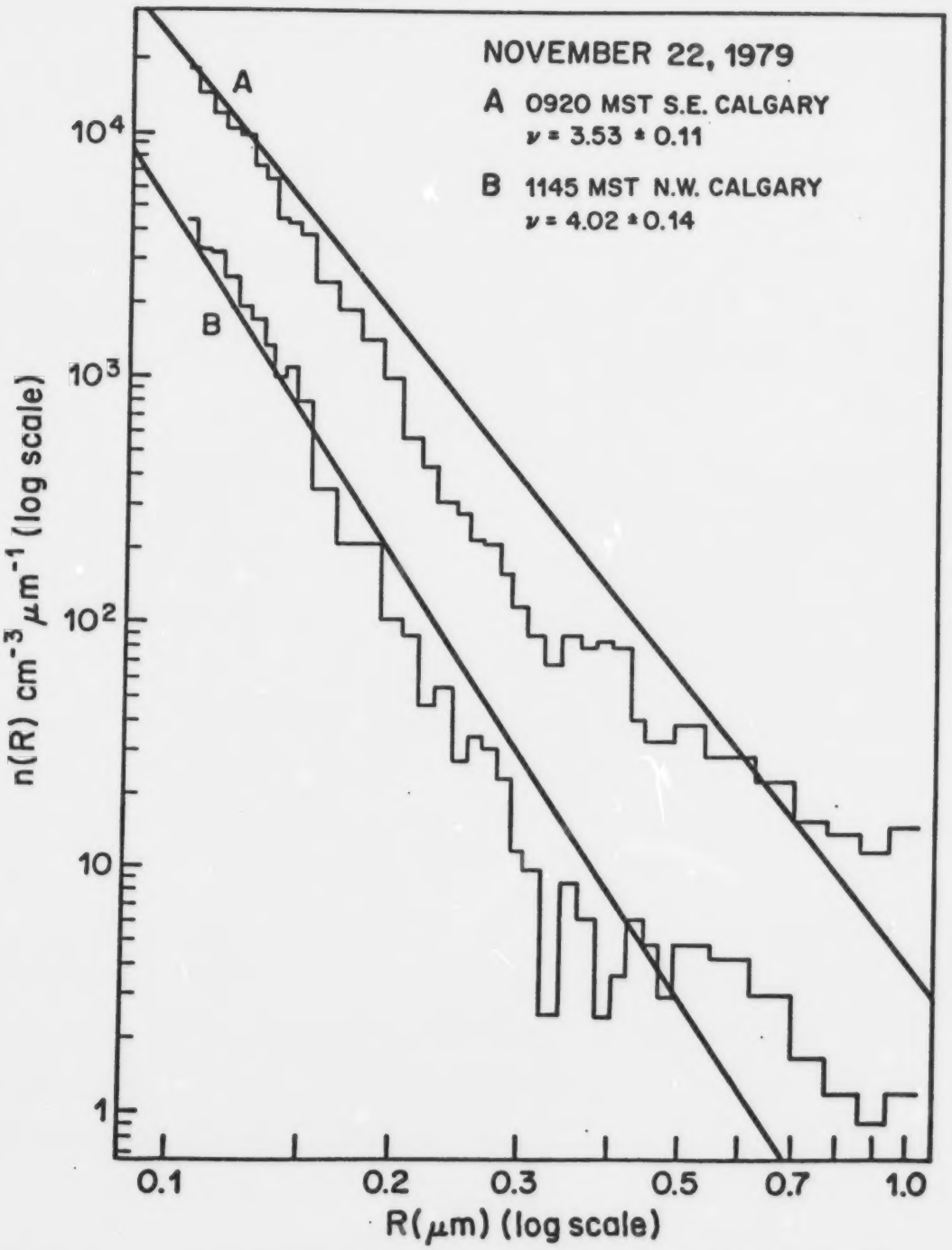

Figure 4.1. Log n(R) versus log R for ambient aerosol in SE and NW Calgary, Nov. 22, 1979.

for the measurements. Values of ν were derived by fitting a straight line to each distribution using the method of least squares best fit. Table 4.1 gives all values obtained for both S.E. and N.E. locations.

An inspection of Table 4.1 shows that even with the 1-2 hour time difference between consecutive S.E. and N.W. observations the particle concentration, n(R) at R = 0.1 μm and at R = 0.5 μm, the scattering coefficient a(480), and the exponent ν all change monotonically in going from one location to the other. The same trend occurs for the COH data recorded at sites very close to the S.E. and N.W. locations. A visual summary of the way in which ν varies between the S.E. and N.W. locations is shown in Fig. 4.2. For all consecutive S.E.-N.W. observations made here it is found that the absolute value of ν(N.W.) is greater than that for ν(S.E.). The difference $\Delta\nu = \nu$(N.W.) - ν(S.E.) is given in Table 4.1 and has an average value 0.49 for these results. Since the standard error for $\Delta\nu$ is less than 0.28 this difference of 0.49 is significant.

A similar comparison of the scattering coefficients for the two locations shows that a(S.E.) > a(N.W.) with mean values of (1.29±0.69) x 10^{-4} m^{-1} and (0.47±0.11) x 10^{-4} m^{-1} for the S.E. and N.W. respectively. The corresponding values of COH are 0.63±0.37 and 0.15±0.08 COH/L.Ft. for S.E. and N.W. respectively. A graphical summary of all a(480) and ν values recorded in this study is given in Fig. 4.3. Relative humidity was monitored to ensure that in general, the scattering coefficients measured by the nephelometer are acceptable.

The results of this transit study indicate that the N.W. sector of Calgary is in general less polluted than the S.E. sector. However, it must be noted that the observations were necessarily limited to one particular time of the year only and the number of observations made was quite small. Evenso, the results do suggest that the absolute

Table 4.1

Summary of mobile unit aerosol data

Date Time (MST)	Site	a(480) $\times 10^4$ m^{-1}	COH (1000 L.Ft.)$^{-1}$	n(R) cm^{-3} μm^{-1} at R = 0.1μm	R = 0.5μm	ν	Δν	R.H. (%)	Wind (km hr^{-1})
Oct. 19									
1120	N.W.	0.62	0.20	6346.0	6.72	-4.32	0.57	82	NW 15
1340	S.E.	2.40	*	31422.4	82.37	-3.75		75	NE 12
Oct. 23									
1020	N.W.	0.30	0.20	817.5	5.36	-3.17	0.14	48	W 15
1330	S.E.	0.60	0.60	2281.2	18.88	-3.03		40	NW 3
Oct. 24									
1145	S.E.	1.20	0.50	6764.7	25.94	-3.51	0.59	50	SW 5
1450	N.W.	0.65	*	4664.2	7.00	-4.10		42	ESE 10
Nov. 21									
1150	S.E.	0.55	0.60	2428.7	11.73	-3.37	0.18	38	W 3
1435	N.W.	0.35	0.10	2786.2	10.10	-3.55	0.54	26	NW 6
1645	S.E.	2.50	1.30	6510.3	54.96	-3.01	0.40	30	W 4
1920	N.W.	0.42	0.20	1229.4	5.54	-3.41		38	NNW 8
Nov. 22									
0715	N.W.	0.40	0.10	1030.1	3.01	-3.68	0.45	47	S 7
0920	S.E.	2.10	1.30	10291.1	38.00	-3.53	0.49	45	SSW 3
1115	N.W.	0.45	0.20	2129.1	3.63	-4.02	0.44	36	SW 6
1235	S.E.	1.30	0.80	6256.5	21.42	-3.58	0.14	28	S 4
1420	N.W.	0.40	0.20	1774.5	1.53	-3.44		24	S 9
Nov. 29									
0715	N.W.	0.60	0.10	4153.8	5.66	-4.16	0.54	72	NW 10
1150	S.E.	1.20	0.90	5928.3	19.22	-3.62	0.06	52	SE 8
1315	N.W.	0.35	0.10	1533.9	4.49	-3.68	0.31	45	WNW 8
1620	S.E.	1.80	0.60	8614.1	41.01	-3.37	0.37	44	N 3
1740	N.W.	0.40	0.20	1606.8	4.27	-3.74		46	NW 10

cont'd.

Table 4.1

Summary of mobile unit aerosol data

Date Time (MST)	Site	a(480) X10^4 m^{-1}	COH (1000 L.Ft.)$^{-1}$	n(R) cm^{-3} μm^{-1} R = 0.1 μm	R = 0.5μm	ν	Δν	R.H. (%)	Wind (km hr^{-1})
Nov. 30									
0840	N.W.	0.55	0.20	1447.8	4.41	-3.66	0.63	42	WNW 15
1030	S.E.	1.40	0.20	2257.4	18.42	-3.03	0.49	42	ENE 14
1240	N.W.	0.40	0.20	601.7	2.27	-3.52	0.43	42	WNW 13
1505	S.E.	0.70	0.30	1786.8	13.43	-3.09	1.32	42	S 3
1755	N.W.	0.60	0.20	2342.9	2.16	-4.41		48	NW 10
Dec. 2									
1120	N.W.	0.45	0.00	3958.9	4.43	-4.27	0.84	70	NW 10
1320	S.E.	0.50	0.20	1438.5	6.27	-3.43		68	S 4
1425	S.E.	0.50	0.20	1345.5	6.93	-3.33	0.82	68	SW 4
1655	N.W.	0.60	0.20	5794.7	9.51	-4.05		68	NW 3

*No data available.

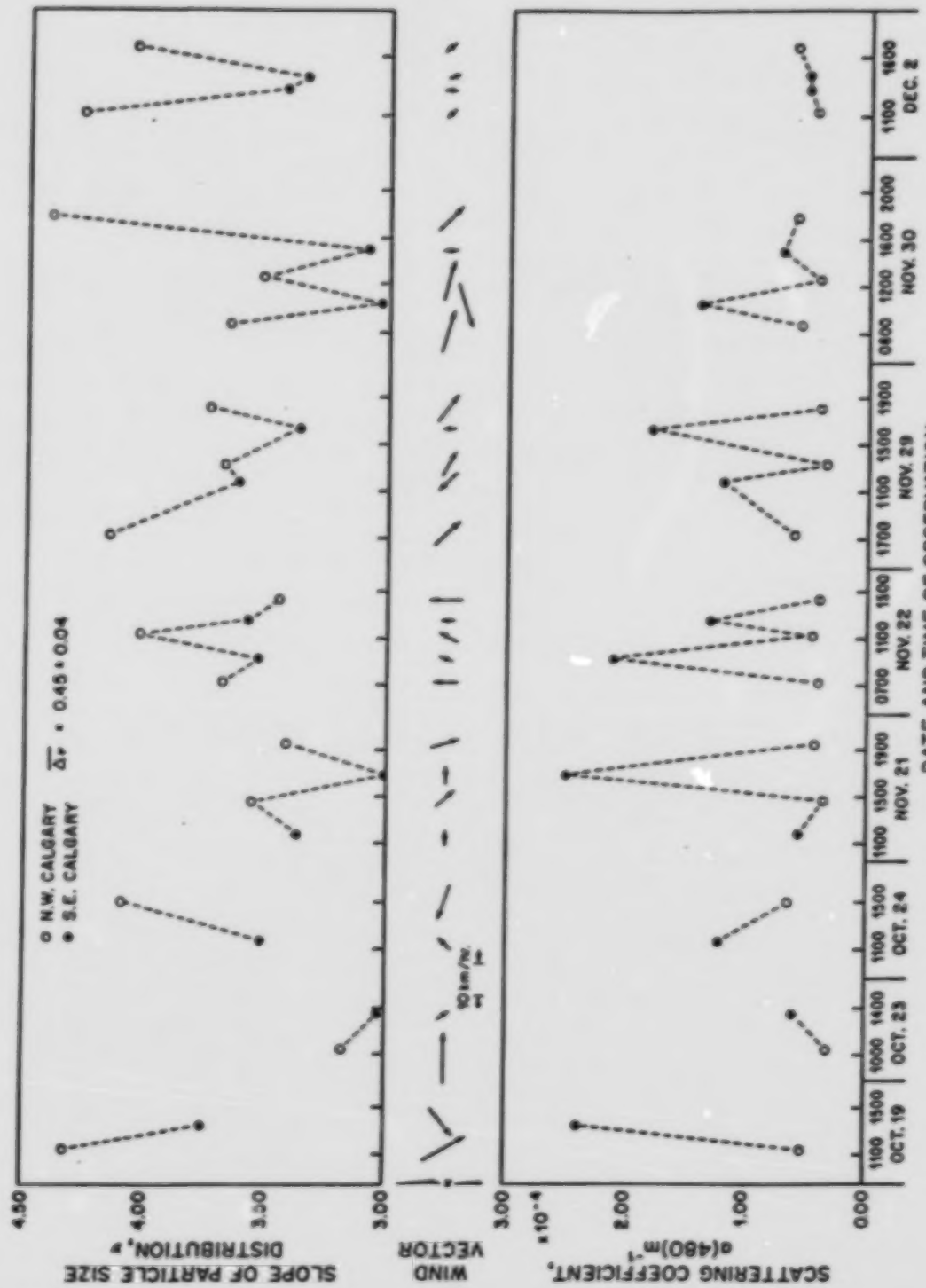

Figure 4.2. Summary of power law exponent ν, wind vector and scattering coefficient σ(480) for the transit study of SE and NW sectors of City of Calgary, October-December, 1979.

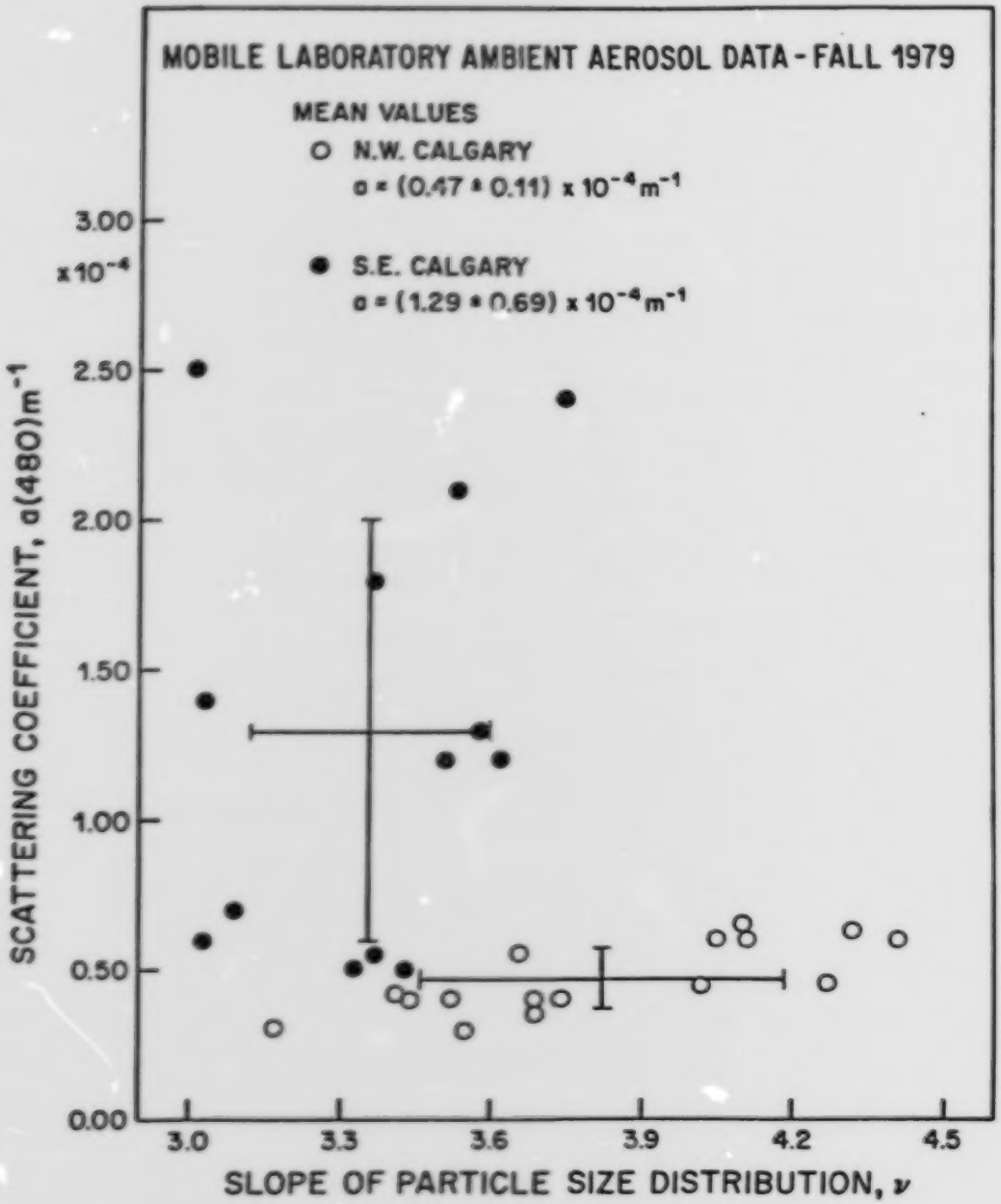

Figure 4.3. Summary all SE and NW sector results for ν and a(480) obtained in the transit study, October-December, 1979.

value of the Junge power law exponent ν is lower for the S.E. aerosol than for the N.W. in the radius size range $R \sim 0.1$ μm to $R \sim 1.0$ μm. In turn this means that the S.E. aerosol contains relatively more larger particles than does the N.W. aerosol. This is evident in the Nov. 22 data shown in Fig. 4.1. If the S.E. sector does contain pollutant sources over and above those normally found in a purely residential area then wind speed and direction over the city should influence the relative values of a(480) and ν found in the N.W. and S.E. sectors. This is indeed the case. On Oct. 23 strong westerly winds maintained both N.W. and S.E. a(480) values at the same relatively low level, characteristic of clean mountain air. On Dec. 2 (Sunday) with no industrial activity in the S.E., again N.W. and S.E. a(480) values are nearly equal. By contrast on other days when the winds are light and of no preferred direction the S.E. sector is more polluted than the N.W. sector.

4.2 Visual range and particle size distribution

The aim of this part of the project was to examine the wavelength dependent aerosol volume differential scattering coefficient $a(\lambda)$ as measured by a spectronephelometer for ambient air, and to relate this to the corresponding aerosol particle size spectrum n(R) as measured by a particle size spectrometer. In the study made here the University of Calgary spectronephelometer and a Particle Measuring Systems Inc., ASAS-300 particle spectrometer were operated on the roof of the Science B building at the University of Calgary in the spring and summer of 1978.

To understand the relationship between the particle size spectrum

and aerosol volume differential scattering coefficient it is necessary to consider some basic elements of Mie scattering theory. The volume differential scattering coefficient for a truly monodisperse aerosol is defined by

$$a(\lambda) = \pi R^2 Q(R,\lambda,m) n \qquad [4.2]$$

where R is the radius of the aerosol particle, n the number per unit volume, and $Q(R,\lambda,m)$ is the Mie scattering efficiency factor (Van de Hulst, 1957). For the case of spherical particles Mie theory can be used to calculate $Q(R,\lambda,m)$, the value of which depends upon particle size R, the refractive index m, and the wavelength of scattered light λ (Kerker 1969). Scattering efficiency factors for selected values of m and relevant ranges of R and λ can be found in the literature (Penndorf, 1958). For a polydisperse aerosol having n(R) particles per unit volume per unit interval of radius the volume differential scattering coefficient is then given by

$$a(\lambda) = \int_0^\infty \pi R^2 Q(R,\lambda,m) n(R) dR \qquad [4.3]$$

Utilization of [4.2] and [4.3] in the calibration of integrating nephelometers or in the analysis of the light scattered in these instruments demands a knowledge of the particle size distribution n(R) as well as the scattering efficiency factor. If $Q(R,\lambda,m)$ is known for the aerosol being studied then these equations can be used to predict the differential scattering coefficient to be expected from a known aerosol distribution, or conversely to derive information on the aerosol particle size distribution from the measured differential volume scattering coefficient.

As mentioned in Sections 2.3 and 4.1 a fairly common aerosol size distribution often found in the lower atmosphere is one which follows

a power law size distribution over the size range $R \sim 0.1$ μm to $R \sim 10$ μm. See [4.1]. In practice particles belonging to such a power law distribution for which $R < 0.1$ μm and $R > 1$ μm give negligible contribution to $a(\lambda)$ in the visible region of the spectrum. Hence the size distribution of a particular aerosol measured within the range $R = 0.1$ to 1.0 μm can be used with the aid of [4.3] to predict the differential scattering coefficient which should result from that aerosol. With the above restrictions imposed on $n(R)$ it is readily shown that [4.3] then leads to

$$a(\lambda) = K\lambda^{-\alpha} \qquad [4.4]$$

where K is a constant and $\alpha = \nu - 3$. The wavelength exponent α is sometimes called the Angström coefficient on account of a similar empirical relationship found by Angström (1929). It follows now that, provided the aerosol being studied has a power law distribution in the size range $R = 0.1$ to 1.0 μm, a measurement of the wavelength dependence of the volume scattering coefficient can be used to calculate the power law size exponent $\bar{\nu}$. In the work reported here the calculated value $\bar{\nu}$ is compared with the measured value ν obtained directly from the ASAS-300 particle size spectra.

Figs. 4.4 to 4.7 inclusive show the measured particle size spectrum $n(R)$ for clean air, light haze, light pollution, and light fog conditions respectively. Figs. 4.8 to 4.11 inclusive give the corresponding measured volume differential scattering coefficient $a(\lambda)$ over the wavelength range $\lambda = 400$ to 700 nm. A least squares straight line fit to both sets of data has been carried out and the straight lines are

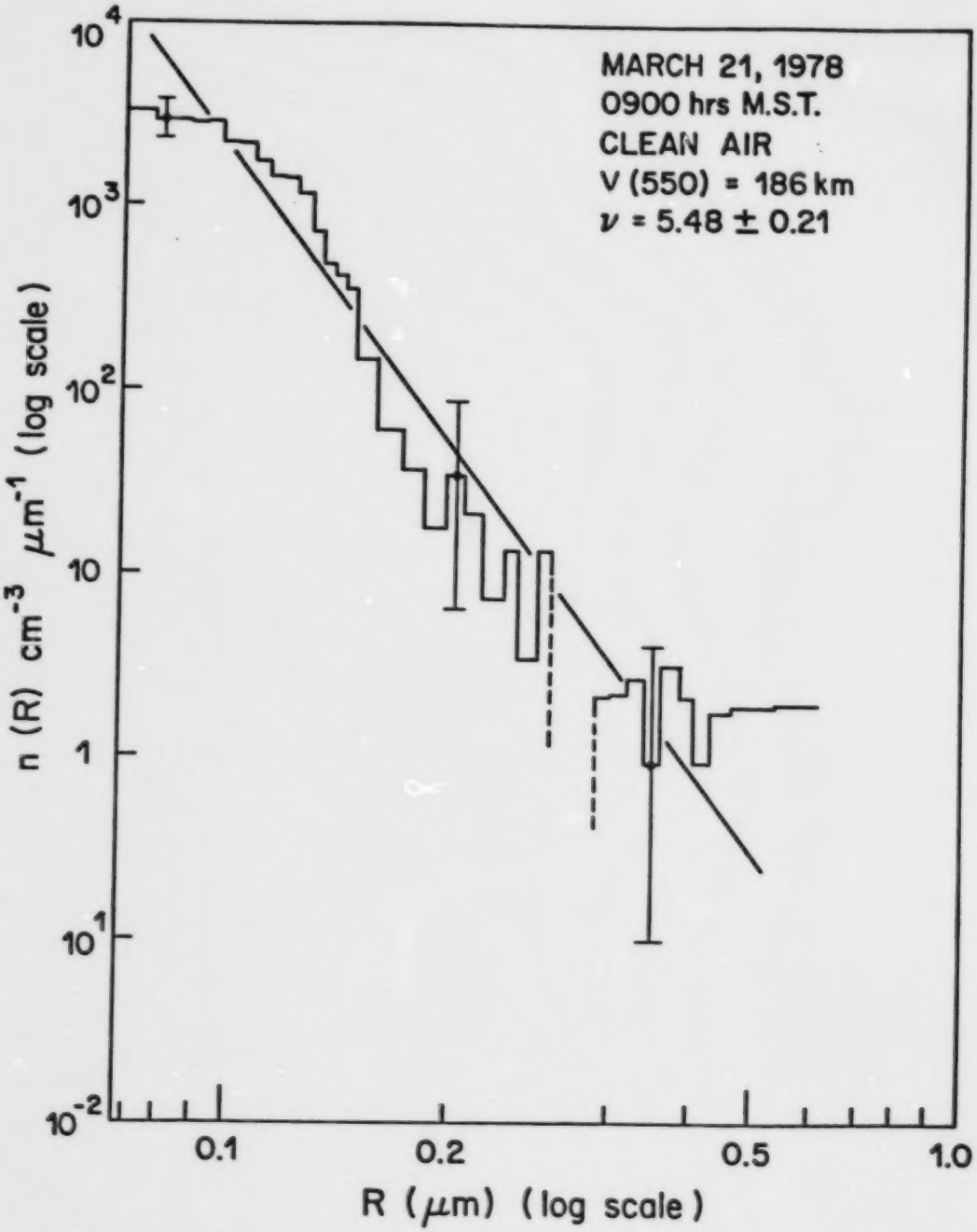

Figure 4.4. Particle size spectrum n(R) versus particle size R for clean air.

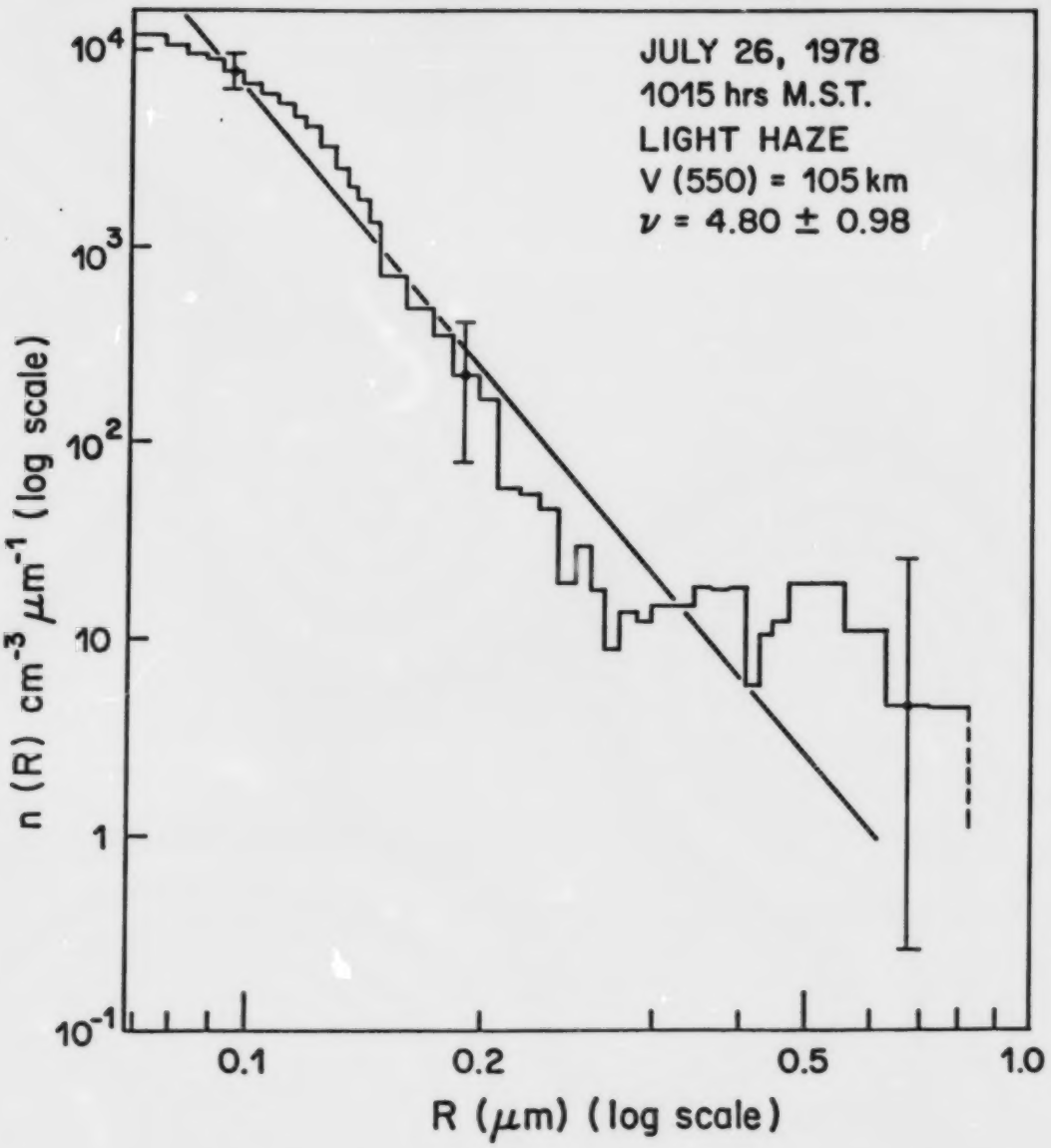

Figure 4.5. Particle size spectrum n(R) versus particle size R for light haze.

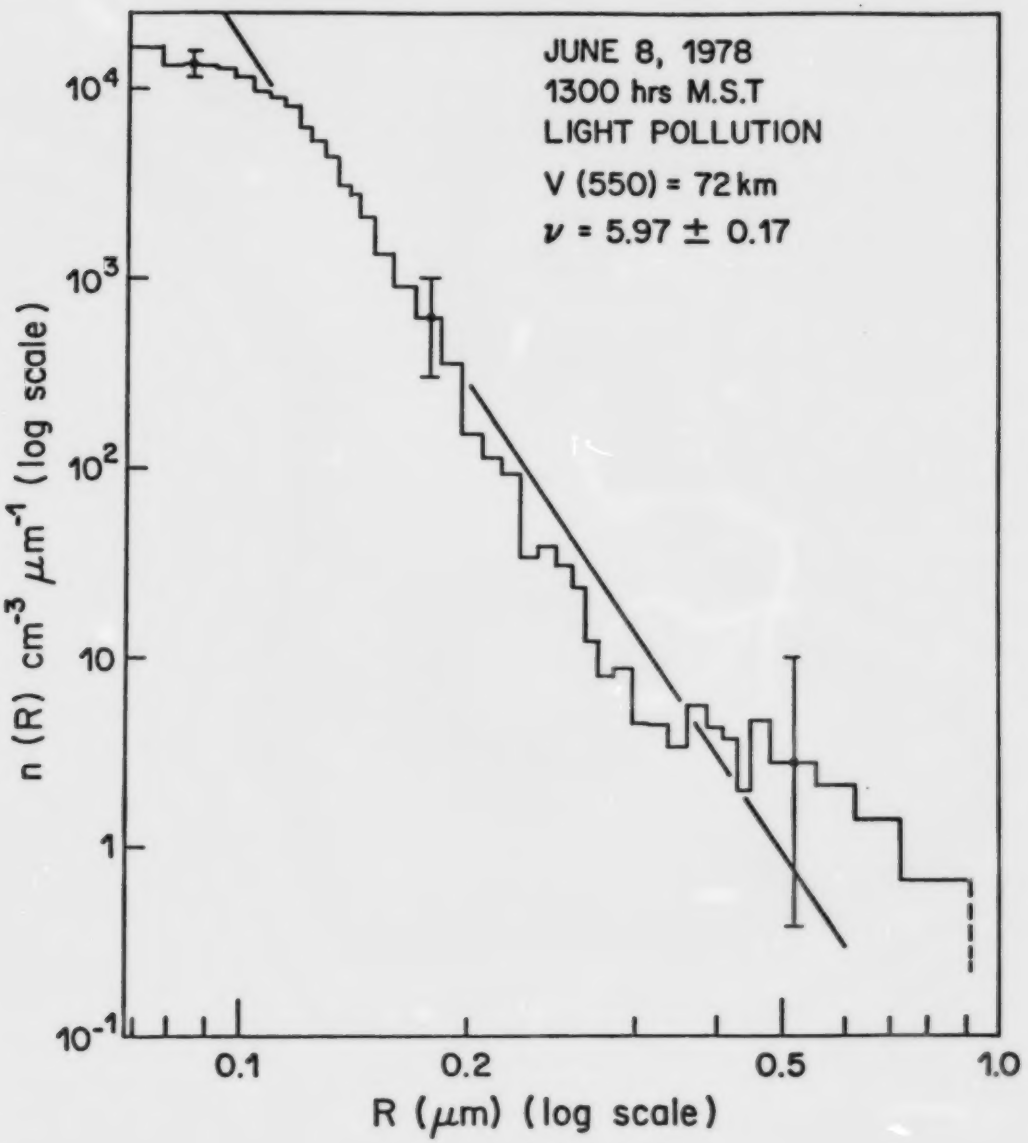

Figure 4.6. Particle size spectrum n(R) versus particle size R for light pollution.

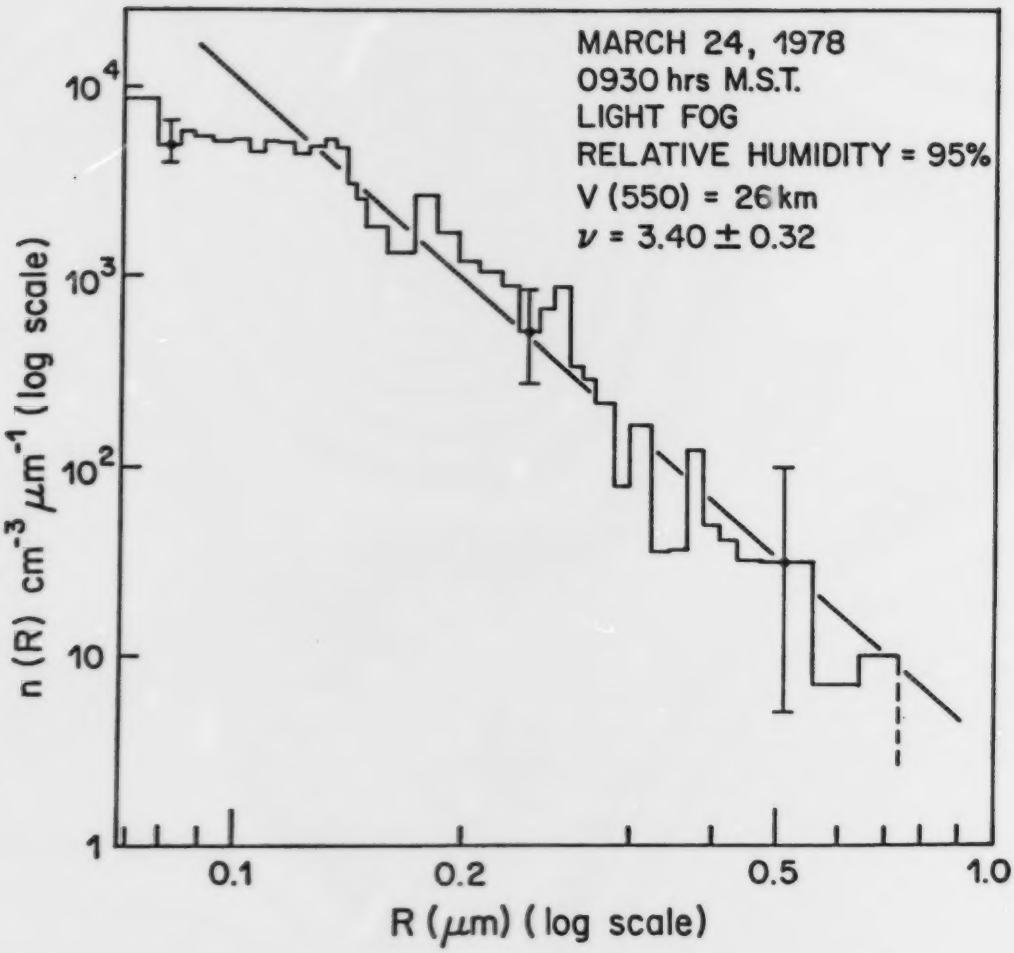

Figure 4.7. Particle size spectrum n(R) versus particle size R for light fog.

shown in the figures. In the case of the n(R) spectra the slopes of the lines give the power law exponent ν which is tabulated in Table 4.2. The Angström exponent α derived from the slope of the straight line fit to the $a(\lambda)$ data has been used to calculate $\bar{\nu}$ which is also given in Table 4.2. For comparison the scattering coefficient for pure air is shown in Figs. 4.8 to 4.11.

The volume scattering coefficient at 550 nm is related to the standard visibility V(550) by

$$V(550) = \frac{3.912}{a(550)} \qquad [4.5]$$

and has been tabulated here for the four atmospheric conditions studied. The visibility varies from 186 km for clean air to 26 km for light fog. A detailed discussion of underlying contrast theory leading to [4.5] as well as the effect of nephelometer characteristics on the measurement of visual range has been given by Harrison, (1979).

The results given in Table 4.2 are not in complete agreement with one another. This can be attributed to, (a) the fact that the underlying Mie theory assumes the ambient aerosol particles to be spherical, which they are not, and (b) the departure of the real particle size spectrum from an ideal power law distribution. In a study carried out by Curcio (1961) the difference between ν and $\bar{\nu}$ for real atmospheric aerosol distributions is of the same relative magnitude as that observed here. The gradual decrease in both ν and $\bar{\nu}$ as n(R) increases is a general characteristic of most natural aerosols and is the reason why the atmosphere appears blue for clean air and white for a very hazy atmosphere. In terms of the scattering coefficient, the

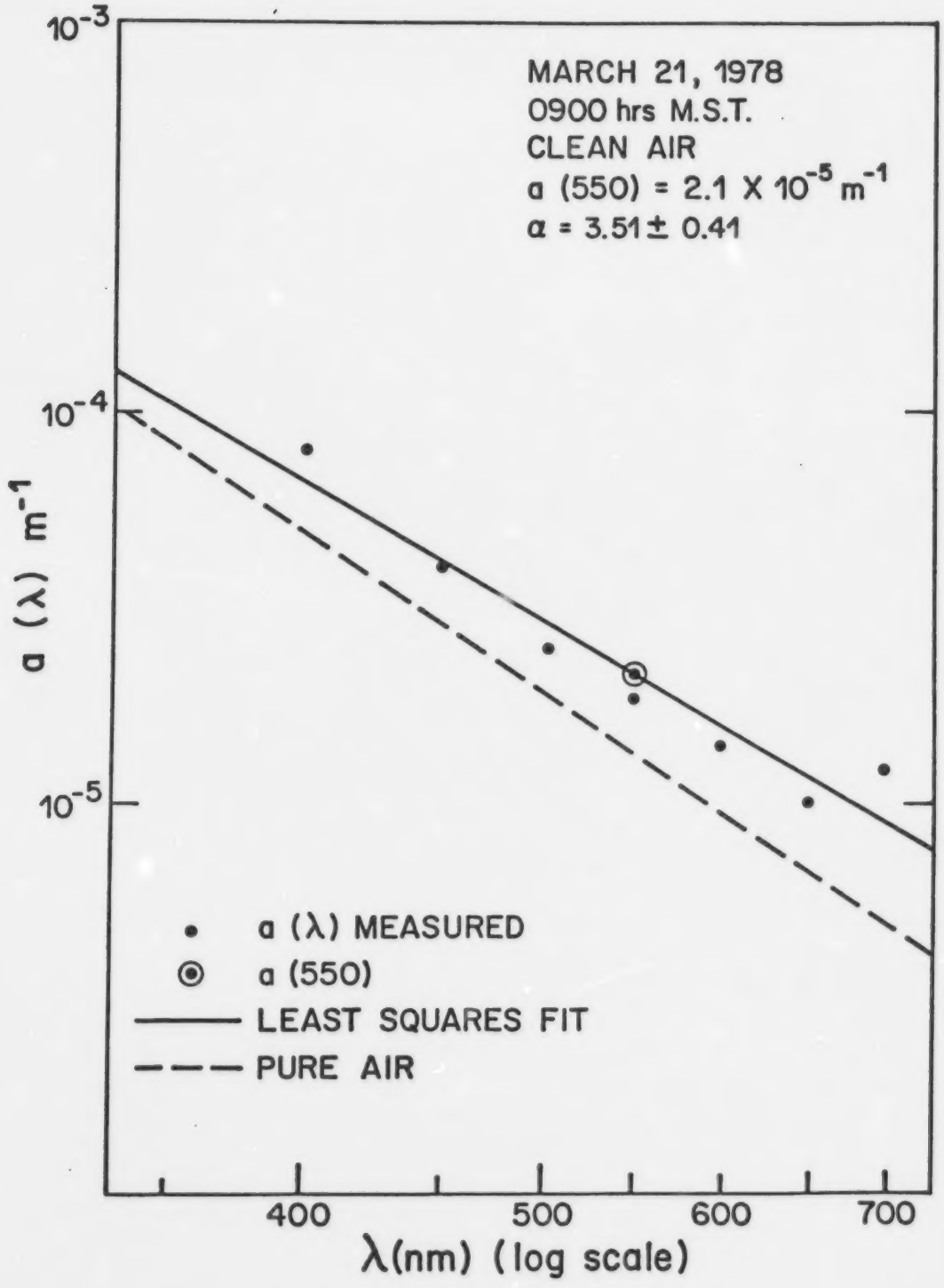

Figure 4.8. Volume differential scattering coefficient a(λ) versus wavelength (λ) for light haze.

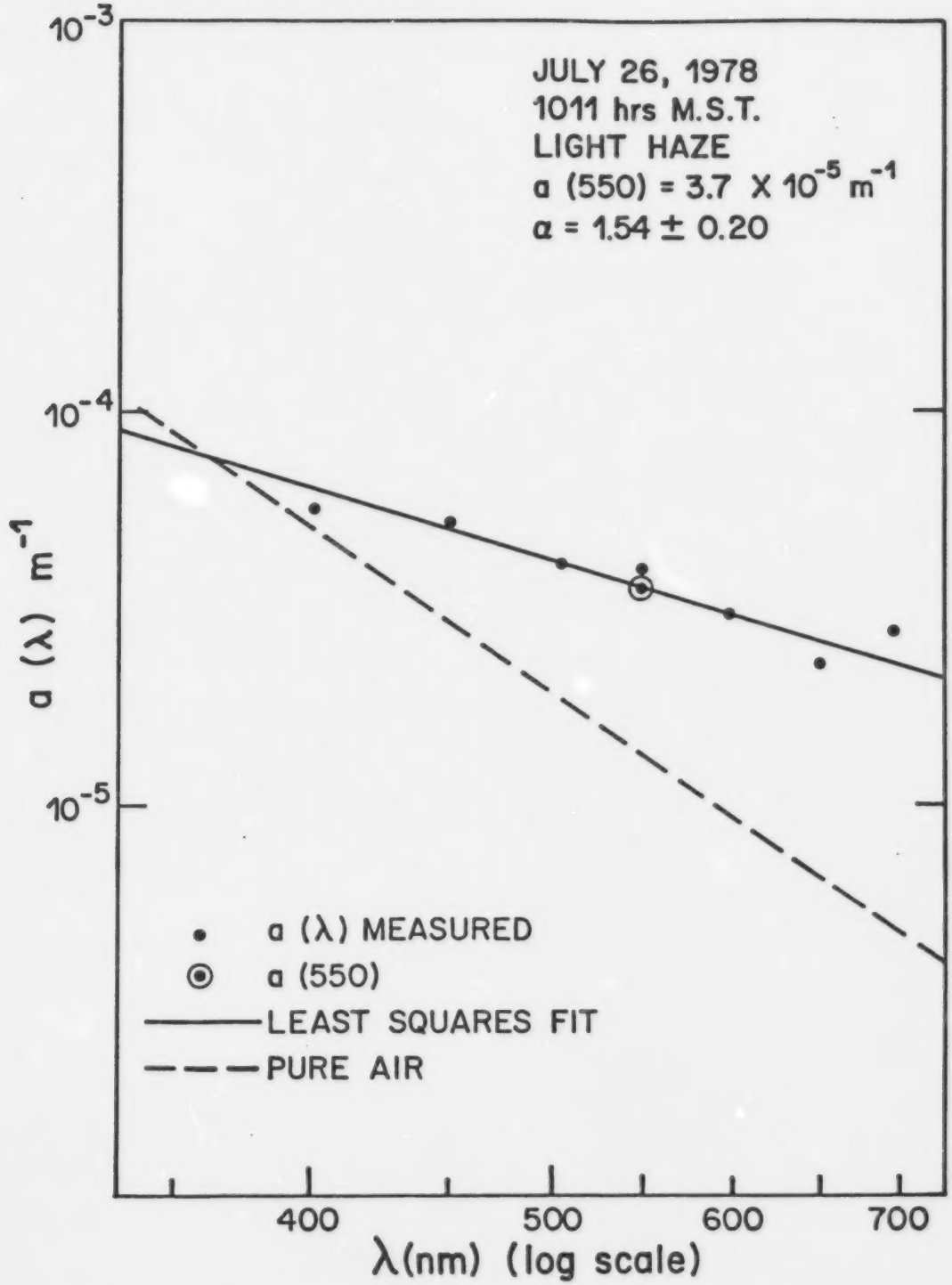

Egure 4.9. Volume differential scattering coefficient a(λ) versus wavelength (λ) for light haze.

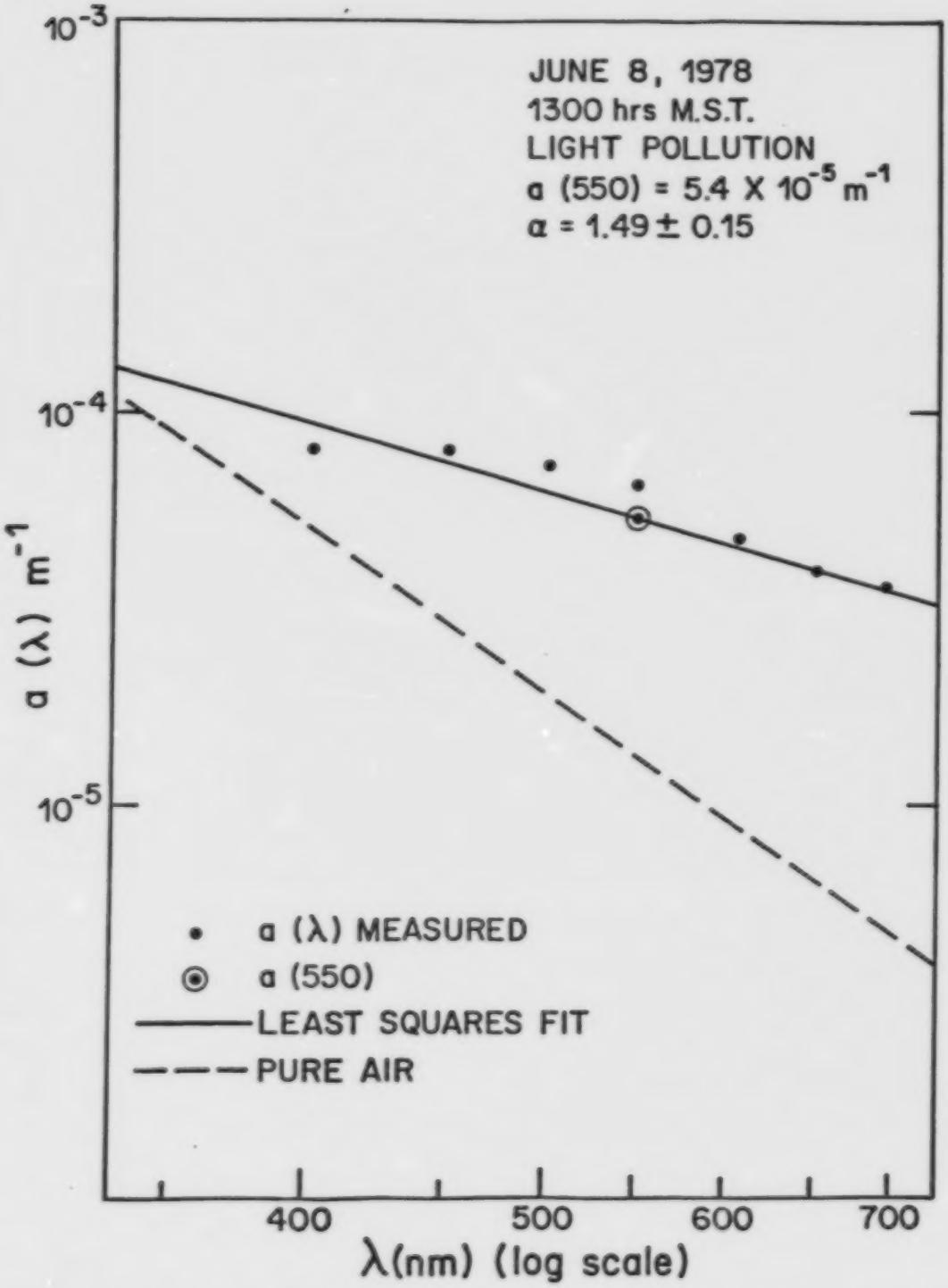

Figure 4.10. Volume differential scattering coefficient a(λ) versus wavelength (λ) for light pollution.

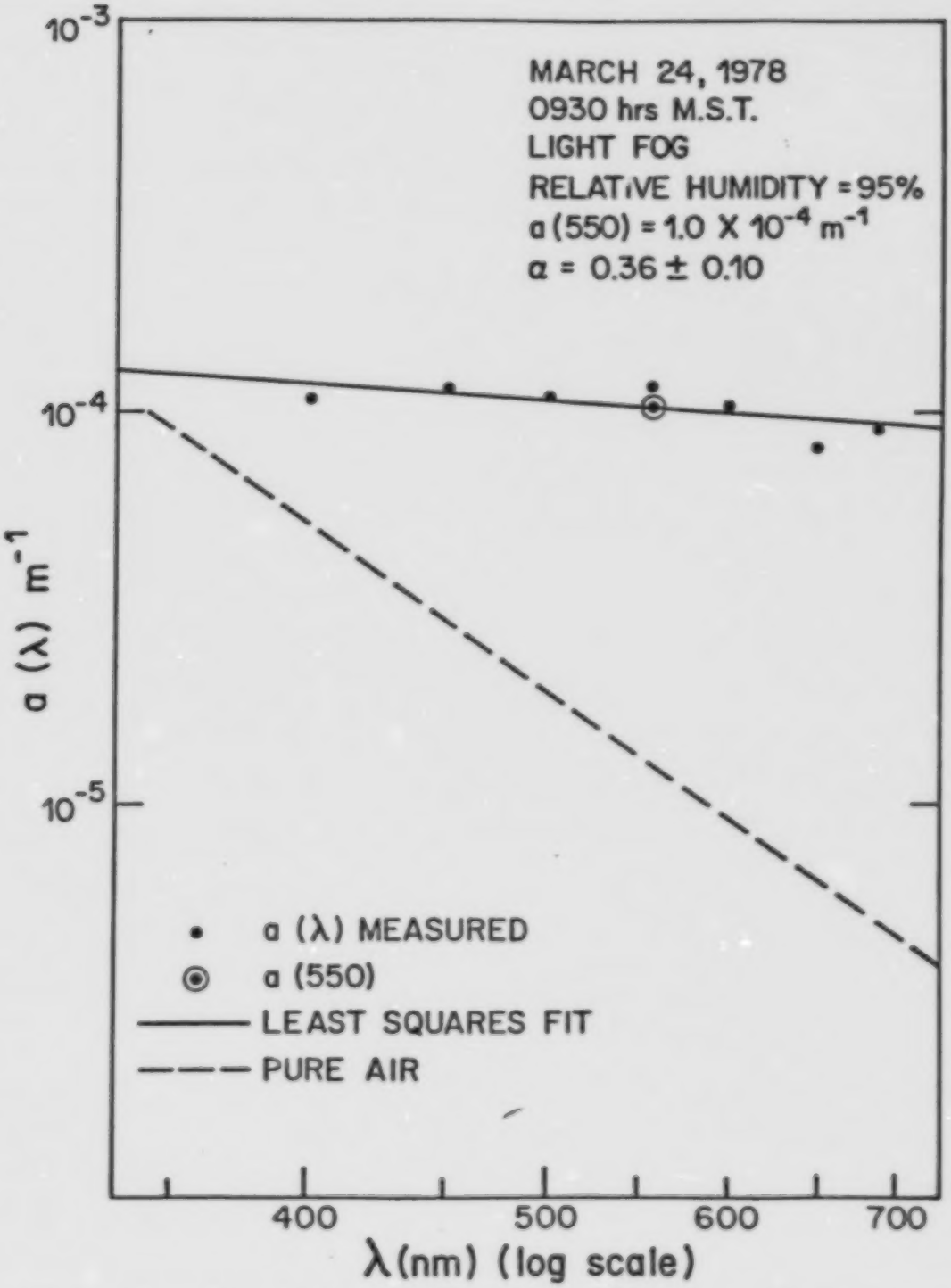

Figure 4.11. Volume differential scattering coefficient a(λ) versus wavelength (λ) for light fog.

air scatters relatively more at longer wavelengths in the latter case than in the former. In conclusion it can be said that for Calgary air the particle size distribution is related to the scattering coefficient and hence to visual range as expected from scattering theory and in accordance with the results of other workers.

Table 4.2

Comparison of measured (ν) and calculated ($\bar{\nu}$) power law exponent with standard visibility V(550).

Atmospheric condition	ν	$\bar{\nu}$	*n(R) cm^{-3} μm^{-1}	V(550) km
Clean air	5.48	6.51	2.1×10^3	186
Light haze	4.80	4.54	6.5×10^3	105
Light pollution	5.97	4.49	1.6×10^4	72
Light fog	3.40	3.36	1.1×10^4	26

*Measured at R = 0.1 μm.

4.3 Impactor data and particle size distribution

In this section a comparison is made between the particle size distribution of ambient aerosol measured with a Particle Measuring Systems, Inc., particle size spectrometer (ASAS-300) and the particle size distribution of the same aerosol deduced from Andersen Impactor data. While the nature of the aerosol size distribution in atmospheric air is known to vary widely with the type of air sampled (Slinn, 1975) many natural aerosols follow a lognormal distribution especially if the source

is singular, (Davies, 1974b). In this study ambient air was sampled by both instruments situated on the roof of the Science B building at the University of Calgary campus. Westerly winds carrying dry mountain air from the Rocky Mountains ensured that urban pollution was directed away from the sampling equipment. Sampling was done during November and December 1978 when the air was particularly cold and dry and when the ground was snow covered with below freezing temperatures. Aerosol particles were collected in the five stages of a model 65-000 Andersen Impactor operated at a flow rate of 20 c.f.m. A high volume air sampler was operated in parallel with the Andersen air sampler as a check on the total mass collected by the latter.

The particle size spectrometer (ASAS-300) was calibrated as described in Section 3.1. Prior to the investigation reported here however, a microprocessor was developed to carry out the $\Delta N/\Delta R$ calculation of particle size distributions and to record that data on paper tape. This was necessary in view of the relatively long sample times needed for the Andersen Impactor. The paper tape data was then transferred to a CDC computer for further analysis.

For a lognormal mass size distribution of aerosol particles.

$$\frac{\Delta M}{M\ \Delta \log D} = \frac{1}{\sqrt{2\pi}\ \log \delta_g} \exp - \left[\frac{(\log D - \log D_m')^2}{2 \log^2 \delta_g} \right] \qquad [4.6]$$

where $\Delta M/M$ is the fractional mass concentration in the log diameter interval $\Delta \log D$, δ_g is the geometric standard deviation and D_m' is the mass median diameter, (Mercer, 1973). When the fractional mass is determined gravimetrically from cascade impactor data, D is the

aerodynamic equivalent diameter and the particles are assumed to be spherical. The corresponding number size distribution is

$$n(R) = \frac{\Delta N}{\Delta R} = \frac{M}{2.3(4/3)\pi R^4 \rho} \left(\frac{\Delta M}{M \, \Delta \log R} \right) \qquad [4.7]$$

where N is the total number of particles, M the total mass concentration, ρ is the average bulk density of aerosol material and R is the particle radius. It should be noted that $\Delta \log D = \Delta \log R$. If log n(R) is plotted against log R then the slope $[=\nu_1]$ of the resulting curve is given by

$$\frac{d}{d\log R}\left[\log n(R)\right] = \frac{d}{d\log R}\left[\log\left(\frac{\Delta M}{M \, \Delta \log R}\right)\right] - 4 \qquad [4.8]$$

On the assumption that the aerosol size distribution is truly lognormal a log-probability plot of cumulative mass percentage less than or equal to a diameter D vs. log D gives a straight line, (Cadle, 1975). From this plot both δ_g and D_m' can be determined thus characterizing the lognormal distribution. An example of this procedure for the data collected November 22-24, 1978 is shown in Fig. 4.12. Having found δ_g and D_m' it then follows that if the value of ρ is either known or assumed [4.6], [4.7] and [4.8] can be used to calculate n(R) and ν_1. In the latter case the equations simplify to

$$\nu_1 = \frac{\log D - \log D_m'}{2.3 \log^2 \delta_g} + 4 \qquad [4.9]$$

A summary of all pertinent results of impactor mass measurements is given in Table 4.3. The mean mass diameter D_m was calculated from

$$\ln D_m = \ln D_m' - 1.5 \ln^2 \delta_g \qquad [4.10]$$

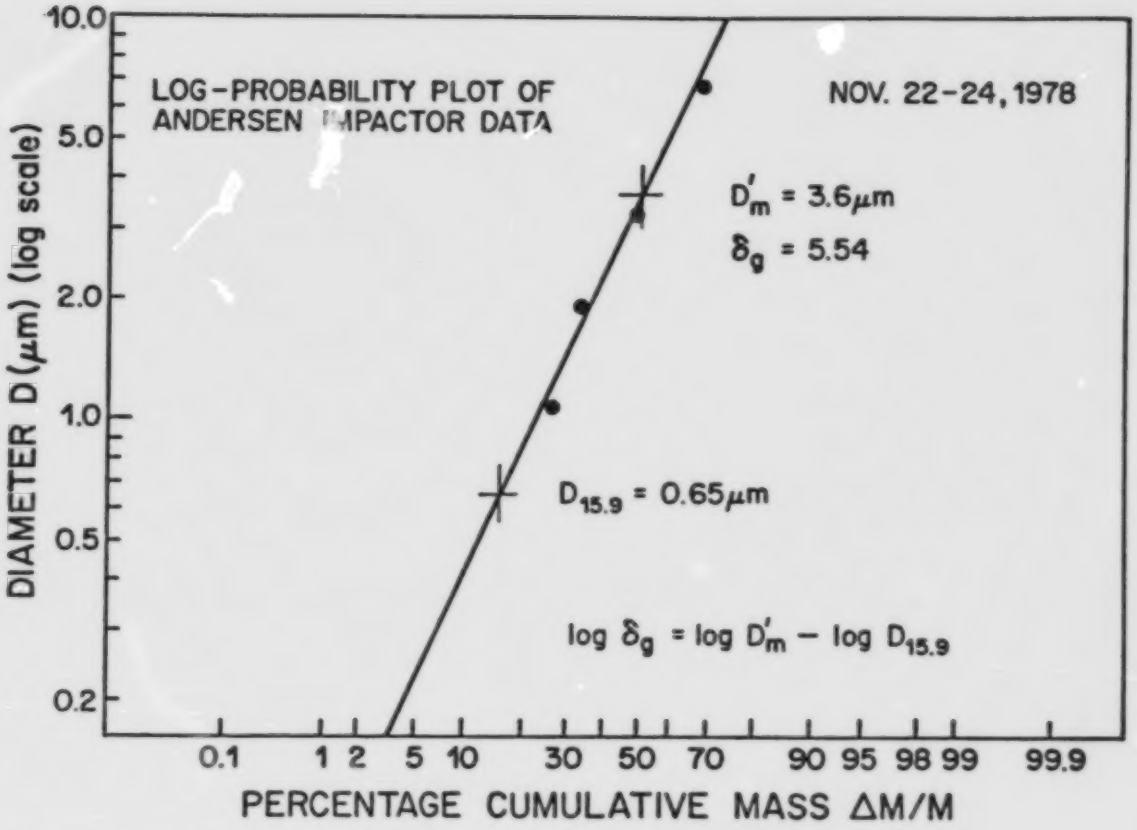

Figure 4.12. Log-probability plot of Andersen impactor data for November 22-24, 1978.

Table 4.3

Summary of Andersen Impactor Data for
University of Calgary Campus, Winter 1978/79.

Period	Total Particulate conc^{n} (μg m^{-3})	% Mass (M) in Dia (D) Range (μm) >7.0	3.3-7.0	2.0-3.3	1.1-2.0	<1.1	M.M.D. D_m' (μm)	Geom. S.D. δ_g	Sample Time (Hrs)
Nov. 22-24	36.00	31.53	18.96	15.92	6.32	27.27	3.6	5.5	51.4
24-27	28.31	22.67	17.26	13.53	11.96	34.46	2.2	5.4	72.4
27-(1)	38.92	33.06	17.77	13.88	7.99	27.30	3.4	6.1	90.3
Dec. 1-4	20.84	18.28	18.26	9.93	10.74	42.79	1.6	6.7	72.5
4-8	37.58	31.15	19.03	12.99	9.12	27.71	3.2	5.8	94.7
11-14	40.60	33.38	18.54	13.42	7.23	27.42	3.5	5.8	74.3
14-17	41.92	31.02	19.59	13.19	8.75	27.45	3.2	5.7	68.0
17-20	57.70	36.79	16.78	10.80	8.53	27.09	3.6	7.3	71.0
Mean	37.73	29.74	18.32	12.96	8.83	30.19	3.0	6.0	

Table 4.3

Summary of Andersen Impactor Data for
University of Calgary Campus, Winter 1978/79.

Period	ΔM/MΔlogD in Dia (D) Range (μm) >7.0	3.3-7.0	2.0-3.3	1.1-2.0	<1.1	ν_1(Calc) at R=0.5μm (lognormal)	ν_2(Meas) From ASAS Spectrum	Mean Mass Dia. D_m (μm)
Nov. 22-24	0.27	0.58	0.73	0.24	0.13	3.56	3.96	4.4×10^{-2}
24-27	0.20	0.53	0.62	0.46	0.17	3.72	4.28	4.6×10^{-4}
27-(1)	0.29	0.54	0.64	0.31	0.13	3.63	3.60	2.6×10^{-2}
Dec. 1-4	0.16	0.56	0.46	0.41	0.21	3.87	4.31	7.3×10^{-3}
4-8	0.27	0.58	0.60	0.35	0.14	3.62	3.99	3.1×10^{-2}
11-14	0.29	0.57	0.62	0.28	0.13	3.60	3.53	3.3×10^{-2}
14-17	0.27	0.60	0.61	0.34	0.13	3.83	3.67	1.8×10^{-2}
17-20	0.32	0.51	0.50	0.33	0.13	3.68	4.21	3.0×10^{-3}
Mean	0.26	0.56	0.60	0.34	0.15	3.69±.10	3.94±.29	2.0×10^{-2}

Point histogram plots of $\Delta M/M\ \Delta \log D$ vs. logD for each of the eight observation periods are given in Figs. 4.13 to 4.20 inclusive. The corresponding log-probability plots of $(\Delta M/M) \times 100$ vs. logD yielded the values of D_m' and δ_g given in Table 4.3 though only one example of these plots (November 22-24, 1978) is shown here (Fig. 4.12). The least squares straight line drawn through the four data points of each log-probability plot represent the lognormal mass distribution which best fits the impactor data. If $D_{15.9}$ and D_m' are the diameters for which the percentage cumulative mass is 15.9% and 50% respectively then

$$\log D_m' = \log \delta_g + \log D_{15.9} \qquad [4.11]$$

for a lognormal distribution. This procedure for finding D_m' and δ_g assumes that the parent aerosol distribution is monomodal. An analysis of aerosols in the Nagoya area showed a bimodal distribution with one mode due to natural sources, the other due to man-made sources, (Kadowaki, 1976). A similar study by Patterson and Wagman, (1977) in the state of New York revealed a near monomodal distribution of $\Delta M/M\Delta \log D$ vs. logD with $D_m' = 7.8$ μm for very clean background air as studied here. It can be concluded therefore that the natural continental and mountain background aerosol sampled here is most likely monomodal. The fact the $\bar{M} = 37.73$ μg m^{-3} shows that the air sampled here was characteristic of continental-background aerosol and relatively devoid of urban pollution.

The lognormal best fit distributions based on the values of D_m' and δ_g in Table 4.3 and calculated from [4.6] are plotted in Figs. 4.13 to 4.20 with the measured point histogram data. The peak of the lognormal or Gaussian curve falls between 1 μm and 4 μm for all eight samples.

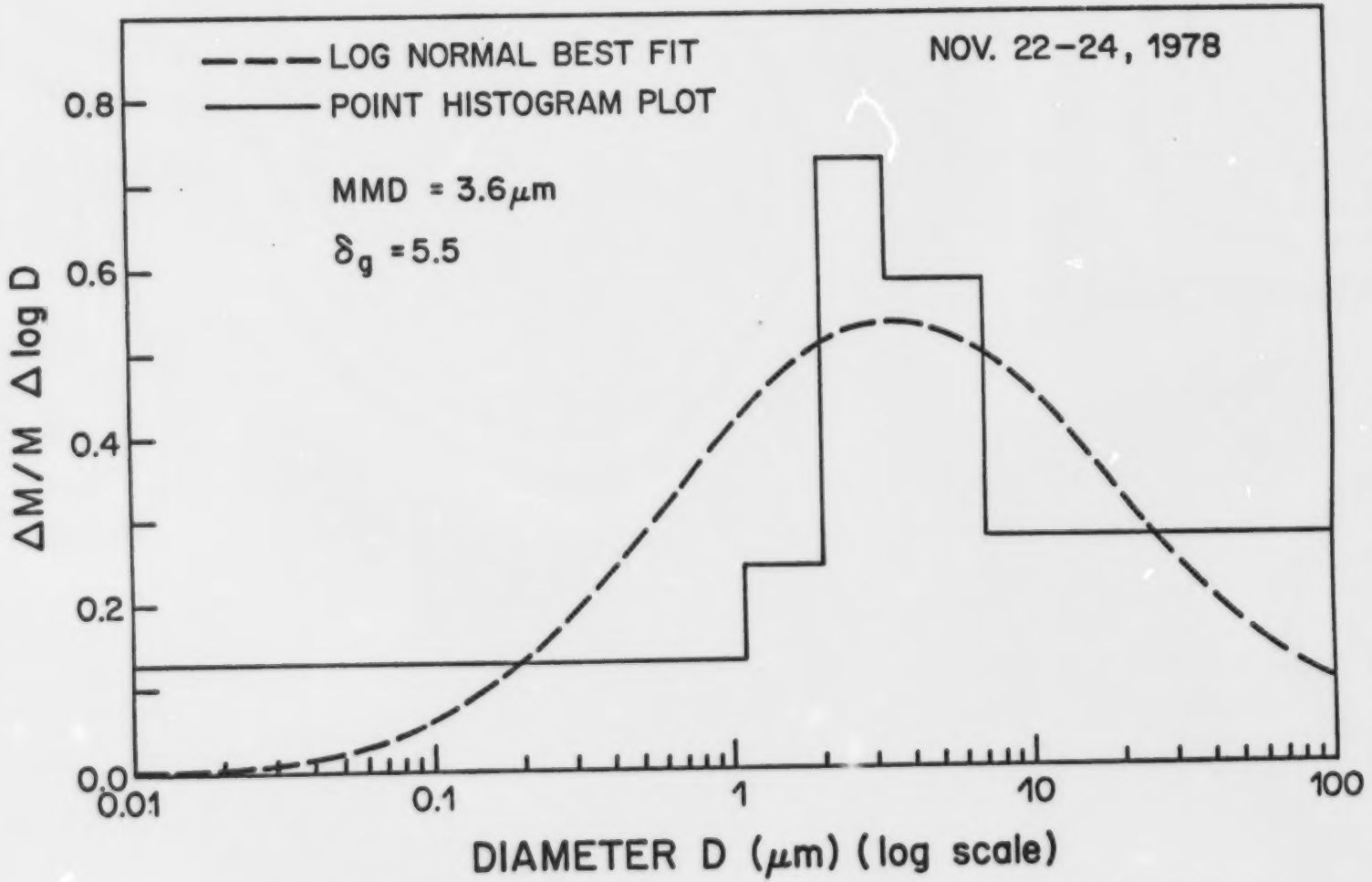

Figure 4.13. Log-normal best fit and point histogram plot of ΔM/MΔlog D versus D for Andersen impactor samples Nov. 22-24, 1978.

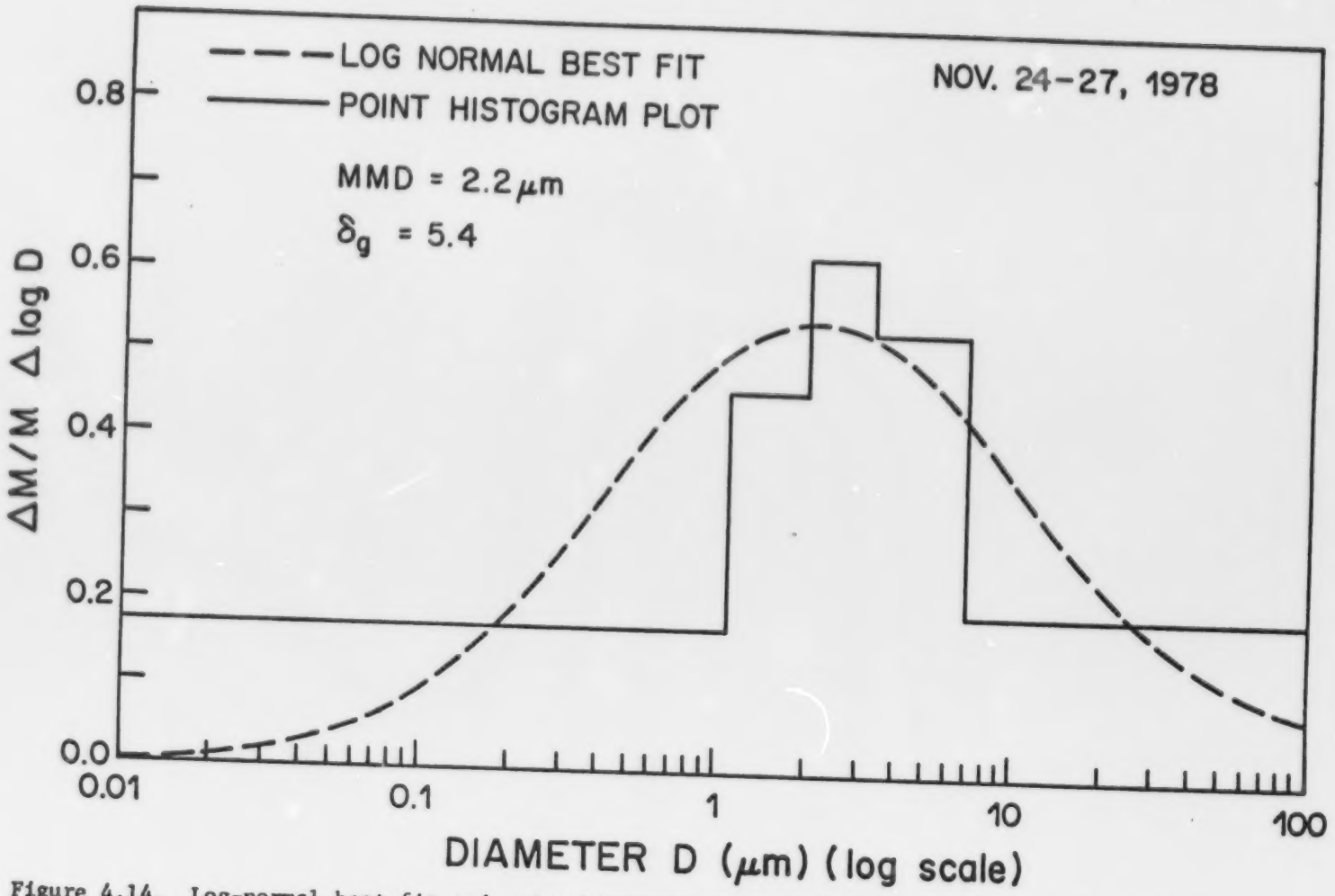

Figure 4.14. Log-normal best fit and point histogram plot of ΔM/MΔlog D versus D for Andersen impactor samples Nov. 24-27, 1978.

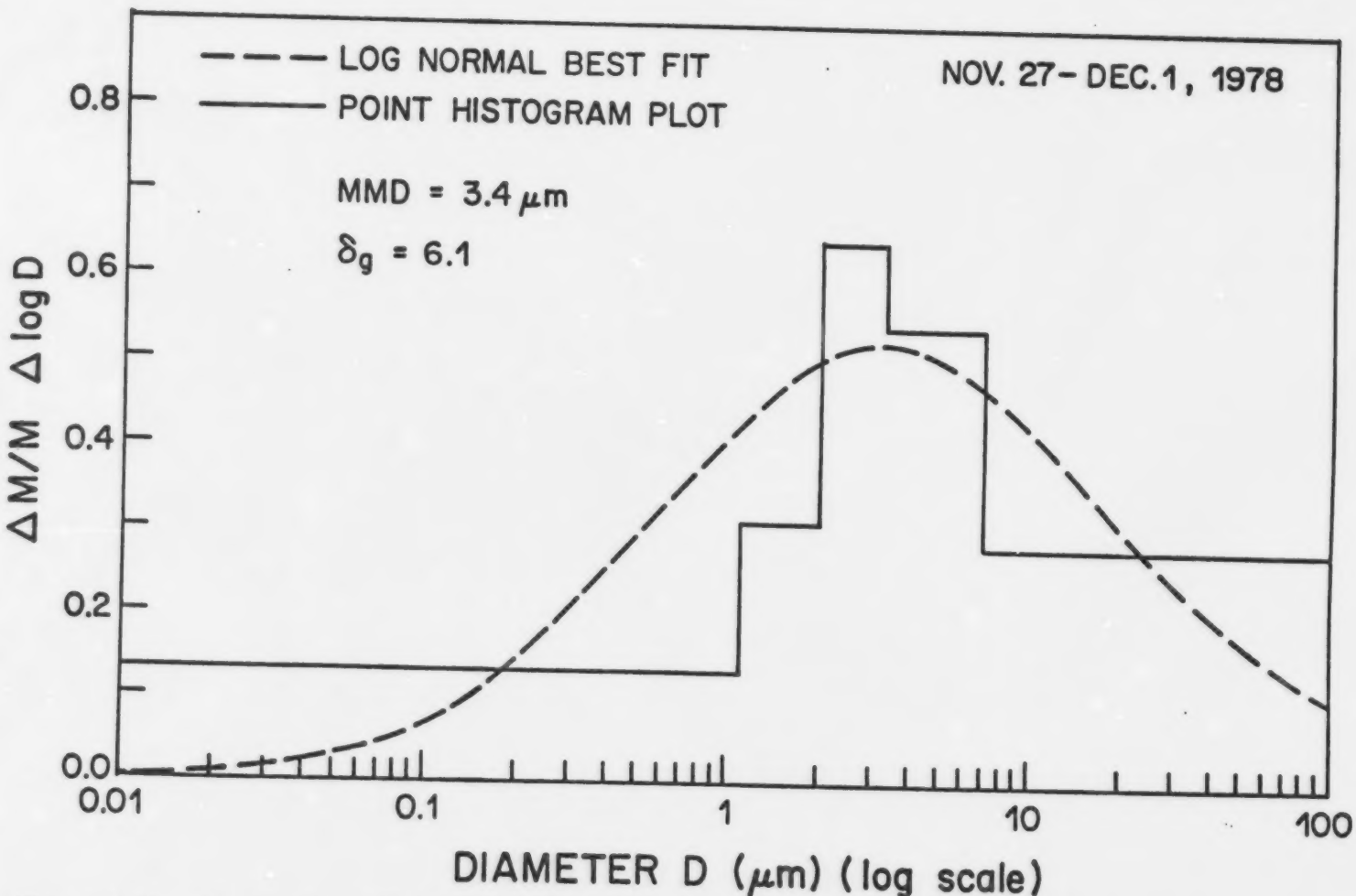

Figure 4.15. Log-normal best fit and point histogram plot of ΔM/MΔlog D versus D for Andersen impactor samples Nov. 27-Dec. 1, 1978.

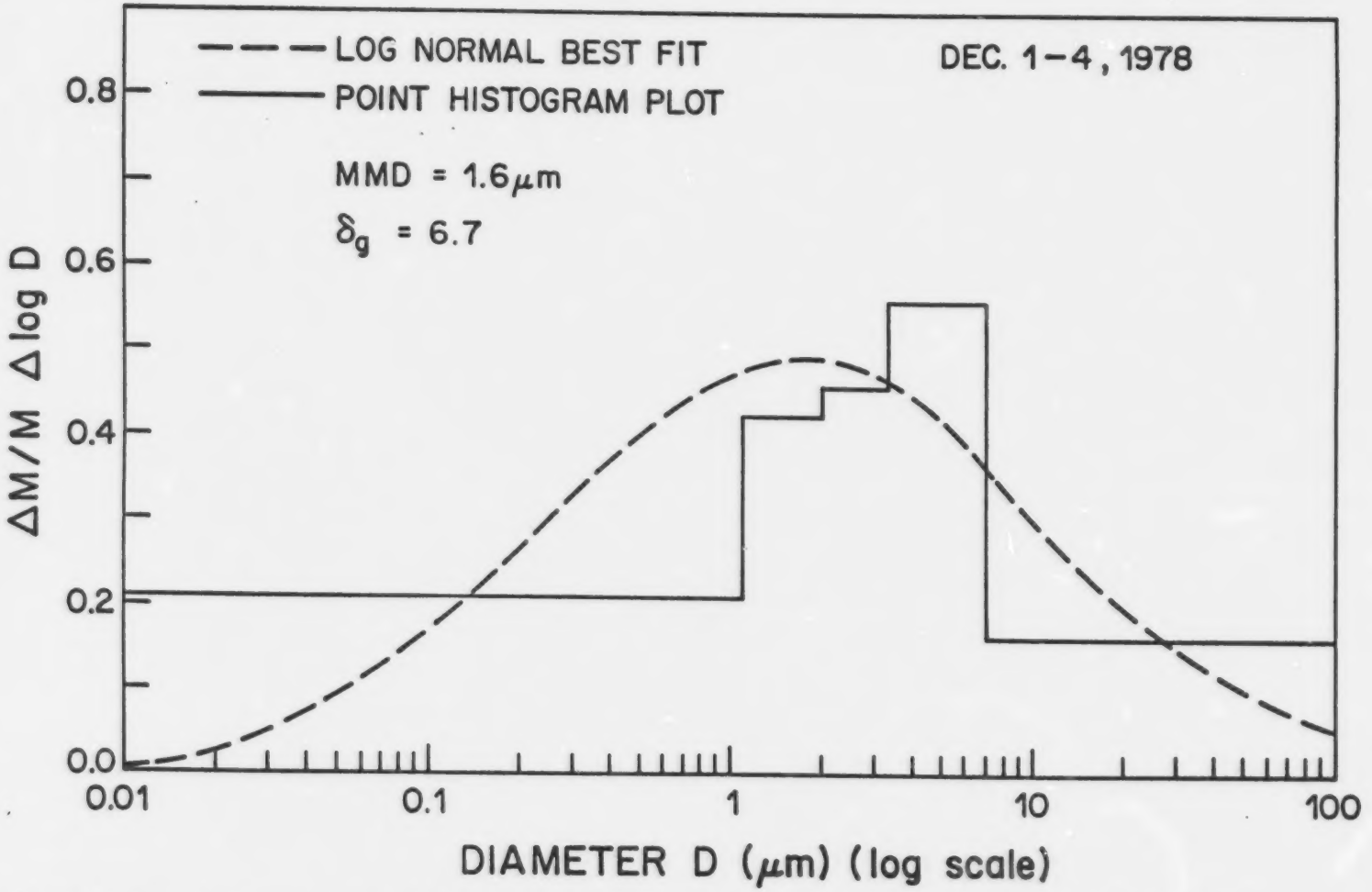

Figure 4.16. Log-normal best fit and point histogram plot of ΔM/MΔlog D versus D for Andersen impactor samples Dec. 1-4, 1978.

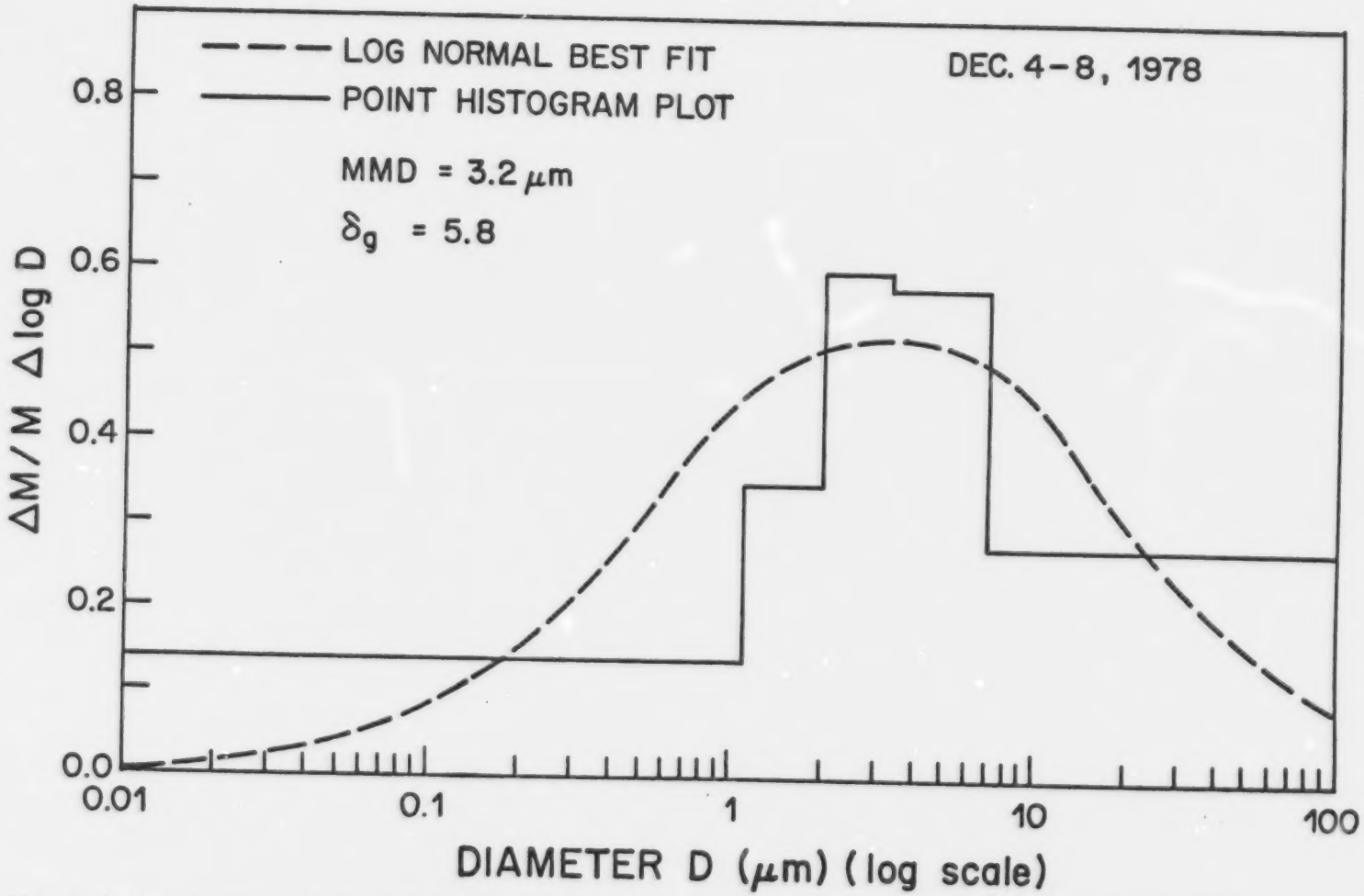

Figure 4.17. Log-normal best fit and point histogram plot of ΔM/MΔlog D versus D for Andersen impactor samples Dec. 4-8, 1978.

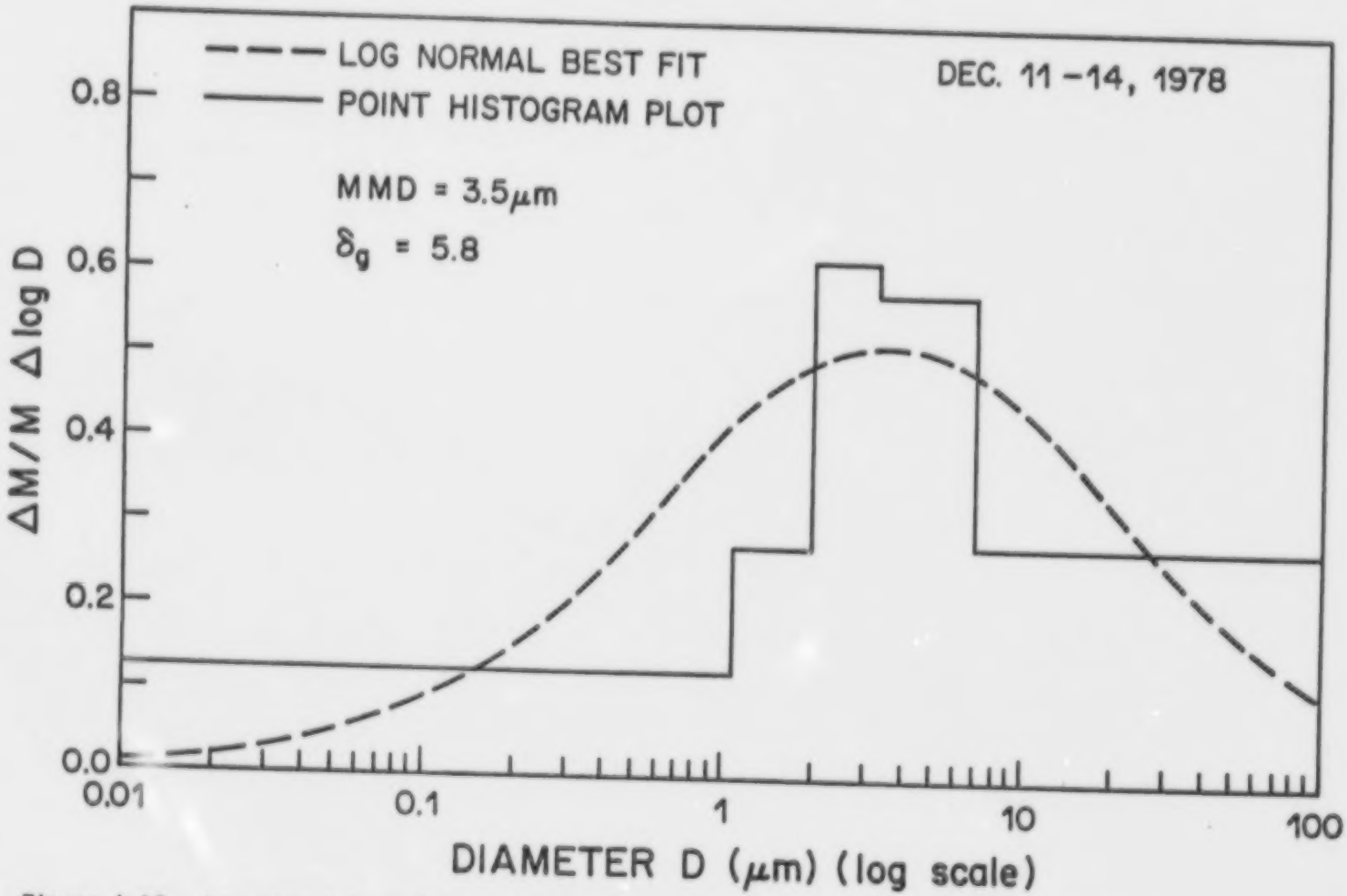

Figure 4.18. Log-normal best fit and point histogram plot of ΔM/MΔlog D versus D for Andersen impactor samples Dec. 11-14, 1978.

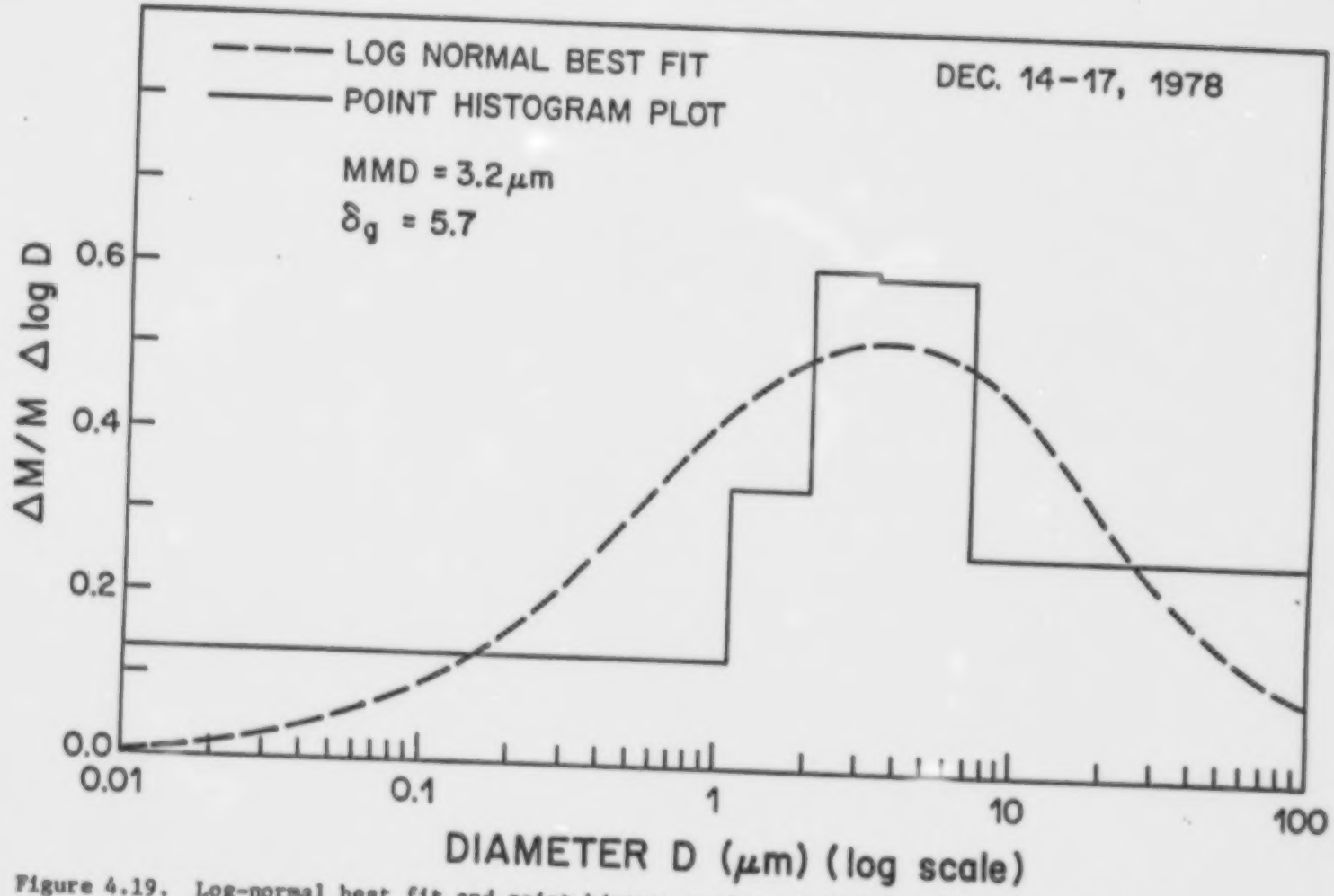

Figure 4.19. Log-normal best fit and point histogram plot of ΔM/MΔlog D versus D for Andersen impactor samples Dec. 14-17, 1978.

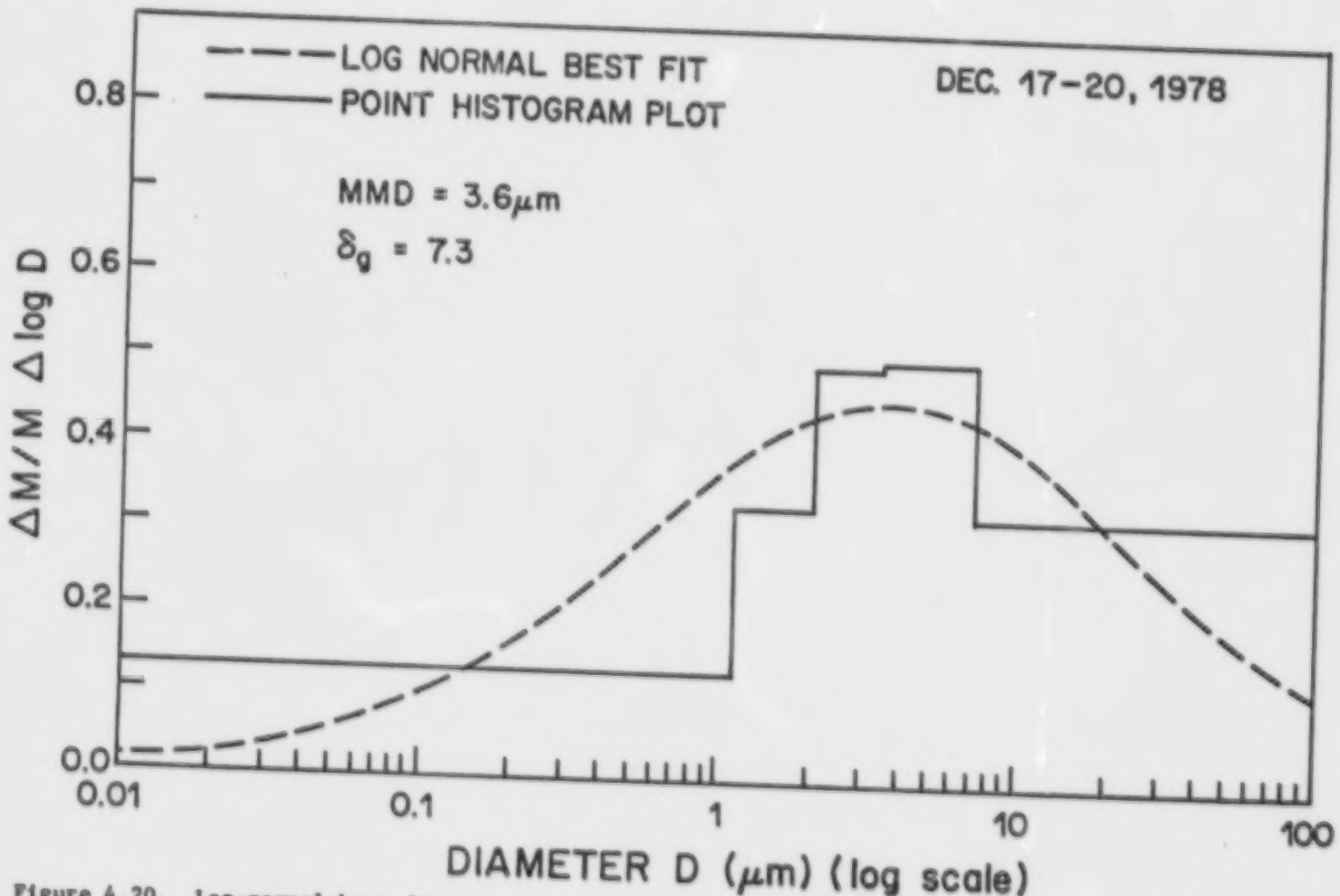

Figure 4.20. Log-normal best fit and point histogram plot of ΔM/MΔlog D versus D for Andersen impactor samples Dec. 17-20, 1978.

Having determined the values of D_m' and δ_g for each impactor sample, [4.6] and [4.8] were used to calculate n(R) for the lognormal distribution and for R = 0.07μm to R = 1.5μm. In this calculation the aerosol density was assumed to be 1.5 g cm^{-3}. The results of these calculations are shown in the plots of log n(R) vs log R in Figs. 4.21 to 4.28 inclusive. The slope (ν_1) for each of these derived lognormal distributions was calculated from [4.9] for D = 1.0 μm (i.e. R = 0.5 μm) and is given in Table 4.3. It is clear from Figs. 4.21 to 4.28 that the slope ν_1 is almost constant over the range of particle size of interest here. A full discussion of the underlying reasons for this behaviour of ν_1 is given by Harrison and Mathai, (1979).

For each of the eight sampling periods studied an average particle number size distribution was measured directly with the ASAS-300 spectrometer. These results are given in histogram form in Figs. 4.21 to 4.28. The different size intervals ΔlogR arise from instrumental characteristics. A least squares best fit straight line to each histogram is also shown and the corresponding slopes ν_2 are given in Table 4.3.

The values of ν_1 and ν_2 are all in the range 3.6 to 4.3 which is to be expected for continental and mountain aerosols in this size range, (Davies, 1974). The fact that there is no significant difference between ν_1 and ν_2 suggests that the Andersen impactor and particle spectrometer give mutually consistent results for the parent particle size distribution i.e. one instrument validates the other. The result that in all cases n(R) derived from impactor data > n(R) measured by

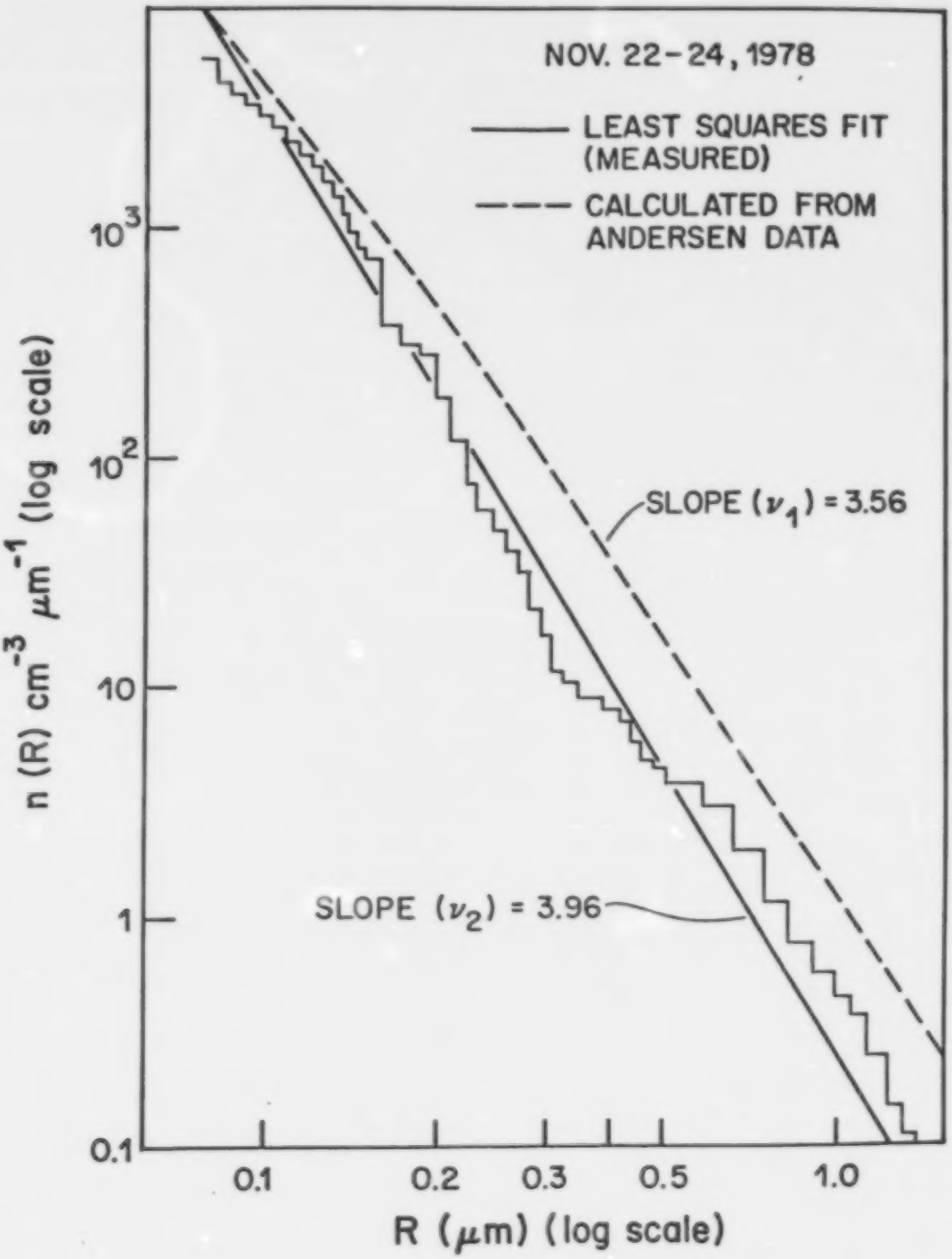

Figure 4.21. Particle size spectrum n(R) calculated from Andersen impactor data and measured by ASAS-300 versus R for samples Nov. 22-24, 1978.

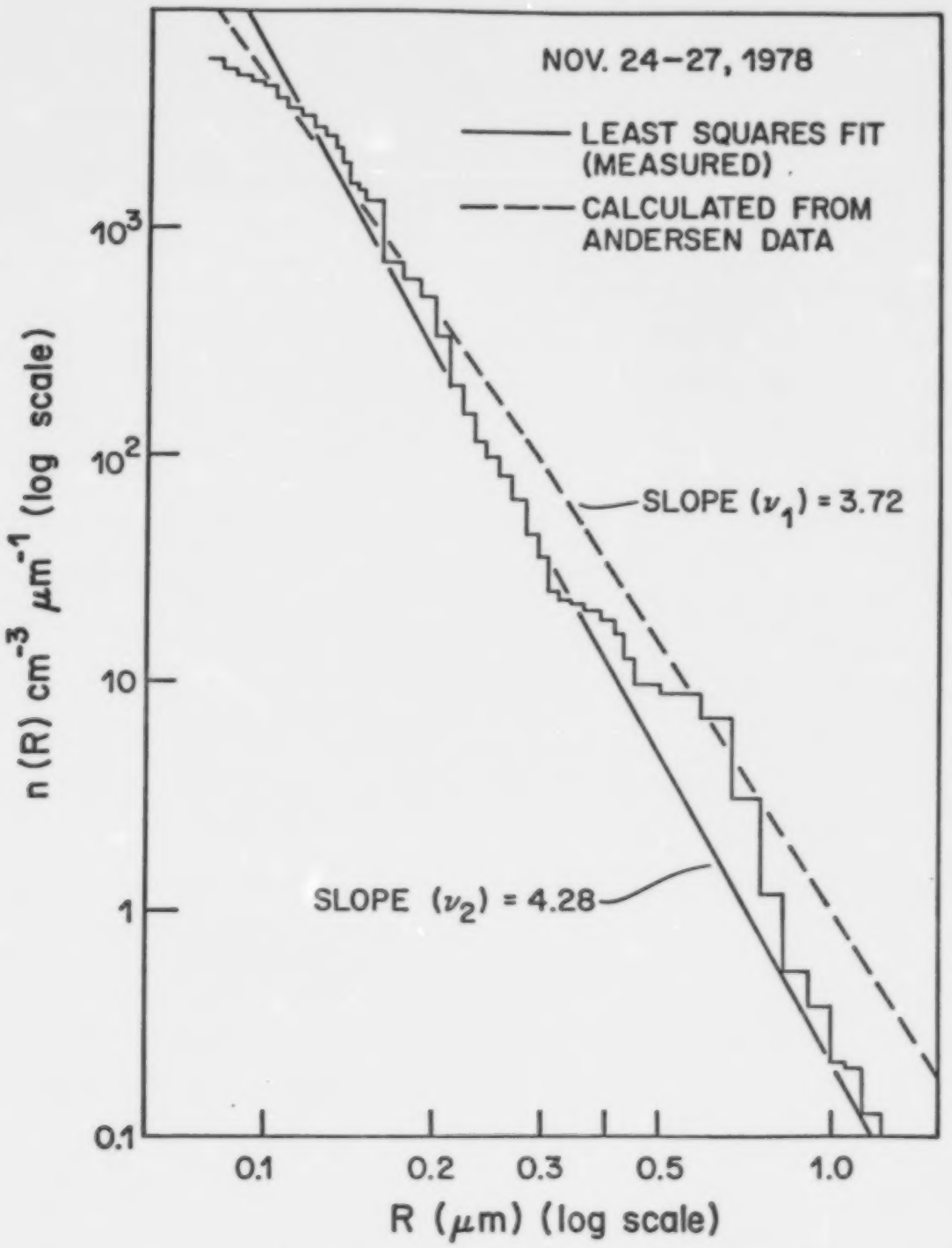

Figure 4.22. Particle size spectrum n(R) calculated from Anderson impactor data and measured by ASAS-300 versus R for samples Nov. 24-27, 1978.

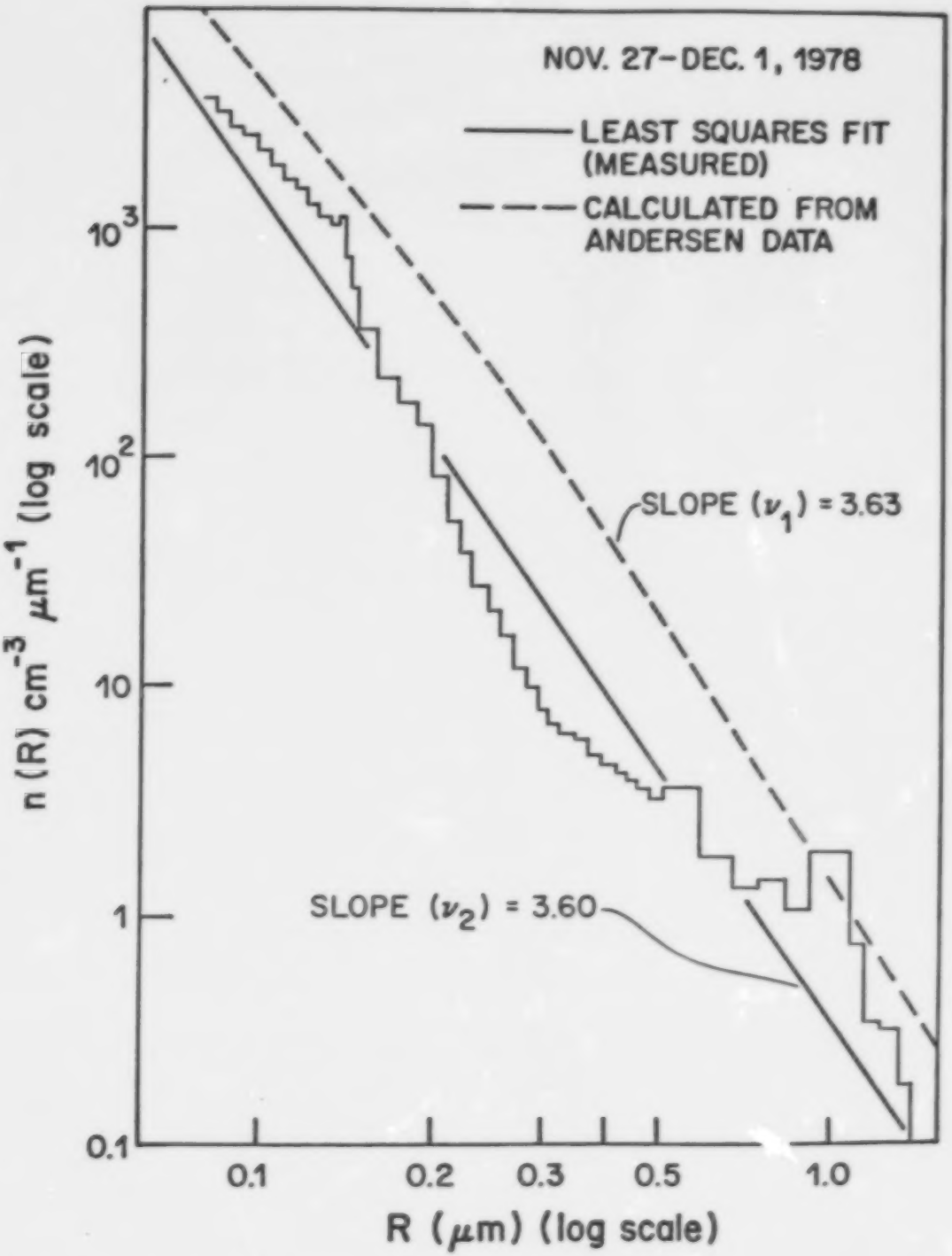

Figure 4.23. Particle size spectrum n(R) calculated from Andersen impactor data and measured by ASAS-300 versus R for samples Nov. 27-Dec. 1, 1978.

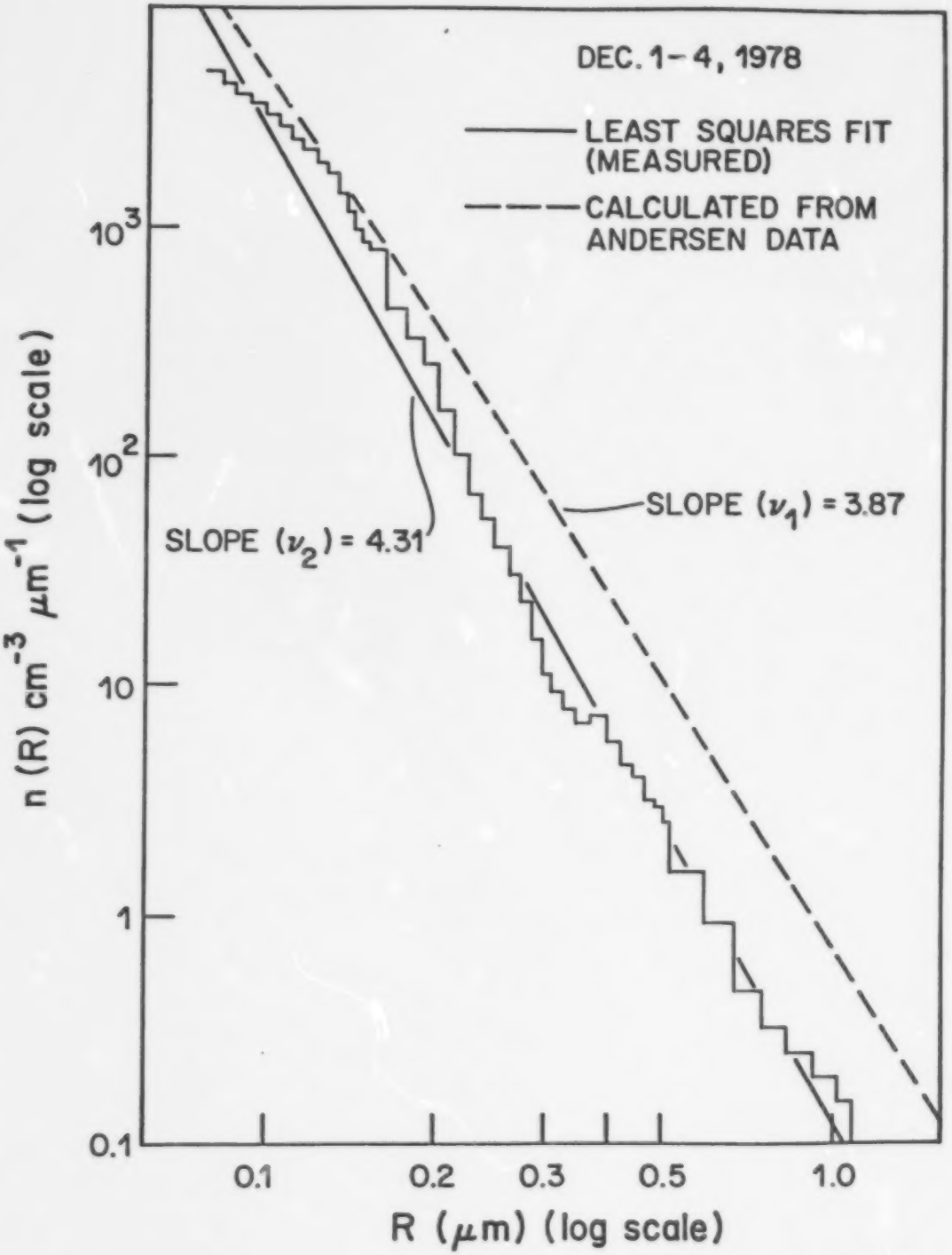

Figure 4.24. Particle size spectrum n(R) calculated from Andersen impactor data and measured by ASAS-300 versus R for samples Dec. 1-4, 1978.

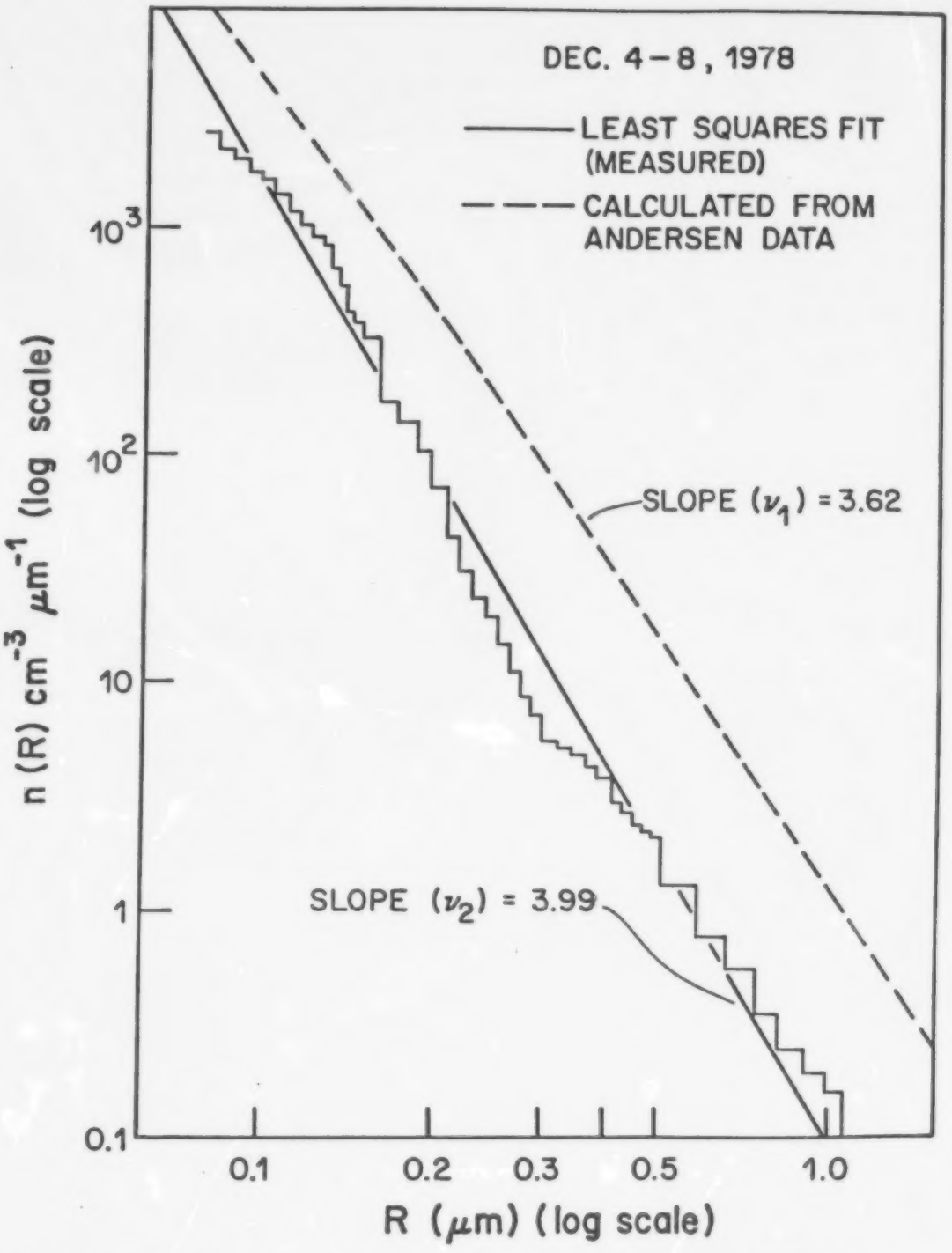

Figure 4.25. Particle size spectrum n(R) calculated from Andersen impactor data and measured by ASAS-300 versus R for samples Dec. 4-8, 1978.

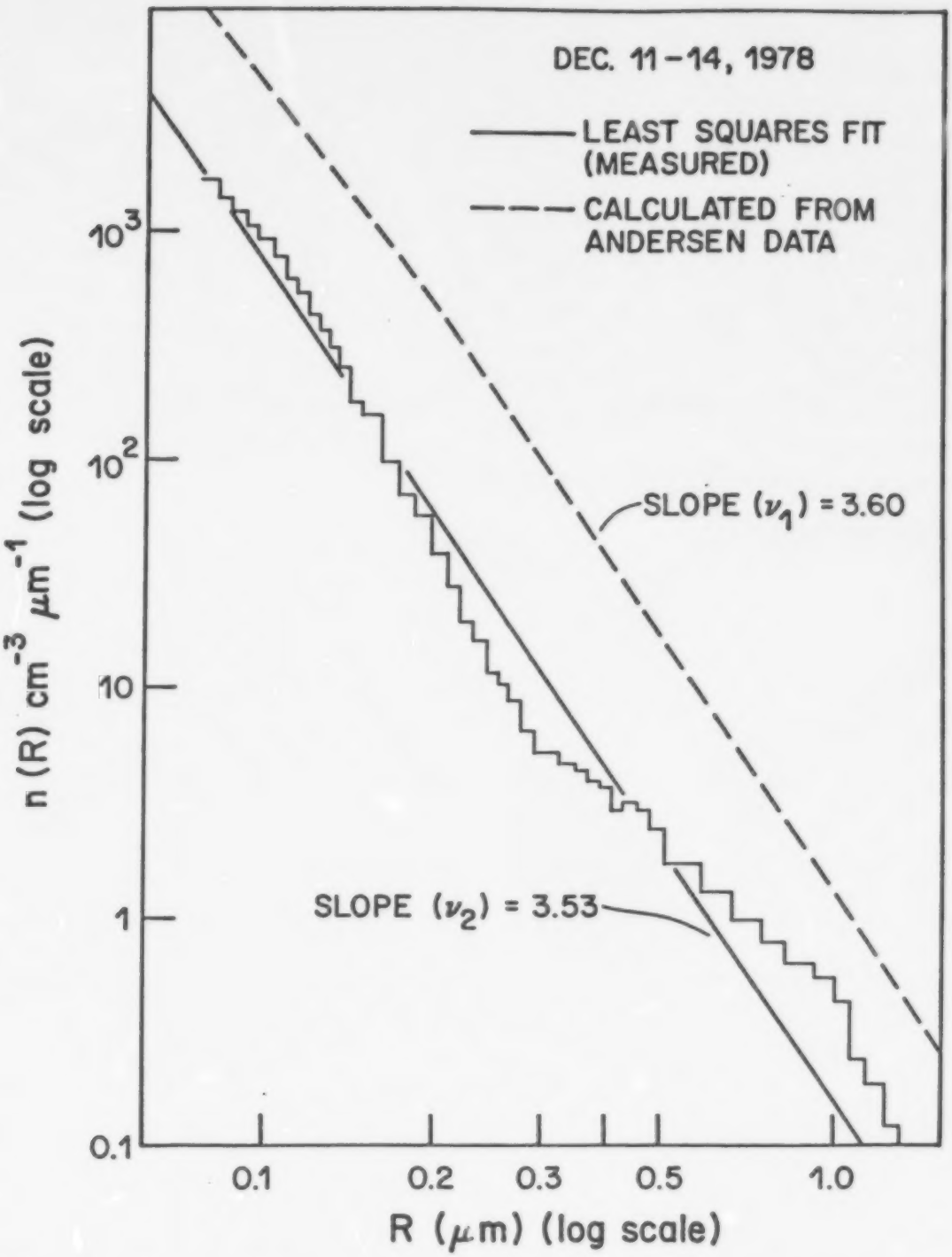

Figure 4.26. Particle size spectrum n(R) calculated from Andersen impactor data and measured by ASAS-300 versus R for samples Dec. 11-14, 1978.

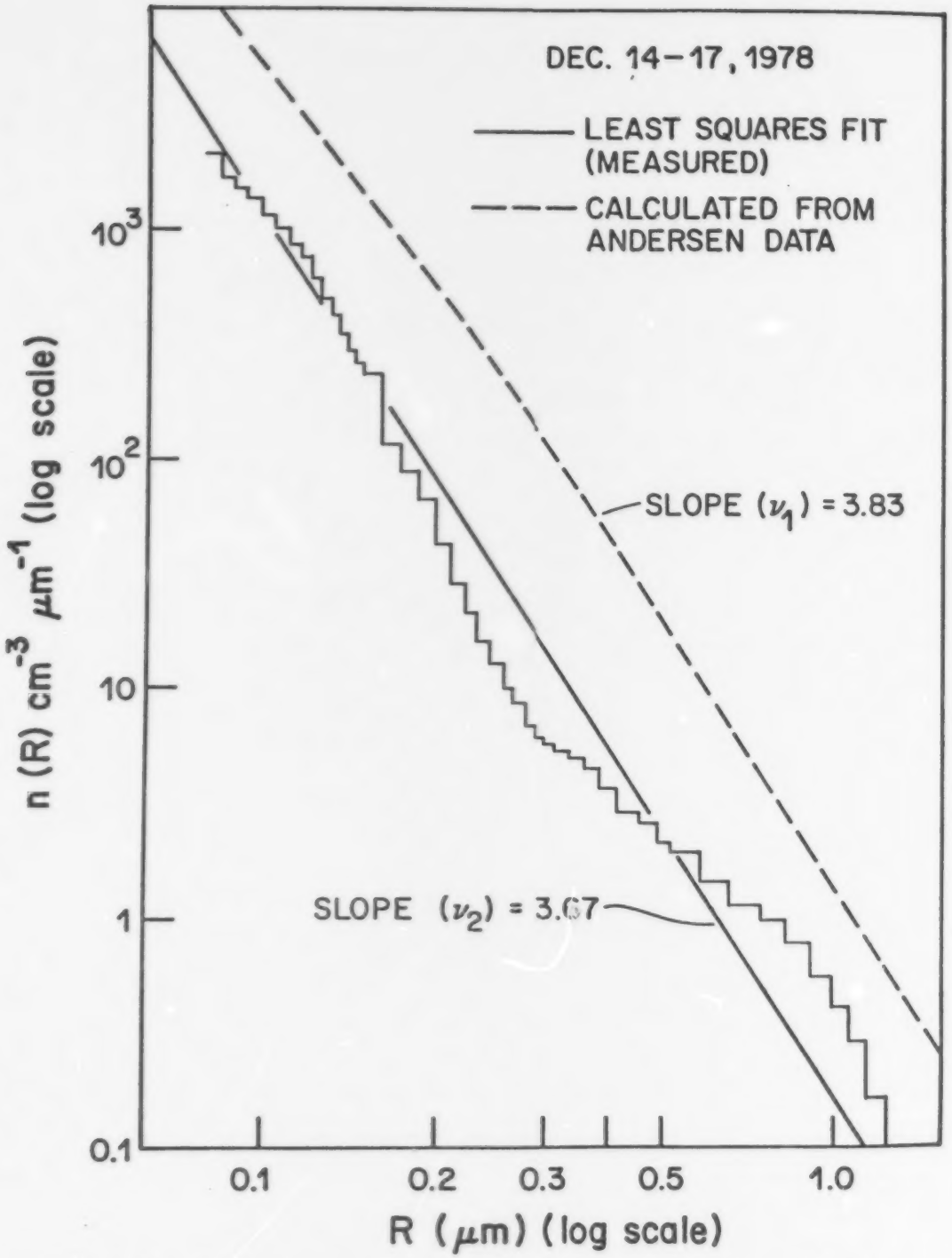

Figure 4.27. Particle size spectrum n(R) calculated from Andersen impactor data and measured by ASAS-300 versus R for samples Dec. 14-17, 1978.

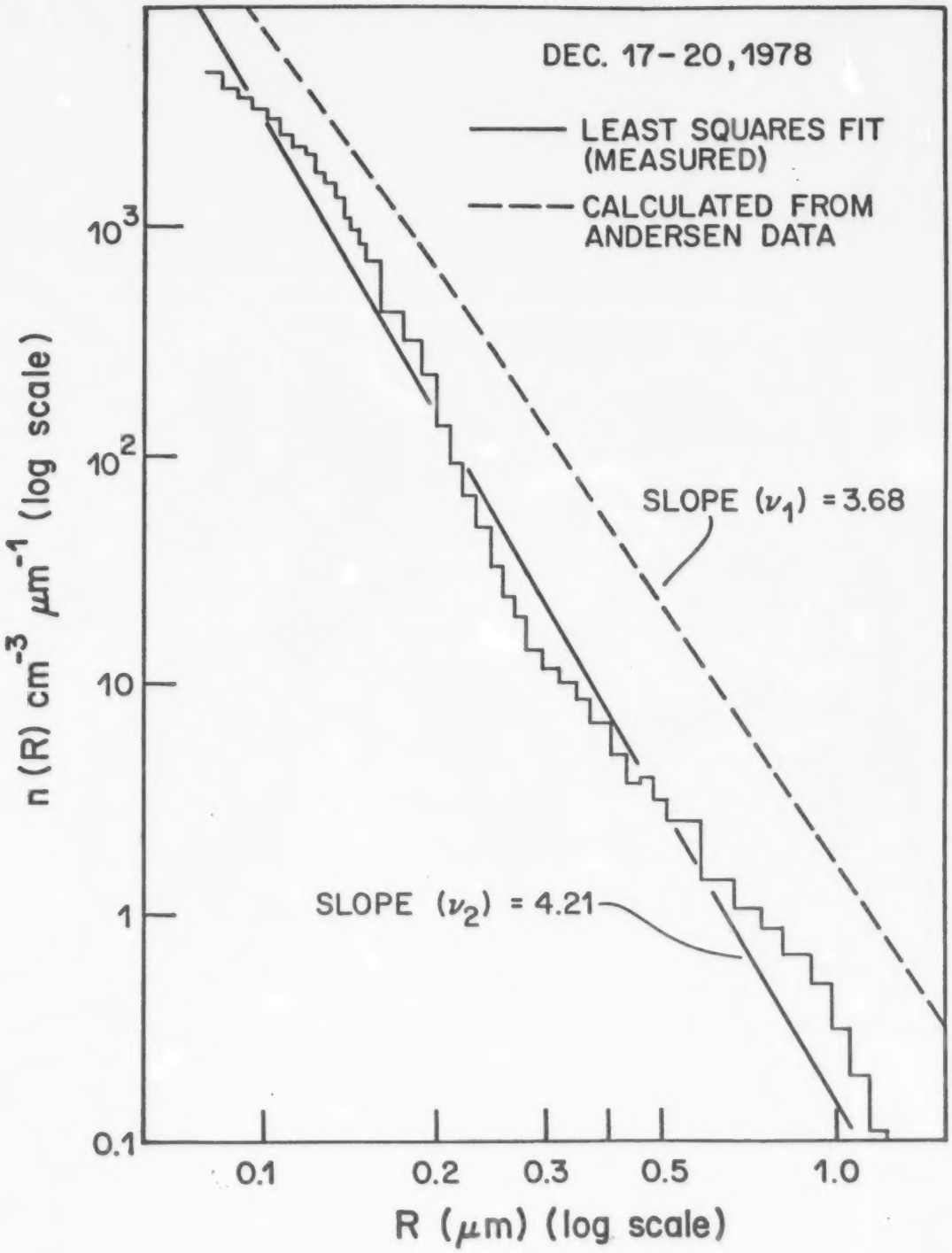

Figure 4.28. Particle size spectrum n(R) calculated from Andersen impactor data and measured by ASAS-300 versus R for samples Dec. 17-20, 1978.

the ASAS-300 can be attributed directly to the assumption that $\rho = 1.5$ g cm^{-3} in the calculations (see above). If ρ is increased to ~ 2.2 g cm^{-3} then $n(R)$ is the same for both impactor and ASAS data. Bulk densities ranging from 1.8 g cm^{-3} to 2.9 g cm^{-3} for dry continental and mountain air have been reported by Hänel and Thudium (1977) so that $\rho = 2.2$ g cm^{-3} would seem to be a reasonable value to assume for the region around Calgary.

4.4 Influence of chinook on particle size distribution

The chinook is characterized by unusually strong, warm and dry westerly winds which descend the eastern slopes of the Rocky mountains, (Glen, 1961). However, a definition of the chinook condition together with a thorough understanding of its effects on urban air quality is still a matter of some controversy, (Longely, 1967; Brinkmann, 1969; Lester 1976a, 1976b; Danielewicz, 1977; Alberta Environment, 1977; and Nkemdirim and Leggat, 1978). Calgary is in the unique position of presenting an urban environment to the chinook phenomenon and yet relatively little is known of the resulting effects of the chinook on aerosol particle size distribution, chemical properties of aerosols, visual range, etc. The purpose of this preliminary study was to ascertain what effect if any a chinook might have on the particle size distribution during a chinook event.

The ASAS-300 particle spectrometer, the MRI integrating nephelometer model 1550 and an Aerovironment model 300 monostatic acoustic sounder (see Section 3.1) were obtained on loan from the Physics Department, University of Calgary, for the months of January and February 1979. During

this period one definite chinook occurred on February 17/18 for which a complete history of relevant parameters was obtained as described below.

Both particle spectrometer and nephelometer were operated at a height of 12 m above ground level in the centre of downtown Calgary (John Bowlen building) while the acoustic sounder was operated a few blocks away in the Stampede grounds (see Section 3.2) and provided information on the turbulence profile of the boundary layer.

While the atmospheric aerosol is composed of suspended particulates varying in size and concentration over several orders of magnitude only those particles in the size range R (radius) $\sim$ 0.1 μm to R $\sim$ 1.0 μm are significant in the reduction of visual range (see Section 4.2). Furthermore for aerosols of urban or continental origin the size distribution usually follows the Junge power law

$$n(R) = c\, R^{-\nu}$$

where c is a constant and the exponent ν has a value between $\sim$ 3.0 and $\sim$ 5.0. One aim of this study was to examine the variation, if any, of the value of ν through a chinook event, the parent particle spectrum n(R) being measured with the ASAS spectrometer. The corresponding volume differential scattering coefficient $a(\lambda)$ is given by [4.3] in terms of the particle size spectrum n(R) and was measured here with the MRI integrating nephelometer for which the effective wavelength is 480 nm, (Harrison, 1979).

Meteorological data used in this work was collected by Alberta Environment at the Bonnybrook Tower, Calgary. This site is 3.5 km distant

from the John Bowlen building. Temperatures were recorded at three heights on the tower: T_L at 30 feet, T_M at 150 feet and T_H at 300 feet above ground level. Any descending warm air is easily recognized from the corresponding temperature records.

The expected pattern of events through a typical chinook commences with clean warm air descending the slopes of the Rocky mountains and penetration of cold arctic air which is near ground level. The resultant descending interface between cold air and warm chinook air is turbulent producing descending multiple layers as indicated on the acoustic sounder chart records. As these multiple layers approach ground level, the ground temperature rises and a layer of ground based turbulence having a characteristic diffuse and variable boundary is recorded by the sounder, (indicated by dark lines on the acoustic sounder records). This turbulent layer is quite distinguishable from more common normal inversion patterns. It may take several hours or even days for these layers to disappear, long after the surface westerly wind has subsided (Hicks and Mathews, 1979).

Fig. 4.29 shows the acoustic sounder records for three chinook periods on February 17/18, March 3, and March 9/10 (Mathai, Harrison and Mathews, 1980). Only the first of these was covered by the study reported here. In all cases, however, descending multiple layers depicting the onset of chinook conditions are evident, followed by near ground turbulent layers. For the February 17/18 event the interface between cold and warm air reached the 200 m level at approximately 1700 MST on February 17. This was followed by a period of $\sim$ 17 hrs. of low altitude turbulence which was accompanied by a strong temperature inversion. In Fig. 4.30 the values of $(T_H - T_L)$

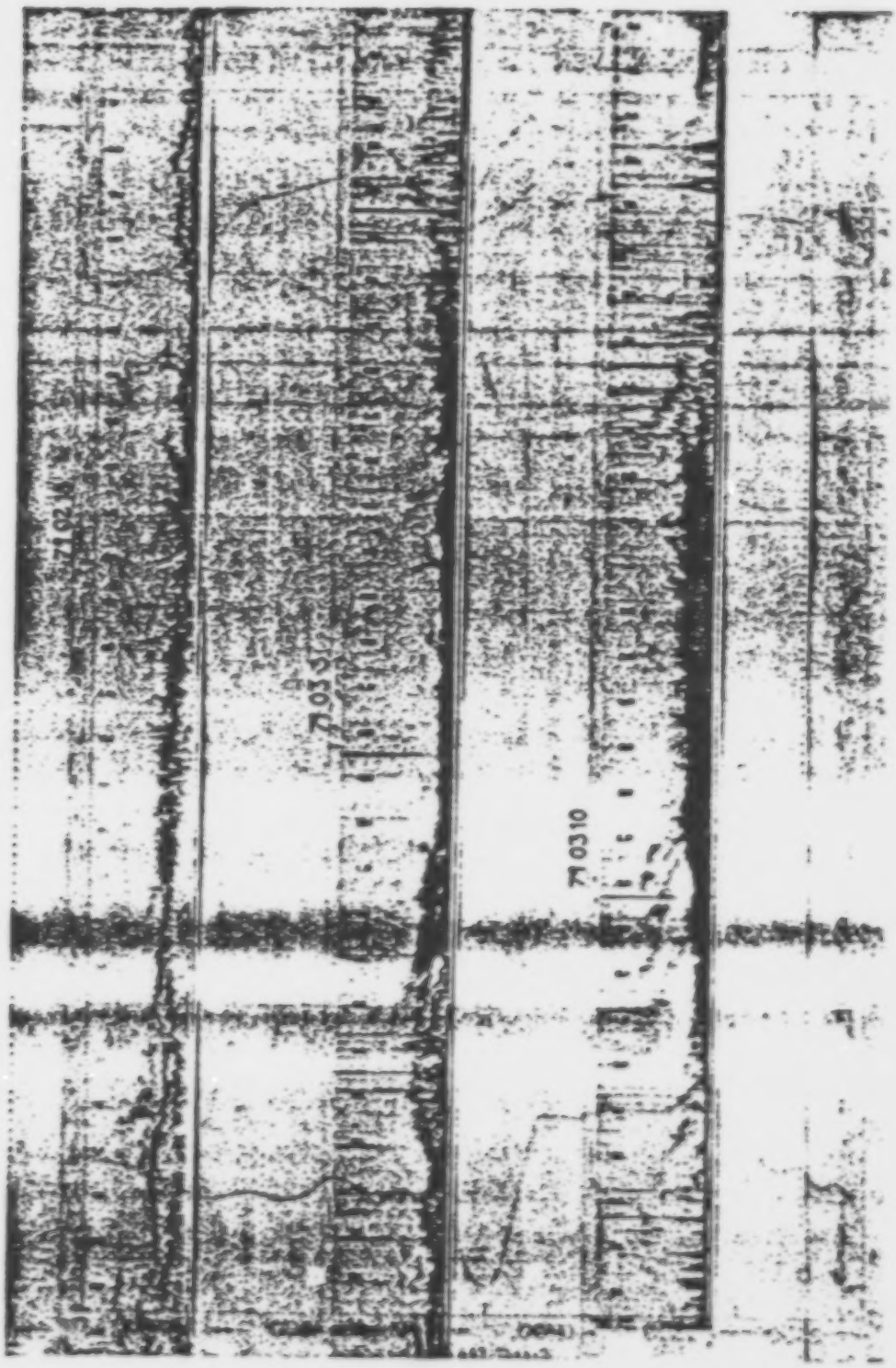

Figure 4.29. Acoustic sounder records for three chinook periods: 17/18 February, 3 March, 9/10 March.

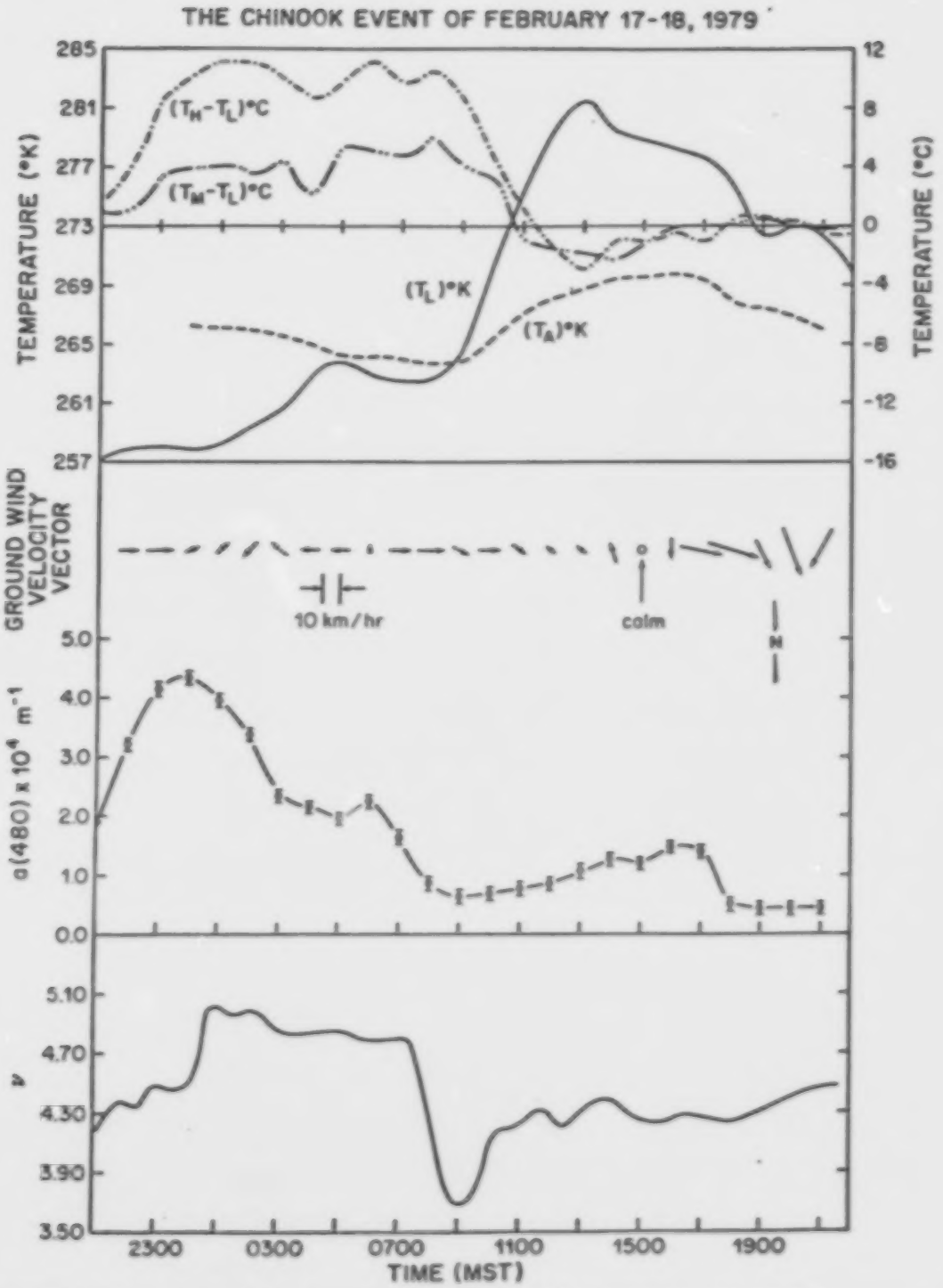

Figure 4.30. Detailed meteorological data (temperature and wind vector), volume scattering coefficient a(480), and particle size power law exponent ν for the chinook of Feb. 17/18, 1978.

and (T_M-T_L) are plotted for this entire period and show maximum values $\sim 11^{\circ}C$ and $\sim 5^{\circ}C$ respectively. Fig. 4.30 also shows other meteorological data (wind velocity vector and ground temperature T_L) as well as the volume scattering coefficient a(480) and power law exponent ν for this chinook period. The temperature, wind data, and nephelometer a(480) values are one hour averages. The ASAS spectrometer sampling time was 10 minutes (or less) for each of the four size ranges so that a complete spectrum was obtained at forty minute (or less) intervals.

During the build-up of the temperature inversion condition the wind is strong and from the west-southwesterly direction which is usual for a chinook in Calgary. At this time the particle size power law exponent ν increased from $\sim$ 4.1 to $\sim$ 5.0 and the scattering coefficient a(480) increased to a maximum value of 4.3×10^{-4} m^{-1} which usually gives low visibility and the visual appearance of a "brown smog layer" over the city. The increase in slope of the n(R) spectrum along with an increase in net particle concentration and higher pollution is commonly observed for the urban air over Calgary and is probably due to stagnant city air acquiring relatively more small particles ($\sim$ 0.1 μm) from automobile exhaust than large particles ($\sim$ 1 μm).

At about 0700 MST on Feb. 18, the temperature inversion starts breaking up and warm air starts replacing the polluted city air. The ground temperature starts rising rapidly producing a $19^{\circ}K$ change in less than five hours. The hourly temperatures for Feb. 18, averaged over the last thirteen years are plotted for comparison, T_A, (the dashed curve in Fig. 4.30), with a minimum of $263.6^{\circ}K$ and a maximum of $276.4^{\circ}K$.

It is not possible to specify the extent to which the hourly temperature changes during the chinook were due to diurnal contributions as these changes are dependent on a number of factors such as cloud cover, snow depth on the ground and the time of day. Danielewicz (1977) has calculated the mean range in temperature due to the diurnal effect in Calgary during January, February and March to be 4.7°K. Therefore, it can be concluded that the chinook contributed significantly to the high of 281.5°K at 1300 MST after a low of 257.7°K at 0030 MST on Feb. 18.

As the warm air starts descending rapidly as indicated by T_H, T_M, and T_L values at about 0700 MST, the value of the slope, ν, drops from about 4.8 to 3.7 within the short time of one hour. Also, the value of a(480) decreases gradually during the early morning hours to a low value of 0.64×10^{-4} m^{-1} at 0800 MST. The drop in the value of ν is due to the relatively large decrease in the number of particles with small radii compared with that for larger radii. The coincidence of the abrupt fall in the value of ν and a(480) with the disappearance of the temperature inversion and the rapid increase in ground level temperature, between 0900 and 1100 MST on Feb. 18 is clearly evident in Fig. 4.30.

It might be concluded from this detailed study of a single chinook event that city pollution levels increase during the accompanying temperature inversion. This is in agreement with the conclusions arrived at by Nkemdirim and Leggat, (1978) and Hicks and Mathews, (1979). This study indicates that ν <u>increases</u> with an increase in particulate concentration and decrease in visibility for city air. However, it should be noted that in a natural (continental) haze ν <u>decreases</u> with

decreasing visibility. See Section 4.2. This behaviour of natural air is in accord with Mie scattering theory and the assumption of a power law size distribution, Bullrich, (1964). It is clear that the chinook condition poses a somewhat unusual circumstance which needs to be investigated further.

4.5 Nephelometer, impactor and CRMU data correlation

The relationship between mass concentration of atmospheric particulates and the associated scattering coefficient in the visible region is important if integrating nephelometer measurements are to be used to infer mass loading of the atmosphere. The earlier and extensive studies of Charlson, (1969) on polluted air show that the ratio of volume differential scattering coefficient $a(\lambda)$ to mass concentration M is about 2.2 g^{-1} m^2 when $a(\lambda)$ is referred to an effective wavelength of 550 nm. More recently similar studies by Kretzschmar, (1975); Clarke et.al., (1977); and White and Roberts, (1977) give similar values of this ratio for polluted air. On the other hand Patterson and Gillette, (1977) have obtained values of $a(\lambda)/M$ an order of magnitude lower for airborne soil particles than for polluted air indicating the wide variability of this ratio under different environmental conditions. In the work reported below $a(\lambda)/M$ has been measured for relatively pollution free air believed to be characteristic of a mountain and continental background.

4.5.1 In the first part of this investigation the broad-band (white light) scattering coefficient $a(m^{-1})$ was determined with an integrating nephelometer (MRI model 1550) and the mass loading of

the atmosphere was measured with a Smoke Sampler (Research Appliance Co.). The latter instrument involves the collection of particles on a filter paper tape followed by a measurement of visible light absorption of the "dust spot" produced on the paper.

The nephelometer was operated on the roof of the Science B building at the University of Calgary (UC) while the smoke sampler was operated on the ground along with other monitoring equipment at the University of Calgary as part of the Alberta Environment pollution monitoring programme (CRMU). The CRMU data is recorded on strip chart paper and eye estimates of hourly average values are then made and tabulated for analysis. In the case of the smoke sampler records, the resolution obtained is very poor as evidenced by the examples shown in Figs. 4.31 to 4.33 inclusive, where the resolution is 0.1 COH per 1000 L.Ft. Hence for a relatively clean atmosphere with a smoke concentration of say, 0.2 COH per 1000 L.Ft., the resolution would be no better than 50%. This point should be borne in mind when comparing smoke sampler measurements with those of the nephelometer.

The data shown in Figs. 4.31 to 4.33 covers the period February 1, 1978 to March 31, 1978 and was selected for a detailed correlation analysis of CRMU and UC measurements. Of particular interest here is a comparison of the volume scattering coefficient a(m^{-1}) and the smoke index s (COH per 1000 L. Ft.). However, for the sake of completion the volume scattering coefficient is also compared with NO_x(n), ozone (o), hydrocarbon(h), and carbon monoxide(c) concentrations. During this two month period the mean values of a and s are 0.86×10^{-4} m^{-1} and 0.17 COH per 1000 L. Ft. with standard deviations of 0.85×10^{-4} m^{-1} and

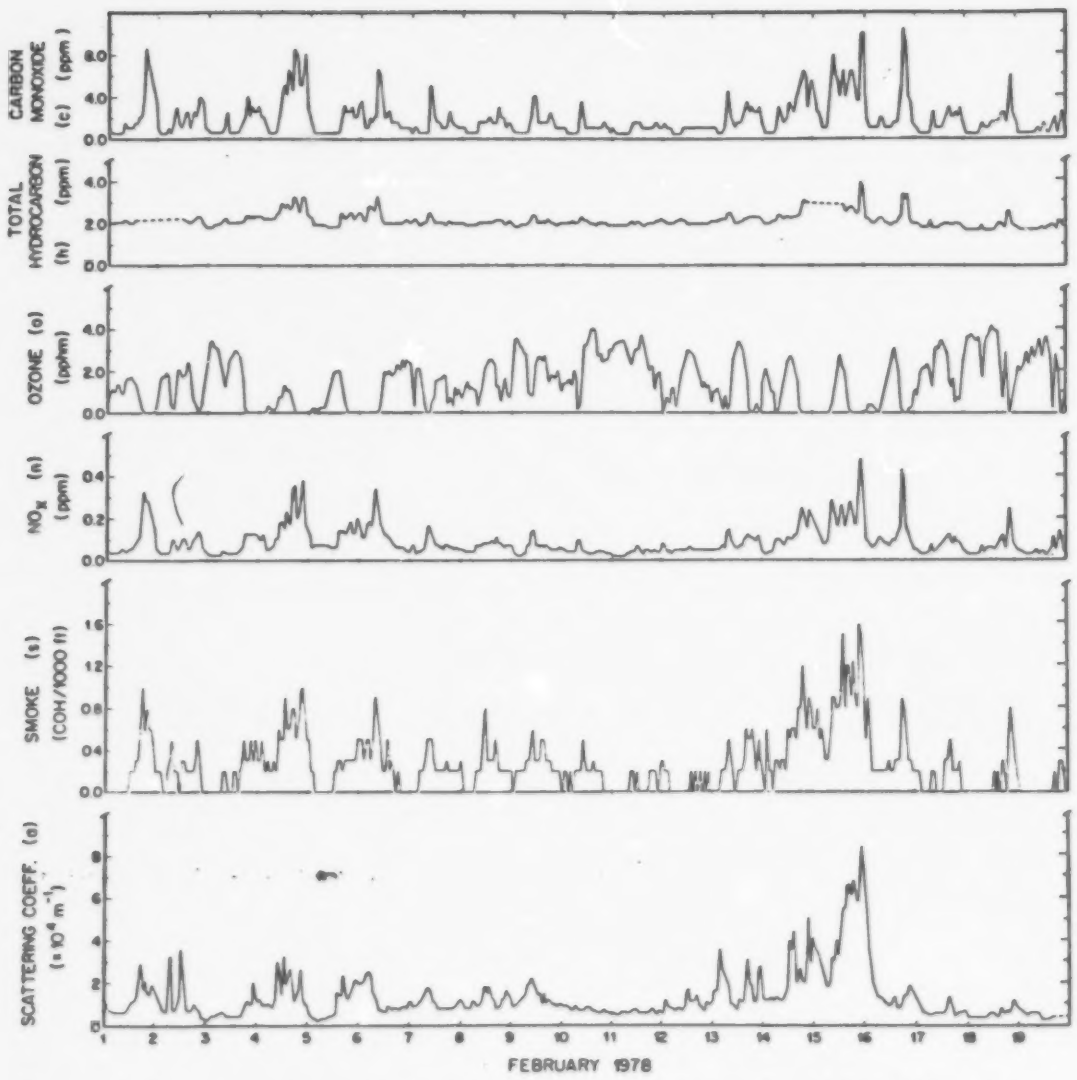

Figure 4.31. Volume scattering coefficient (a), smoke index (s), NO_x concentration (n), ozone concentration (o), hydrocarbon concentration (h), and carbon monoxide concentration (c) for the University of Calgary, Feb. 1-19, 1978.

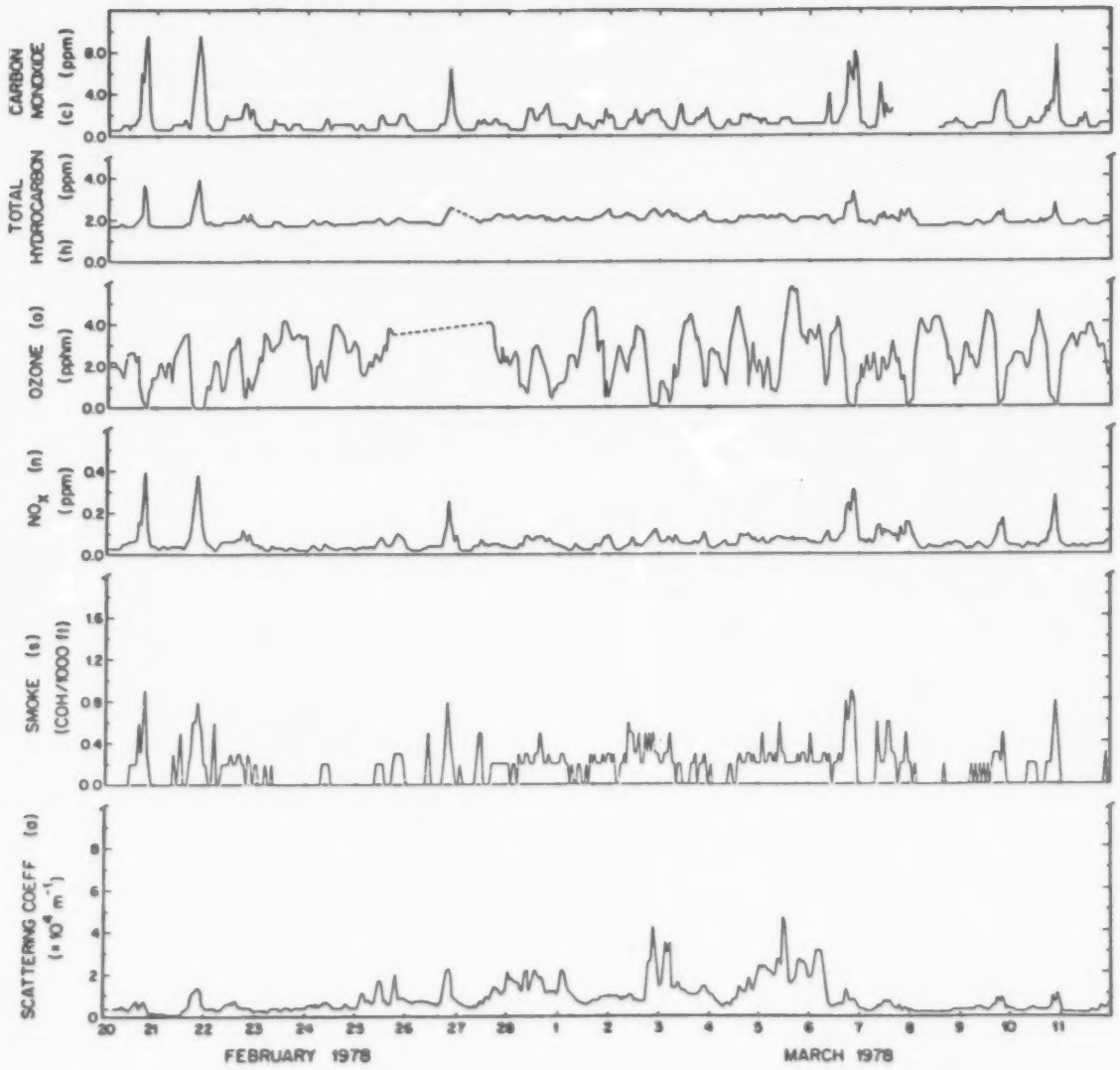

Figure 4.32. Volume scattering coefficient (a), smoke index (s), NO_x concentration (n), ozone concentration (o), hydrocarbon concentration (h), and carbon monoxide concentration (c) for the University of Calgary, Feb. 20-March 11, 1978.

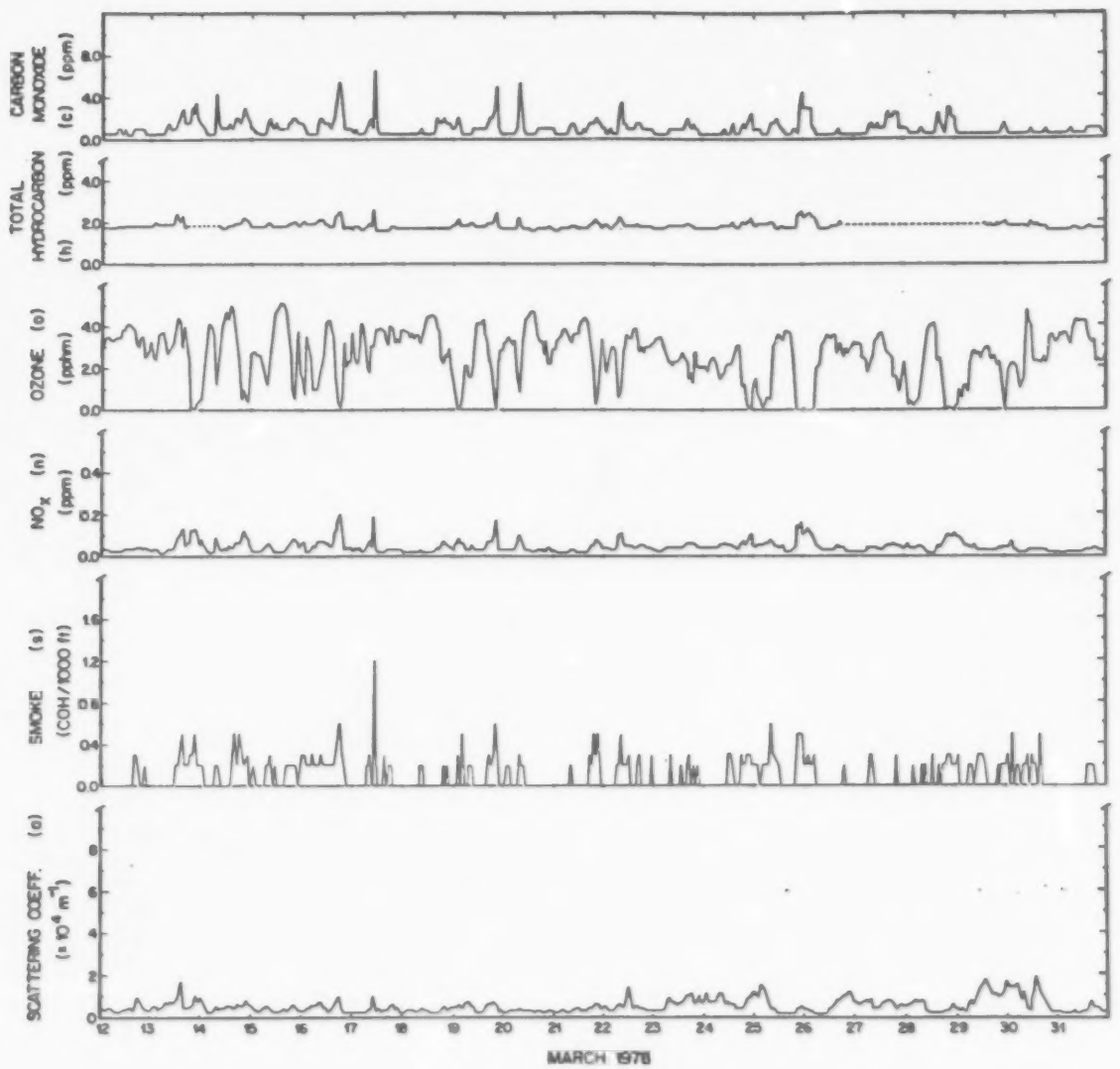

Figure 4.33. Volume scattering coefficient (a), smoke index (s), NO_x concentration (n), ozone concentration (o), hydrocarbon concentration (h), and carbon monoxide concentation (c) for the University of Calgary, March 11-31, 1978.

0.22 COH per 1000 respectively. This gives an indication of the extent of the fluctuations encountered in both a and s during the observing period. Maximum values of a and s (8.4×10^{-4} m^{-1} and 1.6 COH per 1000 L. Ft. respectively) were recorded on February 25, 1978, while minimum values of a and s (0.1×10^{-4} m^{-1} and 0.0 COH per 1000 L. Ft. respectively) were recorded on February 21, 1978. Mean values for n,o,h, and c are 0.063 ppm, 2.72 pphm, 3.76 ppm and 1.39 ppm respectively. A visual inspection of Figs. 4.31 to 4.33 shows that all six parameters measured fluctuate in unison with one another. A quantitative estimate of this observation was made by calculating the simple product moment correlation coefficient r for each of the 15 possible pairs of parameters and for the complete 1416 data points of each parameter covering the selected two month period. The results of this correlation analysis are given in Table 4.4. An application of Student's t test to these results has also been carried out to determine the percentage probability of obtaining each of these calculated r values for a true value r=0. The percentage probabilities for zero correlation are also given in Table 4.4. In all cases except ozone these probabilities are very small indicating a strong correlation between the parameters investigated. The poor correlation with ozone derives from the O_3-NO_x photochemistry. Of particular significance is the correlation between the integrating nephelometer and the smoke sampler.

Whereas the integrating nephelometer detects and measures ambient aerosol particles by virtue of their visible light <u>scattering</u> properties (Mie scattering), the smoke sampler relies upon visible light <u>absorption</u> of a collected sample for the measurement of ambient aerosol particles. The Mie scattering coefficient is strongly dependent

upon both wavelength and particle size (Van de Hulst, 1957), whereas the absorption coefficient of a dust sample depends only on the gross characteristics of the constituent particles. Hence it is conceivable that for certain particle size distributions there might be either a weak correlation or no correlation at all between the two methods of measurement. This could be particularly true in situations where the shape of the particle size distribution changed significantly with increasing particle concentration. It is thus important to know whether or not a correlation exists between these two methods of measurement for the ambient aerosol in the Calgary atmosphere. The result obtained here shows that the integrating nephelometer would indeed be a very good monitor of ambient aerosol comparable to, if not better than, the standard smoke sampler currently employed.

Table 4.4

Correlation coefficients for CRMU and UC data
February 1, 1978 to March 31, 1978.

	Calculated r (% Probability for r=0)				
Parameter	a (scattering coefficient)	s	n	o	h
s(smoke)	0.66 (<0.1)				
n(NO_x)	0.55 (<0.1)	0.81 (<0.1)			
o(ozone)	-0.05 (<5.0)	-0.07 (<1.0)	-0.09 (<0.1)		
h(hydrocarbon)	0.12 (<0.1)	0.15 (<0.1)	0.19 (<0.1)	-0.03 (<20.0)	
c(carbon monoxide)	0.46 (<0.1)	0.77 (<0.1)	0.91 (<0.1)	-0.08 (<1.0)	0.17 (<0.1)

4.5.2 In the second part of this study the volume differential scattering coefficient $a(\lambda)$ was measured with a multiwavelength nephelometer operated at 557 nm and the mass concentration was measured with a high volume air sampler, (see Section 3.1). Both instruments were operated on the roof of Science B building on the University of Calgary campus (site b) during a summer period (May-June, 1978) and a winter period (November-December, 1978). The ambient air sampled was relatively free from urban pollution as evidenced by the low mass concentrations recorded and due to the almost continual prevalence of westerly winds bringing continental background aerosol to the NW sector of the city. A summary of the results obtained in this study is given in Table 4.5.

The ratio a(557)/M observed here for both summer and winter is low compared to the value 2.2 g^{-1} m^2 given by Charlson, (1969) for polluted air, a result verified by Clarke et.al., (1977) and White and Roberts, (1977). However, as pointed out by Davies, (1975) this ratio must depend on the parent particle size number distribution and cannot be expected to have the same value in different environments. An example of this variability was found by Patterson and Gillette, (1977) for airborne soil particles where the ratio varied by more than an order of magnitude with a minimum value $\sim$ 0.3 g^{-1} m^2. For the background continental-mountain air sampled in this study the mass is distributed mainly between 1 and 100 μm whereas for urban polluted air the mass is concentrated more between 0.1 μm and 10 μm, (Slinn, 1975). Since particles above $\sim$ 1 μm contribute relatively little to the scattering

Table 4.5

Aerosol mass concentration and differential scattering coefficient for summer and winter 1978.

Sampling Period 1978	M ($\mu g\ m^{-3}$)	a(557) ($\times 10^5\ m^{-1}$)	a(557)/M ($g^{-1}\ m^2$)	Sampling Period 1978	M ($\mu g\ m^{-3}$)	a(557) ($\times 10^5\ m^{-1}$)	a(557)/M ($g^{-1}\ m^2$)
May 4-11	27.6	4.3	1.60	Nov. 22-24	36.0	2.9	0.80
May 25-June 1	18.6	1.8	0.97	Nov. 24-27	28.3	4.4	1.50
June 1-8	38.6	2.6	0.67	Nov. 27-Dec. 1	38.9	2.7	0.69
June 8-16	25.5	1.4	0.56	Dec. 1-4	20.8	3.4	1.6
June 16-22	27.3	1.9	0.70	Dec. 4-8	37.6	2.0	0.54
June 22-29	32.4	2.5	0.76	Dec. 8-11	31.3	2.3	0.73
June 29-July 6	38.1	2.0	0.53	Dec. 11-14	40.6	2.2	0.53
MEAN VALUES	29.7		0.83		33.4		0.91

of visible light, the ratio a(557)/M should be higher for urban air than for the air sampled here. Hence the low values reported here are to be expected.

Finally it might be noted that there are no significant differences in summer and winter values of either the scattering coefficient or mass concentration. This infers that the visibility in the mountain region west of Calgary has the same quality year round conforming with the observation that mountain peaks 80-100 km distant are more often than not visible from the observation site.

5. CONCLUSIONS

The majority of investigations reported above concern the particle size distribution of ambient aerosol as measured in the Calgary boundary layer. From the results obtained over the two year period of the study it can be concluded that in the important size range $R \sim 0.1$ μm to $R \sim 1.0$ μm the particle size distribution is best represented by the power law or lognormal forms. Both are approximately equivalent in this size range. The absolute value of the power law exponent $|\nu|$ is smaller in the SE sector of the city (industrial) than in the NW sector (residential). It can be inferred that industrial activity in the SE injects relatively more larger particles into the boundary layer than corresponding residential effluents in the NW. Similarly a(480) is generally greater in the SE sector than in the NW, notwithstanding the effects of wind speed and direction.

The nature of the particle size distribution in the range $R \sim 0.1$ μm to $R \sim 1.0$ μm determines the wavelength dependence of

scattered light in the visible region. A study made here of the Angstrom coefficient α in clean and polluted air showed that the relationship $\alpha = \nu - 3$ was followed and that clean air scatters relatively more blue light than red. Polluted air scatters more at longer wavelengths which accounts in part for the appearance of a white or brown haze during periods of mild pollution or light fog.

A comparison of Andersen impactor data with particle size distributions determined directly with the ASAS-300 spectrometer has shown that the distribution is generally monomodal in the range $R \sim 0.1$ μm to 1.0 μm. The impactor has been shown to give a lognormal mass distribution in agreement with the spectrometer distributions. Slopes of plots of log n(R) versus log R derived by both methods were found to agree with one another within the limits of experimental error, (3.69±0.1 and 3.94±0.29). The density of the ambient aerosol was estimated to be ~ 2.2 g cm^{-3}, in agreement with that found by other workers. The mass size distribution found to be near lognormal had a MMD = 3.0 μm and a GSD = 6.0. The mass concentration varied between the limits 20 and 58 μg m^{-3} with a mean value of 38 μg m^{-3}.

In a somewhat different vein the particle size distribution was monitored through a chinook and temperature inversion event. The power law exponent ν was found to increase during the inversion build-up phase along with increases in both n(R) and a(480). Following the chinook winds, however, ν decreased from ~ 4.7 to ~ 3.6 in less than an hour.

A comparison of nephelometer measurements of both differential and broad-band aerosol scattering coefficients with high volume air

sampler and COH data for the same aerosol has shown a general agreement between the results from the different instruments. The nephelometer appears to have a better resolution capability than the smoke sampler employed here, otherwise both instruments exhibited a high correlation with one another. The ratio of a(557)/M for the Calgary environment was found to be 0.83 g^{-1} m^2 for the summer and 0.91 g^{-1} m^2 for the winter months. Both values are somewhat lower than those found in some other urban areas of North America but larger than values found by other workers in non-urban areas.

6. RECOMMENDATIONS

The overall recommendation that might be made concerning possible future research studies of the ambient aerosol over Calgary is that the investigation made here of chinook and temperature effects be continued. Due to the unpredictable nature of these phenomena a continuous and prolonged monitoring programme should be initiated involving particle size distribution, nephelometer, acoustic sounder, visibility and meteorological measurements. Such measurements would be very useful for assessing long term effects of any gradual increase in aerosol pollution and degradation of visibility especially due to the current rapid growth in the City of Calgary. The results obtained in the pilot study here indicate that the power law exponent could be used as one indicator of a chinook occurrence. The setting up of a particle size spectrometer at a particular location (CDMU) along with a commercial nephelometer and an acoustic sounder might be one simple way of initiating such a programme. While no chemical analyses of collected particulates could be undertaken during this two year study period it is recommended

that these be included in any future planning of aerosol analysis on a continuous basis. Based upon the established fact that the optically active atmospheric aerosols are those in the radius range 0.1 to 1.0 μm dichotomous samplers rather than standard high volume samplers should be used to collect fine particulates on filter paper. These samples collected on filter paper may then be used for chemical analysis.

The scientific community in the province should be encouraged to continue (and initiate) basic research in the area of optical properties of atmospheric aerosols and their effects on visibility.

Although it is desirable to have sets of instruments located at various regions of the city, transit studies of both aerosol scattering coefficient and particle size distribution could be a relatively economical yet effective way of monitoring in both industrial and residential areas of Calgary. A refinement of the mobile technique used here could further the day to day mapping of pollutants across the city, taking account of local wind and other meteorological factors.

Regarding visibility studies in the Calgary atmosphere it might be mentioned here that fundamental research studies currently in progress at the University of Calgary involving custom built visible and infra-red telephotometers indicate that telephotometry is becoming the preferred method for measuring visual range. It is recommended that Alberta Environment give some consideration to the inclusion of a commercial telephotometer in any routine monitoring programme of atmospheric air quality over Calgary. This would be particularly appropriate if visibility is considered an important parameter in the programme.

7. ACKNOWLEDGEMENTS

In any study such as that reported here a large number of persons from different organizations and institutions inevitably get involved in one way or another and it is not possible to mention all of these. However, special thanks are extended to Dr. H.S. Sandhu of Alberta Environment who was largely responsible for the initiation of this project and whose continual guidance and encouragement are appreciated; to Mr. G. Peck of the Calgary office of the Alberta Environment for his support in providing space in the John Bowlen building and for help with equipment and services of personnel in his department; to Mr. R.D. Brassard, Air Quality Control Div., Alberta Environment for the loan of the MRI meteorological station; to the Calgary Fire Department for their generous assistance in providing parking space and power for the mobile monitoring unit; to Dr. T. Mathews of the Physics Department, University of Calgary for recognizing the effort put into this work by the principal investigator, often to the detriment of his other University duties; and finally (and by no means least) to Mr. L. Murdock whose technicial ability and assistance at all times prevented the whole project from falling apart.

8. REFERENCES

Ahlquist, N.C., and Charlson, R.J., "A new instrument for evaluating the visual quality of air", J. Air Poll. Control Assoc., 17, 467-469 (1967).

Ahlquist, N.C., and Charlson, R.J., "Measurement of the vertical and horizontal profile of aerosol concentration in urban air with the integrating nephelometer", Environ. Sci. Tech. 2, 363-366 (1968).

Ahlquist, N.C., and Charlson, R.J., "Measurement of the wavelength dependence of atmospheric extinction due to scatter", Atmos. Environ., 3, 551-564 (1969).

Alberta Environment, "Inventory of air pollution sources and emissions in the City of Calgary" (1973).

Alberta Environment, "A preliminary study on the Effect of Chinook on Air pollutant Levels in Calgary", (Dept. of the Environment, Government of Alberta, Edmonton, Canada) (1977).

Andreev, S.S., Ivlev, L.S., Kabanov, M.W., and Pkhalagov, Y.A., "Effect of the relative humidity on the attenuation of optical radiation by aerosols in the atmosphere", Izv. Vyss. Uch. Zav., Fizika, 5, 54-57 (1974).

Angström, A., "On the atmospheric transmission of sun radiation and on dust in the air", Geograf. Ann. Deut., 11, 156 (1929).

Auer, A.H., "The evolution of visibility deterioration and aerosol spectra in the St. Louis urban plume", J. Air Poll. Control Assoc., 27, 1188-1191 (1977).

Blifford, I.H. Jr., and Ringer, L.D., "The size and number distribution of aerosols in the continental troposphere", J. Atmos. Sci., 26, 716-724 (1969).

Brinkmann, W.A., "The Definition of Chinook in the Calgary Area", Unpublished M.Sc. Thesis, University of Calgary, (1969).

Brock, J.R., "On size distributions of atmospheric aerosols", Atmos. Environ., 5, 833-841 (1971).

Bullrich, K., "In Advances in Geophysics", 10, Academic Press, New York, N.Y. (1964).

Buma, T.J., "A statistical study of the relationship between visibility and relative humidity at Leeuwarden", Bull. Amer. Met. Soc., 41, 357-360 (1960).

Cadle, R.D., "The measurement of Airborne Particles, John Wiley and Sons, New York (1975).

Charlson, R.J., Horvath, H., and Pueschel, R.F., "The direct measurement of atmospheric light scattering coefficient for studies of visibility and pollution", Atmos. Environ., 1, 469-478 (1967).

Charlson, R.J., Ahlquist, N.C., and Horvath, H., "On the generality of correlation of atmospheric aerosol mass concentration and light scatter", Atmos. Environ., 2, 455-464, (1968).

Charlson, R.J., "Atmospheric visibility related to mass concentration", Environ. Sci. Tech., 3, 913-917 (1969).

Charlson, R.J., Ahlquist, N.C., Selvidge, H., and MacCready, P.B., Jr., "Monitoring of atmospheric aerosol parameters with the integrating nephelometer. J. Air Poll. Control Assoc., 19, 937-942 (1969).

Charlson, R.J., "Multiwavelength nephelometer measurements in Los Angeles smog aerosol", In Aerosols and Atmospheric Chemistry, by G.M. Hidy, ed. Academic Press, New York (1972).

Charlson, R.J., Porch, W.M., Waggoner, A.P., and Ahlquist, N.C., "Background aerosol light scattering characteristics: nephelometric observations at Mauna Loa observatory compared with results at other remote locations", Tellus, 26, 345-360 (1974).

City of Calgary, "An evaluation of Calgary's present and future air quality with emphasis on the south-east sector, Prepared by Western Research and Development Corporation, Calgary (Ref. No. 2810-R1) (1979).

Clark, W.E. and Whitby, K.T., "Concentration and size distribution measurements of atmospheric aerosols and a test of the theory of self-preserving size distributions", J. Atmos. Sci., 24, 677-687 (1967).

Clarke, A.G., Moghadassi, M.A. and Williams, A., "A comparison of techniques for automatic aerosol mass concentration measurement", J. Aerosol Sci. 8, 73-81, (1977).

Crosby, P., "The measurement of visual range", Nature, 185, 438-439 (1960).

Crosby, P., and Koerber, B.W., "Scattering of light in the lower atmosphere", J. Opt. Soc. Amer., 53, 358-361 (1963).

Curcio, J.A., "Evaluation of atmospheric aerosol particle size distribution from scattering measurements in the visible and infrared", J. Opt. Soc. Am., 51, 548-551 (1961).

Cutten, D.R., Dale, F.R., Crosby, P., Koerber, B.W., and Lloyd, D.T., "A visibility meter for monitoring atmospheric aerosol parameters", Atmos. Environ., 9, 253-260 (1975).

Danieliwicz, Z.W., "Some Characteristics of Large Scale Winter Chinooks in Southern Alberta", Unpublished M.Sc. Thesis, University of Calgary (1977).

Davies, C.N., "Aerosol Science", Academic Press, New York (1966).

Davies, C.N., "Particles in the atmosphere - natural and man-made", Atmos. Environ., 8, 1069-1079 (1973).

Davies, C.N., "Size distribution of atmospheric particles", Aerosol Science, 5, 293-300 (1974a).

Davies, C.N., "Particles in the atmosphere - natural and man-made", Atmos. Environ., 8, 1069-1079 (1974b).

Davies, C.N., "Visual range and size of atmospheric particles", J. Aerosol Sci., 6, 335-347 (1975).

Deluisi, J.J., Furukawa, P.M., Gillette, D.A., Schuster, B.G., Charlson, R.J., Porch, W.M., Fegley, R.W., Herman, B.M., Rabinoff, R.A., Twitty, J.T., and Weiman, J.A., "Results of comprehensive atmospheric aerosol-radiation experiment in the southwestern United States", J. App. Meteor. 15, 441-463, (1976).

Dennis, R., "Handbook on Aerosols", Technical Information Center, Oak Ridge, Tennessee (1976).

Durham, J.L., Wilson, W.E., Ellestad, T.G., Willeke, K., and Whitby, K.T., "Comparison of volume and mass distributions for Denver aerosols", Atmos. Environ., 9, 717-722 (1975).

Eccleston, A J., King, N.K., and Packham, D.R., "The scattering coefficient and mass concentration of smoke from some Australian forest fires. J. Air Poll. Control Assoc., 24, 1047-1050 (1974).

Eldridge, R.G., "Haze and fog aerosol distributions", J. Atmos. Sci., 23, 605-613 (1966).

Eldridge, R.G., "The relationship between visibility and liquid water content in fog", J. Atmos. Sci., 28, 1183-1186 (1971).

Ensor, D.S., and Waggoner, A.P., "Angular truncation error in the integrating nephelometer", Atmos. Environ., 4, 481-487 (1970).

Freidlander, S.K., "Similarity considerations for the particle size spectrum of a coagulating, sedimenting aerosol", J. Meteor., 17, 479-483 (1960).

Fuchs, N.A., "The Mechanics of Aerosols", Pergamon Press, New York, (1964).

Garland, J.A., "Condensation on ammonium sulphate particles and its effect on visibility", Atmos. Environ., 3, 347-354 (1969).

Garland, J.A., and Rae, J.B., "An integrating nephelometer for atmospheric studies and visibility warning devices", J. Phys. E:Scientific Instruments, 3, 275-280, (1970).

Glen, C.L., "The Chinook", Weatherwise, 14, 175-180 (1961).

Griggs, M., "Relationship of optical observations to aerosol mass loading", J. Air Poll. Control Assoc., 22, 356-358 (1972).

Gucker, F.T., and Peterson, A.H., "A comparison photometer to measure light scattering of aerosols and gases, using the latter as light scattering standards", J. Colloid Sci., 10, 12-23, (1955).

Hänel, G. and Thudium, J., "Mean bulk densities of samples of dry atmospheric aerosol particles: A summary of measured data", Pageoph. 115, 799-803, Birkhäuser Verlag, Basel, Switzerland, (1977).

Harrison, A.W., "Rayleigh volume scattering coefficients for freon-12, freon-22 and sulphur hexafluoride", Can. J. Phys., 55, 1898-1901, (1977a).

Harrison, A.W., "Spectronephelometer studies of aerosols", Can. J. Phys., 56, 1594-1600, (1977b).

Harrison, A.W., "An automatic scanning integrating spectronephelometer, Can. J. Phys., 55, 1399-1406 (1977c).

Harrison, A.W., "Nephelometer estimates of visual range", Atmos. Environ., 13, 645-652 (1979).

Harrison, A.W. and Mathai, C.V., "Size distribution of winter continental-mountain aerosols 0.07 - 1.5 μm", Can. J. Phys., 57, No. 9, 1557-1564 (1979).

Heintzenberg, J., "Determination in-situ of the size distribution of atmospheric aerosol", J. Aerosol. Sci., 6, 291-303 (1975).

Hicks, R.B., Smith, D., Irwin, P.J. and Mathews, T., "Preliminary Results of Atmospheric Acoustic Sounding at Calgary", Boundary Layer Meteor., 12, 201-212 (1977).

Hicks, R.B. and Mathews, T., "Impact of Chinooks on Calgary's Air Quality:Acoustic Sounder Observations of Atmospheric Stability", Water, Air, Soil Pollut., 11, 159-172 (1979).

Horvath, H., and Noll, K.E., "The relationship between atmospheric light scattering coefficient and visibility", Atmos. Environ., 3, 543-550 (1969).

Jennings, S.G., and Elleson, R.K., "Aerosol particle size distributions in the 0.25 - 5.0 μm radius range in Northern England", Atmos. Environ., 11, 361-366 (1977).

Junge, C.E., "Atmospheric Chemistry", In Advances in Geophysics, Vol. 4, Academic Press, New York (1958).

Junge, C.E., "Air Chemistry and Radioactivity", Academic Press, New York (1963).

Junge, C.E., Comments on "Concentration and size distribution measurements of atmospheric aerosols and a test of the theory of self-preserving size distributions", J. Atmos. Sci., 26, 603-608 (1969).

Kadowaki, S., "Size distribution of atmospheric total aerosols, sulphate, ammonium and nitrate particulates in the Nagoya area. Atmos. Environ., 10, 39-43 (1976).

Kelkar, D.N., and Joshi, P.V., "A note on the size distribution of aerosols in urban atmospheres", Atmos. Environ., 11, 531-534 (1977).

Kerker, M., "The scattering of light", Academic Press, New York, N.Y. (1969).

Kretzschnar, J.G., "Comparison between three different methods for the estimation of the total suspended matter in urban air", Atmos., Environ., 9, 931-934 (1975).

Korerber, B.W., and Dale, F.R., "A rugged visibility meter for monitoring atmospheric aerosol parameters", W.R.E. Technical Note - 582 (AP), Australian Defence Scientific Service, Adelaide (1972).

Leaderer, B.P., "Summary of the New York summer aerosol study (NYSAS)", J. Air Poll. Control Assoc. 28, 321-327 (1978).

Lester, P.L., "A Qualitative Definition of the Chinook of Southern Alberta", Report 177, Environmental Science Centre, The University of Calgary (1976a).

Lester, P.L., "Evidence of Long Lee Waves in Southern Alberta", Atmosphere, 14, 28-36 (1976b).

Livshits, G.S., Solovyeva, A.N., and Travina, T.B., "On the relationship between the scattering factor of atmospheric haze and relative humidity", Izv. Atmos. Oceanic Phys., 10, 991-992 (1974).

Longely, R.W., "The Frequency of Winter Chinooks in Alberta", Atmosphere, 5, 4-16 (1967).

Lundgren, D.A., and Cooper, D.W., "Effect of humidity on light scattering methods of measuring particle concentration", J. Air Poll. Control Assoc., 19, 243-247 (1969).

Lyons, T.J., and Cutten, D.R., "Atmospheric pollutant and temperature traverses in an urban area", Atmos. Environ., 9, 731-737 (1975).

Mainwaring, S.J., and Harsha, S., "Size distribution of aerosols in Melbourne city air", Atmos. Environ., 10, 57-60 (1976).

Mathai, C.V., Harrison, A.W. and Mathews T., "Aerosol particle size distribution (0.1 to 1.0 μm) During the Chinooks of 1979 over Calgary, Canada", J. App. Meteor. 19, 515-520 (1980).

Mathews, T. and Hicks, R.B., "Typical Features of Atmospheric Turbulence Profiles Associated with Chinooks", Atmosphere-Ocean, 17, 125-134 (1979).

McCartney, E.J., "Optics of the Atmosphere", John Wiley and Sons, New York (1976).

McCormick, R.A., and Holzworth, G.C., "Air pollution climatology in Air Pollution", Vol. I, Academic Press, New York (1976).

Megaw, W.J., "The background aerosol", Contemporary Physics, 4, (1973).

Mercer, T.T., "Aerosol technology in hazard evaluation", Academic Press, New York, 81 and 243 (1973).

Meszaros, A., "On the size distribution of atmospheric aerosol particles of different composition", Atmos. Environ., 11, 1075-1081 (1977).

Middleton, W.E.K., "Vision through the atmosphere", University of Toronto Press (1968).

Nkemdirim, L.C. and Leggat, K., "The effect of chinook weather on urban heat island and air pollution", Water, Air, Soil Pollut., 9, 53-67 (1978).

Noll, K.E., Mueller, P.K., and Imada, M., "Visibility and aerosol concentration in urban air", Atmos. Environ., 2, 465-475 (1968).

Orsini, C.Q., Kaufmann, H.C., Akselsson, K.R., Winchester, J.W., and Nielson, J.W., "Variation of elemental composition with particle size in the St. Louis aerosol", Nucl. Instrum. Methods, 142, 91-96 (1977).

Paterson, M.P., "Visibility, Humidity and Smoke in Sydney", Atmos. Environ., 7, 281-290 (1973).

Patterson, E.M., Gillette, D.A., and Grams, G.W., "The relation between visibility and the size-number distribution of airborne soil particles", J. App. Meteor., 15, 470-478 (1976).

Patterson, R.K., and Gillette, D.A., "Measurements of visibility vs mass-concentration for airborne soil particles", Atmos. Environ., 11, 193-196 (1977).

Patterson, R.K., and Wagman, J., "Mass and composition of an urban aerosol as a function of particle size for several visibility levels", J. Aerosol Sci., 8, 269-279 (1977).

Penndorf, R.B., "Total Mie Scattering coefficients", J. Opt. Soc. Amer., 47, 1010-1015 (1975).

Peterson, C.M., Paulus, H.J., and Foley, G.H., "The number-size distribution of atmospheric particles during temperature inversions", J. Air Poll. Control Assoc., 19, 795-801, (1969).

Pi, R., "A study of the Calgary ambient aerosol", M.Sc. Thesis, University of Calgary (1979).

Porch, W.M., Charlson, R.J., and Radke, L.F., "Atmospheric aerosol: Does a background level exist?", Science, 170, 315-317 (1970).

Porch, W.M., Ensor, D.S., and Charlson, R.J., "Visibility of distant mountains as a measure of background aerosol pollution", App. Optics 14, 400-403 (1975).

Pueschel, R.F., and Noll, K.E., "Visibility and aerosol size frequency distribution", J. App. Meteor., 6, 1045-1052 (1967).

Rae, J.B., and Garland, J.S., "A stablized integrating nephelometer for visibility studies", Atmos. Environ., 4, 219-223 (1970).

Rassol, S.I., "Chemistry of the Lower Atmosphere", Plenum Press, New York (1973).

Shaw, G.E., "Properties of the background global aerosol and their effects on climate", Science, 192, 1334-1336 (1976).

Sinclair, D., Countess, R.J., and Hoopes, G.S., "Effect of relative humidity on the size of atmospheric aerosol particles", Atmos. Environ., 8, 1111-1118 (1974).

Slin, W.G.N., "Atmospheric particles in surface-level air", Atmos. Environ., 9, 763-764 (1975).

Stein, F., Esmen, N.A., and Corn, M., "The shape of atmospheric particles in Pittsburgh air", Atmos. Environ., 3, 443-453 (1969).

Stern, A.C., "Air Pollution", Vol. I., Academic Press, New York (1976).

Suck, S.H., Middleton, P.B., and Brock, J.R., "On the multimodality of density functions of pollutant aerosols", Atmos. Environ., 11, 251-255 (1977).

Sverdrup, G.M., Whitby, K.T., and Clark, W.E., "Characterization of California aerosols - II. Aerosol size distribution measurements in the Mojave desert", Atmos. Environ., 9, 483-494 (1975).

Tashenov, B.T., Tem, E.L. and Fedulin, I.A., "Determinations of the atmospheric-aerosol spectrum from the optical characteristics of the clear daytime sky", Izv. Atmos. Oceanic Phys., 9, 314-317, (1973).

Thudium, J., "Water uptake and equilibrium sizes of aerosol particles at high relative humidites: Their dependence on the composition of the water soluble material", Pageoph, Vol. 116, Birkhauser Verlag, Basel (1978).

Tombach, I., "Measurement of some optical properties of air pollution with the integrating nephelometer", Amer. Inst. Aeron. Astron. Paper No. 71-1101 (1971).

Twomey, S., "Atmospheric Aerosls", Elsevier Scientific Publishing Company, New York (1977).

Wadely, M.W., Witz, S , Bope, W., and MacPhee, R.D., "Size distribution measurements of particulate matter in Los Angeles and Anaheim using high volume Andersen samplers", J. Air Poll. Control Assoc. 28, 363-367 (1978).

Wangen, L.E., "An atmospheric particulate sampling procedure for gravimetric and elemental analyses", J. Air Poll. Control Assoc., 28, 55-57 (1978).

Whitby, K.T., Husar, R.B., and Liu, B.Y., "The aerosol size distribution of Los Angeles Smog", J. Colloid Interface Sci., 39, 177-204 (1972).

Sem, G.M., Willeke, K., Liu, B.H.Y., and Pui, D.Y.H., "Characterization of California Aerosols - I. Size distributions of freeway aerosols", Atmos. Environ. 9, 463-482 (1975).

Van de Hulst, H.G., "Light scattering by small particles", Wiley, New York, N.Y. (1957).

White, W.H., and Roberts, P.T., "On the nature and origins of visibility reducing aerosols in the Los Angeles air basin", Atmos. Environ., 11, 803-812 (1977).

Willeke, K., Whitby, K.T., Clark, W.E. and Marple, V.A., "Size distribution of Denver aerosols - a comparison of two sites", Atmos. Environ., 8, 609-633 (1974).

Yamamoto, G., and Tanaka, M., "Determination of aerosol size distribution from spectral attenuation measurements", App. Optics 8, 447-453 (1969).

Zdunkowski W.G., and Kuo-Non Liou., "Humidity effects on the radiative properties of a hazy atmosphere in the visible spectrum", Tellus 28, 31-36, (1976).